British Geological Survey

Mineral Reconnaissance Programme

Platinum-group element mineralisation in the Loch Ailsh alkaline igneous complex, north-west Scotland

Department of Trade and Industry

MRP Report 131
Technical Report WF/94/2

Platinum-group element mineralisation in the Loch Ailsh alkaline igneous complex, north-west Scotland

M H Shaw, A G Gunn, K E Rollin and M T Styles

BRITISH GEOLOGICAL SURVEY

Technical Report WF/94/2

Mineral Reconnaissance Programme Report 131

Platinum-group element mineralisation in the Loch Ailsh alkaline igneous complex, north-west Scotland

M H Shaw, A G Gunn, K E Rollin and M T Styles

Compilation
M H Shaw, BSc

Geochemistry
A G Gunn, BA, MSc
M H Shaw, BSc

Geophysics
K E Rollin, BSc

Mineralogy
M T Styles, BSc, PhD

This report was prepared for the Department of Trade and Industry

Maps and diagrams in this report use topography based on Ordnance Survey mapping

Bibliographical reference
Shaw, M H, Gunn, A G, Rollin, K E, and Styles, M T. 1994. Platinum-group element mineralisation in the Loch Ailsh alkaline igneous complex, north-west Scotland. *British Geological Survey Technical Report* WF/94/2 (*BGS Mineral Reconnaissance Programme Report* 131).

Keyworth, Nottingham 1994

BRITISH GEOLOGICAL SURVEY

The full range of Survey publications is available through the Sales Desks at BGS Keyworth, BGS Edinburgh, and at the BGS London Information Office. The adjacent bookshop stocks the more popular books for sale over the counter. Most BGS books and reports are listed in HMSO's Sectional List 45, and can be bought from HMSO and through HMSO agents and retailers. Maps are listed in the BGS Map Catalogue, and can be bought from Ordnance Survey agents as well as from BGS.

The British Geological Survey carries out the geological survey of Great Britain and Northern Ireland (the latter as an agency service for the government of Northern Ireland), and of the surrounding continental shelf, as well as its basic research projects. It also undertakes programmes of British technical aid in geology in developing countries as arranged by the Overseas Development Administration.

The British Geological Survey is a component body of the Natural Environment Research Council.

Keyworth, Nottingham NG12 5GG
☎ 0602-363100 Telex 378173 BGSKEY G
Fax 0602-363200

Murchison House, West Mains Road, Edinburgh EH9 3LA
☎ 031-667 1000 Telex 727343 SEISED G
Fax 031–668 2683

London Information Office at the Natural History Museum, Earth Galleries, Exhibition Road, South Kensington, London SW7 2DE
☎ 071-589 4090 Fax 071-584 8270
☎ 071-938 9056/57

St Just, 30 Pennsylvania Road, Exeter EX4 6BX
☎ 0392-78312 Fax 0392-437505

Bryn Eithyn Hall, Llanfarian, Aberystwyth, Dyfed SY23 4BY
☎ 0970-611038 Fax 0970-624822

Windsor Court, Windsor Terrace, Newcastle upon Tyne NE2 4HB
☎ 091-281 7088 Fax 091-281 9016

Geological Survey of Northern Ireland, 20 College Gardens, Belfast BT9 6BS
☎ 0232-666595 Fax 0232-662835

Maclean Building, Crowmarsh Gifford, Wallingford, Oxfordshire OX10 8BB
☎ 0491-838800 Telex 849365 HYDROL G
Fax 0491-825338

Parent Body

Natural Environment Research Council
Polaris House, North Star Avenue, Swindon, Wiltshire SN2 1EU
☎ 0793-411500 Telex 444293 ENVRE G
Fax 0793-411501

Dr D C Cooper
Minerals Group
British Geological Survey
Keyworth
Nottingham NG12 5GG

Printed in England for the British Geological Survey by Saxon Graphics Limited, Derby

CONTENTS

FIGURES

TABLES

PLATES

SUMMARY

A programme of exploration for the platinum-group elements (PGE) carried out over the Loch Ailsh alkaline intrusive complex in north-west Scotland is described. The area was considered to have potential for two styles of PGE-bearing mineralisation, namely magmatic, associated with cumulus or intercumulus phases and hydrothermal, related to post-cumulus low-temperature PGE concentration and precipitation in structurally-controlled settings.

Reconnaissance sampling of drainage sediments and bedrock indicated localised PGE enrichment in mafic and ultramafic rocks in the south-east and northern parts of the Complex. Concentrations were generally higher in fine-fraction drainage samples than in corresponding panned coarser-fractions. Maximum values in stream sediments are 859 ppb Pt and 43 ppb Pd. Drainage sampling also identified enhanced gold levels in panned concentrates in the northern sector of the Complex and markedly enhanced gold concentrations in stream sediments at several widely-spaced localities.

Detailed basal overburden sampling over the south-east part of the Complex indicated widespread PGE enrichment in pyroxenites. The highest PGE concentrations in overburden, up to 110 ppb Pt and 70 ppb Pd, occur within the central section Allt Cathair Bhan catchment.

Lithogeochemical sampling revealed a widespread low tenor PGE enrichment in the Allt Cathair Bhan valley in pyroxenites, pyroxenite mylonites and pyroxenite skarns consistent with a magmatic origin. Higher PGE contents, up to a maximum of 300 ppb Pt+Pd, occur sporadically in the lower section of the Allt Cathair Bhan valley. In these PGE-enriched rocks sperrylite (PtAs) and isomertieite (Pd+Sb+As) were identified by automated microchemical mapping. Complex tellurides of Pd, Ag, Bi and Pb were also found in these rocks.

A detailed ground magnetic survey was used to define the extent and structure of the concealed parts of the mafic and ultramafic components of the Complex. These investigations indicated that the pyroxenite exposed in the south-east of the Complex underlies a large area of Lower Palaeozoic and Moinian cover. Additionally, VLF-resistivity techniques were employed to search for potentially PGE-enriched sulphide mineralisation but without success.

Geochemical and petrological investigations suggest that the Ailsh pyroxenites are of magmatic origin and that PGE enrichment is associated with late-magmatic volatile-rich fluids deficient in sulphur. Further localised upgrading of the PGE and gold may have occurred at lower temperatures, together with base-metal enrichment.

Full data listings, together with detailed logs of samples, are available from the Mineral Reconnaissance Programme Database, BGS, Keyworth, on request.

INTRODUCTION

The investigations described in this report were carried out over the Loch Ailsh Complex, the location of which is shown on the regional geology map (Figure 1). The survey described was carried out as part of the Department of Trade and Industry-sponsored Mineral Reconnaissance Programme (MRP). The work was conducted in 1989 and 1990, concurrent with a drilling programme for PGE in the marginal pyroxenite of the Loch Borralan pluton two kilometres to the south-west (Shaw et al., 1992).

An association between precious metals and alkaline intrusions of has long been recognised (Eckel, 1938), and many accounts of precious-metal enrichment in porphyry and stockwork deposits, frequently associated with Cu sulphides, are documented. Following renewed interest in the prospectivity of alkaline plutons for the PGE in the 1980s, it was recognised that rapid volatile flux played an important role in the separation of mineral phases within alkaline ultramafic magmas, and possibly, therefore, in PGE enrichment mechanisms: (Werle et al., 1983, Finch et al., 1983). The requirements imposed by models for PGE concentration in layered intrusions were therefore challenged. With this research has come the recognition of the importance of discordant features in mafic and ultramafic rocks as evidence of rapid volatile flux, and as potential hosts for PGE mineralisation (Eckstrand, 1984). Further evidence for the transport of the PGE over a wide range of temperatures and in association with a variety of complexing agents has also recently come to light, thus broadening the range of targets for potential economic PGE mineralisation (Stumpfl, 1993, Coghill and Wilson, 1993).

In response to the stimulus provided by these investigations, the decision was made by the Mineral Reconnaissance Programme to explore for the PGE in the alkaline complexes of north-west Scotland. The discovery of enhanced PGE levels in archived drill core from the Loch Borralan Complex provided stimulus for further investigations at Loch Borralan and on the neighbouring Loch Ailsh Complex.

PHYSIOGRAPHY

The Loch Ailsh Complex is situated on the southern margin of the Ben More Assynt hill massif, in the sparsely populated north-west of Scotland (Figure 1). The small market town and port of Ullapool is situated some 25 km to the south-west. There are a few other small settlements in the area, such as Elphin, some 12 km west of the project area, which accommodates a few dozen people.

The climate of north-west Scotland may be classified as cool wet temperate at sea level. In the Loch Ailsh area, the influence of the adjacent higher ground, which rises to around 600 m elevation, increases the frequency of early and late-seasonal snowfall. At all altitudes the weather pattern is variable, and is seldom stable due to the northerly latitude and frequent exposure to storms from the Atlantic.

The relatively high rainfall in the area generally results in the podzolisation of poorly drained soils. The resultant low soil nutrient status and short growing season severely restrict the area's potential for arable and pastoral farming. Most of the upland is untended and the vegetation dominated by dry

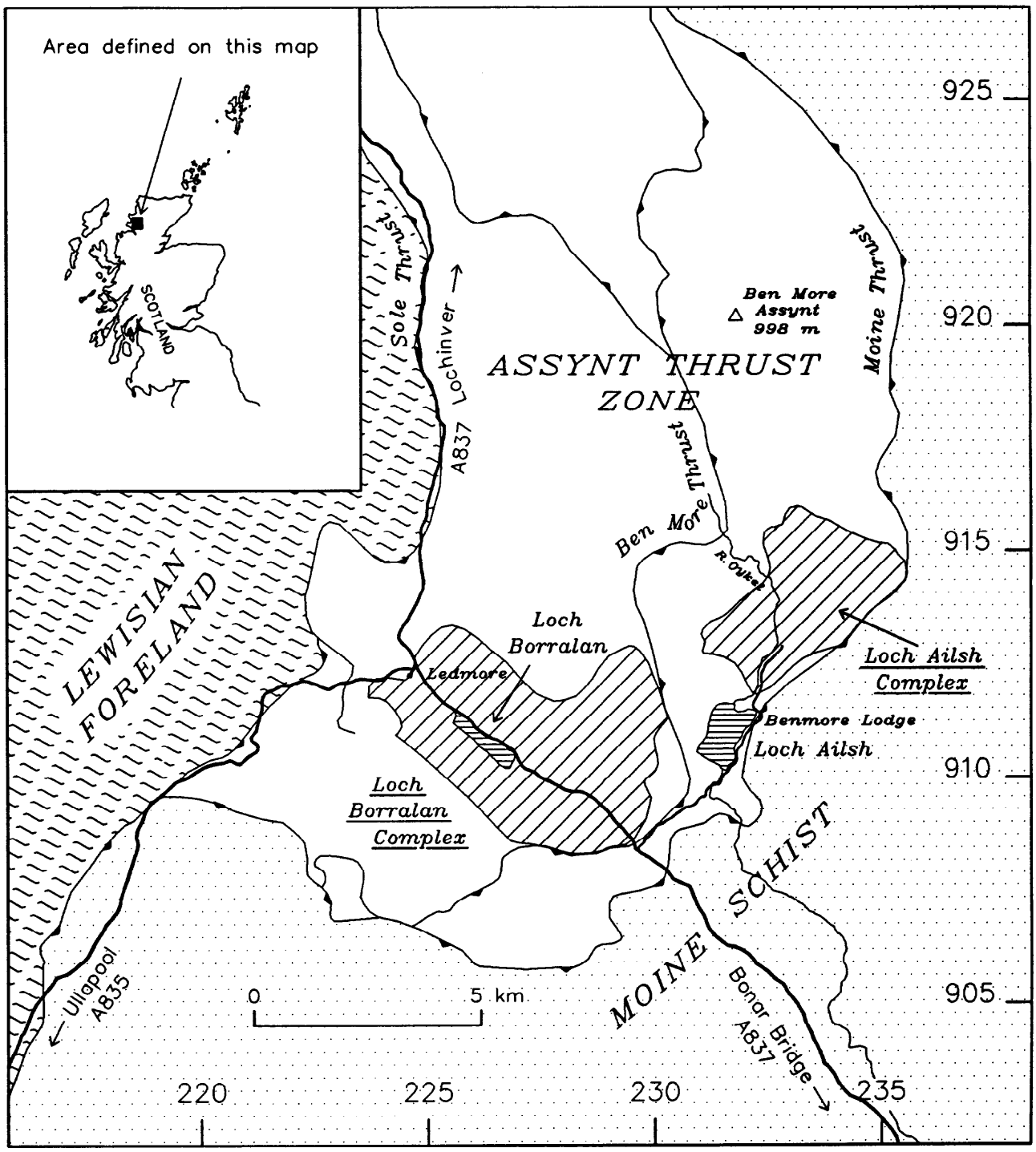

Figure 1 Regional geology map showing location of project area

heath species of heather, bilberry, nardus and festuca grass on the drier ground, and patchy sedge and sphagnum over poorly-drained areas. Naturally regenerated trees are confined to a few inaccessible areas such as rocky ledges. Elsewhere their regeneration is constrained by excessive deer grazing. Commercial afforestation over the southern fringes of the Complex has taken place in the last 15 years, notably in the area between Loch Ailsh and the southern part of the Loch Ailsh Complex.

The project area is situated approximately 6 km north-east of the A837 public road from Bonar Bridge to Ledmore (Figure 1). From the road, vehicle access is provided by a track which runs northwards along the eastern shore of Loch Ailsh and then follows the upper valley of the River Oykel northwards for about one kilometre beyond Benmore Lodge. From this section of track easy foot access can be made over the southern part of the Complex. The northern part is less accessible and involves a half hour walk along a rough stalker's track from the confluence of the River Oykel with the Allt Sail an Ruathair (Figure 2).

Scotland was subjected to extensive glaciation during the Pleistocene. Superficial deposits are predominantly of late-Pleistocene (Devensian) and Holocene age. The sporadic occurrence of rounded clasts of Lewisian gneiss in streams draining the southern part of the Complex, notably within the Allt Cathair Bhan catchment, indicate there has been some glacial or fluvioglacial transport of this material from the higher ground to the north-west. However, the erratics form significantly less than one percent of the cobble-sized fraction in these streams and the main direction of ice and meltwater flow appears to have skirted the Cathair Bhan ridge and followed the line of the Oykel valley. This valley contains an extensive and thick infill of coarse glacial and fluvioglacial material, as does the lower section of the Allt Sail an Ruathair. The deposits are locally of a hummocky nature and visual assessment indicates are that they may exceed 10 m in thickness. Within the Allt Cathair Bhan catchment, the superficial deposits are predominantly derived from in situ weathering and solifluction, and average 2-3 m in thickness. In the Sron Sgaile area (Figure 2), much of the body is concealed beneath a covering of peat, which renders geochemical sampling difficult.

PREVIOUS WORK

There are few records of previous commercial interest in the Loch Ailsh area. The only well-documented project was carried out by Noranda-Kerr (U.K.) Ltd in the early 1970s. The project was in part supported by financial assistance from the Mineral Exploration and Investment Grant Act, 1972 (M.E.I.G.A.).

Between 1970 and 1973 Noranda-Kerr undertook investigations for base-metals at three localities in Scotland, including the Loch Ailsh area. These investigations were based on a model for the stratiform base-metal deposits at Laisvall and Vassbo in Sweden (Tegengren, 1962).

At Loch Ailsh, the company undertook reconnaissance stream sediment sampling over the Lower Palaeozoic succession surrounding the Loch Ailsh Complex, and included marginal areas of the Complex. In addition to sporadic anomalies over the Lower Palaeozoic succession, anomalous Cu levels in soils, in excess of 120 ppm, were obtained from the Allt Cathair Bhan and Black Rock areas of the Complex. A third anomalous area was identified over Sron Sgaile, but soil sample coverage was not complete. The distribution pattern for lead in soils was roughly coincident with that of Cu.

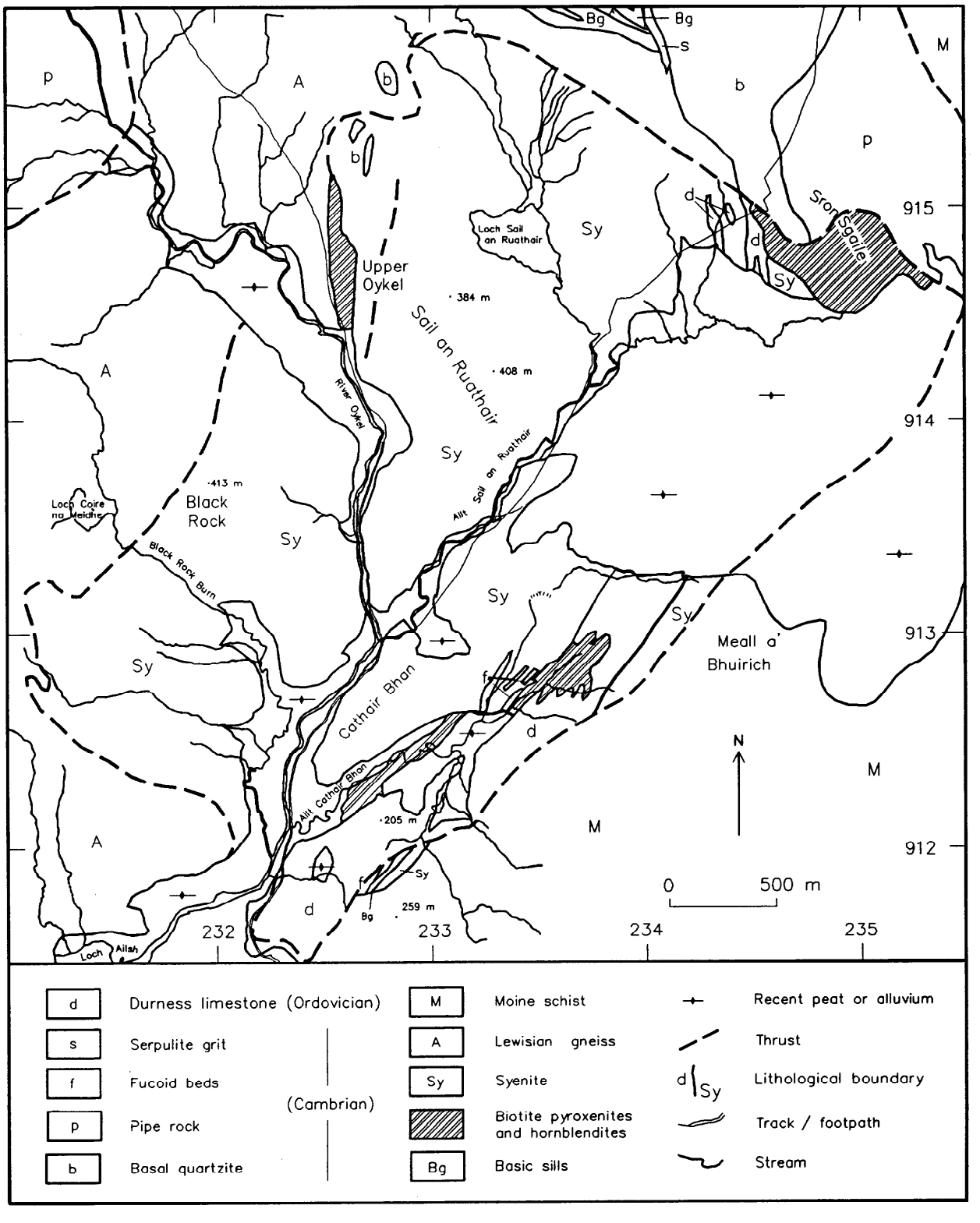

Figure 2 Locational and geological map of Loch Ailsh Complex

The results indicated that three areas of the Complex, each several hundred metres in dimensions, were enriched in base metals. The disposition of these anomalies, particularly the Allt Cathair Bhan anomaly which transects ultramafic as well as Lower Palaeozoic lithologies, were not consistent with the original model. The Allt Cathair Bhan anomaly was investigated further using ground geophysics. Details of this work are given in the geophysics section of this report.

These investigations failed to prove the existence of economic base-metal enrichment. Full details are available for inspection on Open File at BGS, Keyworth as M.E.I.G.A. reports.

The Mineral Reconnaissance Programme of BGS began its exploration for the PGE in alkaline complexes in 1988. The investigations were initially carried out on archived drillcore from 37 boreholes which had been drilled in the late 1970s as part of an evaluation of the phosphate potential of the Loch Borralan body (Notholt and Highley, 1981). The results for trace and precious element data from these investigations (Shaw et al., 1992) indicate that the highest levels of PGE occur in zones associated with calcite veining and chalcopyrite mineralisation. Maximum levels of 328 ppb Pt and 550 ppb Pd were obtained from a 0.5 m intersection in one borehole, with values averaging 450 ppb (combined Pt and Pd) over a 2 m section. Minor enrichment in Au was also detected in association with enhanced Cu in some intervals.

These results provided a stimulus for further drilling at Loch Borralan between September and November 1989. This second phase of study showed that PGE enrichment occurs in association with elevated Cu within low Cr-Ni pyroxenites (Figures 3 and 4). It was considered that this pattern of PGE and Cu enrichment, depletion in Cr-Ni, and variable but generally high large-ion lithophile element (LILE) values, was consistent with an intercumulus (hydromagmatic) style of primary PGE concentration, with localised upgrading in stocks or veins with chalcopyrite mineralisation.

GEOLOGY OF THE LOCH AILSH COMPLEX

The Loch Ailsh pluton is one of five medium-sized alkaline complexes which occur along the north-west margin of the Scottish Caledonides. Radiometric dating indicates that this magmatism took place during the latter stages of the Caledonian orogeny and was episodic over at least 30 Ma (Halliday et al., 1987). U-Pb zircon ages have been quoted at 439 +/-4 Ma for the Loch Ailsh pluton (Halliday et al., 1987) and for Loch Borralan at 430 +/-4 Ma (van Breeman et al., 1979).

The Loch Ailsh Complex is believed to be a sill-like intrusion emplaced between Proterozoic basement rocks and an overlying cover of Lower Palaeozoic sediments (Figure 2). The Complex is roofed by limestones of the Ordovician Durness Group, and xenoliths from this group and the underlying Cambrian succession are locally evident in the catchments of the Metamorphic Burn [233 914], Black Rock Burn [232 913] and the Allt Cathair Bhan [233 912]. Evidence for in situ fractionation within the Complex is sparse, and contacts between the various intrusive components are generally sharp. The Complex comprises lithologies ranging from ultramafic, through basic and hybrid types to a suite of three mineralogically distinctive, rather sodic leucocratic syenites (Parsons, 1965b). The two earlier syenitic units are sill-like in shape and are exposed extensively throughout the Complex. They are intruded by the plug-like form of the later leucosyenite.

Loch Borralan Borehole 2

Location: NC 22462 91140 Azimuth: 270° Inclination: 55°

Depth, inclined: 116.84 m. Depth, true: 82.62 m.

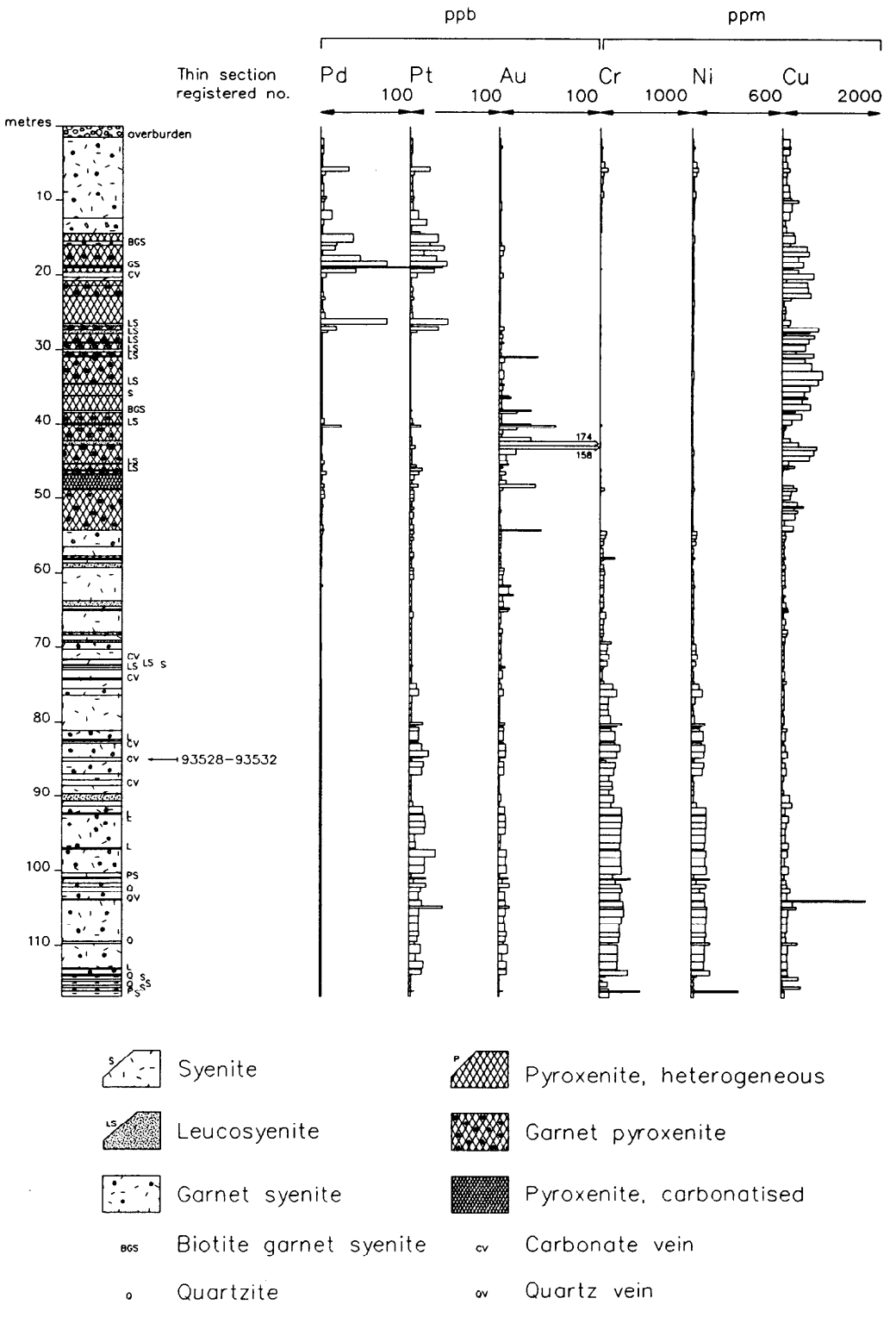

Figure 3 Graphic and lithogeochemical log for Loch Borralan Borehole 2

Loch Borralan Borehole 4

Location: NC 22499 91143 Azimuth: 254° Inclination: 55°

Depth, inclined: 72.70 m. Depth, true: 59.55 m.

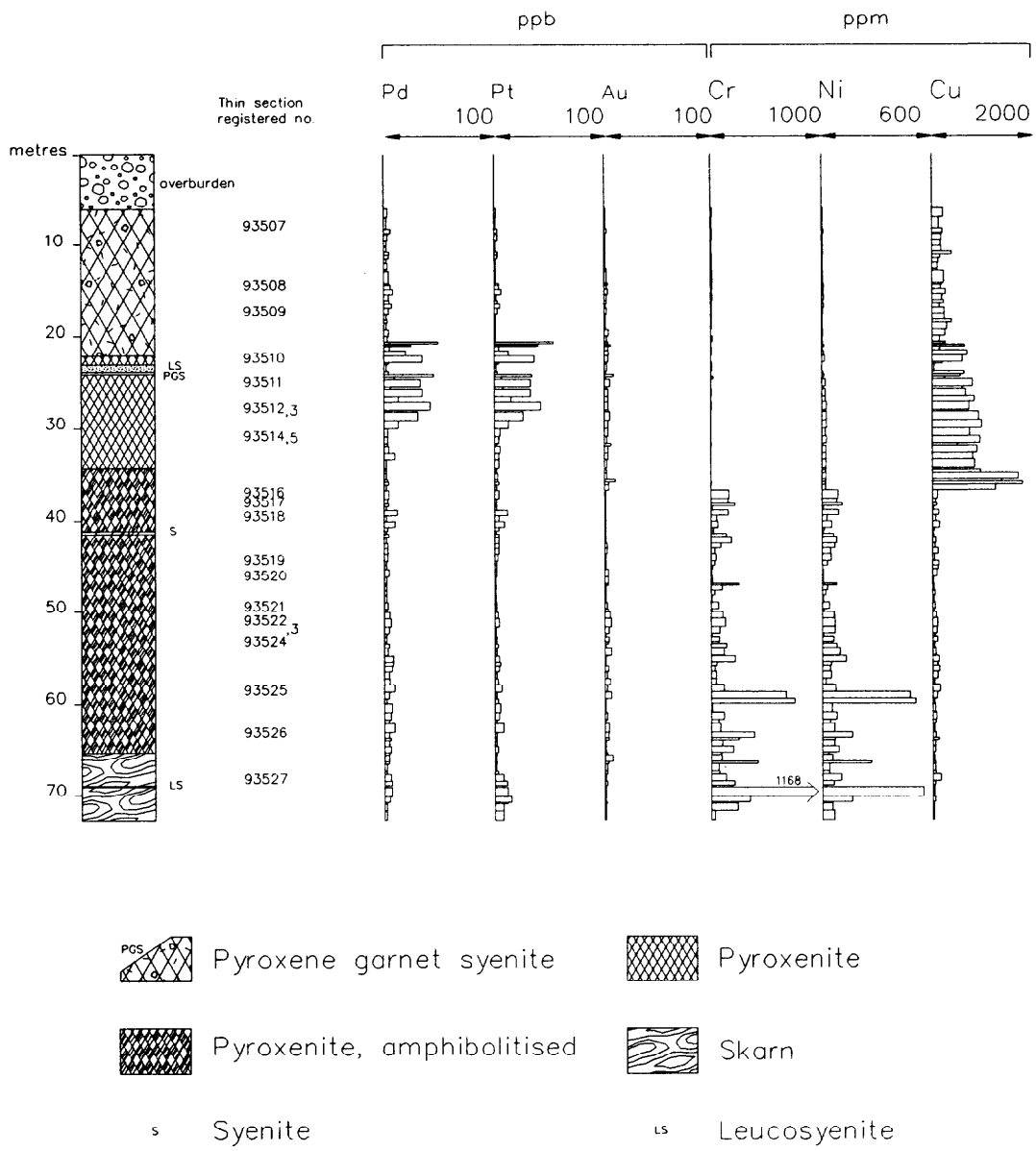

Figure 4 Graphic and lithogeochemical log for Loch Borralan Borehole 4

The location of the Complex is within the Caledonian foreland thrust belt, where rocks of upper Proterozoic age (Moine series) overthrust the Lewisian basement and Cambro-Ordovician cover. The relationships between emplacement and thrusting at Ailsh are not fully understood, but the thrust-bounded margins indicate the Complex may have been moved a considerable distance from the east during thrusting. All lithologies are locally affected by mylonitisation and shearing which, it is believed, are related to one of the major thrust movements (Halliday et al., 1987). However, these fabrics are very localised, which suggests that emplacement may, at least in part, have occurred during periods of quiescence or extensional relaxation.

The genesis of the ultramafic suite at Loch Ailsh has long been a source of conjecture. Phemister and Ross (1926), in their detailed petrological and field account of the Complex, favoured a magmatic model. They argued that evidence from the Sron Sgaile body of an abrupt transition from ultramafic to mafic types suggested that differentiation between these two magmatic types had not taken place in situ.

Parsons (1965a) considered fractionation at depth of feldspathic magma to account for the variation between relatively sodic S1 and S2 syenites and the later, relatively potassic S3 type. In consideration of the genesis of pyroxenites in the Allt Cathair Bhan catchment he concluded from magnetic evidence (Parsons, 1965b) that these formed steeply dipping screens separating syenites and metamorphosed Durness limestone. Petrological studies of pyroxene trends by the same author (Parsons, 1968), indicating the unusually diopsidic nature of pyroxenes in oversaturated syenites, were used to support the contention that metasomatic reaction had occurred between syenitic magma and limestone. This view accorded with those of Shand (1910) and Matthews and Woolley (1977) concerning similar observations on the Loch Borralan Complex.

Although assimilation has undoubtedly occurred locally in both intrusions, the present authors concur with Wyllie (1984) that (in the case of the Loch Ailsh Complex) there is little field evidence or theoretical plausibility for the assimilation model to work on such a large scale. Instead a magmatic origin for the ultramafic rocks of the Loch Ailsh Complex is preferred.

The suite of pyroxenites in the Allt Cathair Bhan catchment were the main targets for the present investigations, and are described in detail below. Rocks believed by Phemister and Ross (1926) to represent hybrids of ultramafic and syenitic magma are found in various parts of the Complex. These range from shonkinites to pulaskites (Parsons, 1965b), and vary by proportion of mafic constituents between 30 and 70%. They are best seen in the vicinity of Black Rock (Figure 2) and in the river section of the River Oykel, immediately below its confluence with the Allt Sail an Ruathair.

The ultramafic, mafic and hybrid phases were succeeded by three syenitic phases S1 - S3 (Parsons, 1965b), showing a progressive decrease in mafic constituents. The earliest syenites (S1) were identified as pulaskites by Phemister and Ross (1926), and contain a significant proportion of mafic constituents - mainly aegirine augite, biotite and riebeckite. They are exposed in the crags surrounding the Loch Sail an Ruathair [233 914]. A second phase (S2), often finer grained and paler in colour than S1 due to the lower proportion of mafics, is exposed in the south-western part of the Complex to the south of Black Rock. The third (S3) type syenite which forms the remainder of the Complex contains less than 3% mafic minerals, but is locally melanite bearing. In the south-west part of the Complex, in the vicinity of the Allt Cathair Bhan and to the west of the Cathair Bhan ridge,

the xenocrystic nature of the S3 syenite is attributable to partial mylonitisation, probably related to late thrusting.

GEOLOGY OF THE ALKALINE ULTRAMAFIC SUITE

Allt Cathair Bhan pyroxenite

Pyroxenites are exposed discontinuously in the Allt Cathair Bhan catchment, which defines the south-eastern margin of the Ailsh intrusion (Figure 2). The pyroxenites are commonly biotitic, although the abundance of biotite varies greatly, resulting in highly variable weathering characteristics. This has given rise to an irregular topography, which is in the main masked by drift.

The pyroxenite is flanked to the north by xenocrystic S3 type leucosyenite, which forms most of the Cathair Bhan ridge. Magnetic data from this and previous studies indicate that the transition is not sharp and that pyroxenite is locally interdigitated with syenite on both the southern and northern flanks of this ridge. Although contact relations are not exposed, ground magnetics picks up this intercalation clearly and the localised presence of pyroxenite has been proven by shallow digging in the present work and by Parsons (1965a).

On the southern side of the Allt Cathair Bhan valley dolomitic limestones of the Durness Group, metamorphosed to forsterite marble, are exposed over a strike length of approximately 1.5 km. In the lower Allt Cathair Bhan catchment area the Durness limestone forms a distinctive plateau at around 200 m elevation - some 30 m higher than the valley floor. Immediately north-east of this plateau is an embayment of low ground where the drift thickens and there is no exposure. Geophysical data indicate that this area is underlain by non-magnetic rocks while geochemical results from overburden sampling suggest the presence of limestone beneath the drift. Limestone outcrop is also found to the north-east of this embayment and forms patchy exposure on the north-west facing, gently-sloping hillside. More continuous exposure is present in the north-eastern tributaries of the Allt Cathair Bhan. The limestone is overthrust on its south-eastern side by quartz-feldspar schists of the Moine series. Within the vicinity of the thrust plane the limestone shows marked strain deformation, but elsewhere it is massive and fresh.

The Allt Cathair Bhan pyroxenites are divided into three sections for descriptive purposes. This permits the separation of the clearly contrasting lower section pyroxenites from the upper section hornblendites by a middle zone containing a wider variety of lithological types.

Lower section

In this section the massive pyroxenite is exposed along the bed of the Allt Cathair Bhan and on its adjacent, generally steep-sided stream banks. The pyroxenite is dark grey and composed of medium to coarse clinopyroxene containing clots or patches of biotite. It varies from a massive green-grey variety with little or no mica to foliated biotite-rich types which are frequently decomposed and friable. Accessory magnetite is abundant in some outcrops and occurs in aggregates which may locally be dominant over pyroxene.

The lower Allt Cathair Bhan pyroxenites display a variety of brittle and ductile deformation features. The pyroxenites are sometimes veined with pink syenite (probably of S3 type) - the veining usually apparent on a millimetric or centimetric scale. The veins and their host pyroxenites are locally disrupted by parallel, generally sub-millimetric calcite-filled brittle shears. Displacement along these shears is seldom more than a few cm. A later phase of ductile deformation may be seen in the form of centimetric mylonite zones, which transect the pyroxenite at almost 90° to the brittle shearing. A thicker example is exposed in the stream bed at [2328 9125], where a 20 - 30 cm zone is also mineralised with sulphides - principally galena and pyrite.

Within the lower Allt Cathair Bhan section the massive pyroxenites contain traces of sulphide mineralisation, principally pyrite and chalcopyrite on joint surfaces. This localised presence of chalcopyrite is indicated by the wide range of Cu values, up to a maximum in excess of 3000 ppm.

Middle section

The middle Allt Cathair Bhan section is defined on the ground by the broader and flatter valley floor. A number of abandoned stream channels occur in this section, as do all the main tributary confluences with the Allt Cathair Bhan. Bedrock exposure is sparse and is confined to a few outcrops in the vicinity of the stream.

The principal lithology exposed in this section is biotite-rich pyroxenite. Outcrop is not readily apparent as these rocks have been severely chemically degraded. The degraded biotite pyroxenite is best displayed in a 2 m high streambank exposure [2330 9125]. The texture of the rock appears to be locally cataclastic, with coarse angular clasts of grey biotite pyroxenite seated in an orange micaceous clay matrix. Another exposure of similar material 30 m downstream is cut by an undisturbed syenite veinlet several metres long. Apart from these two exposures the extent of this rock type cannot otherwise be determined due to the presence of drift cover.

Some 60 m upstream of the aforementioned site, fragments of diopside-chlorite-tremolite skarn may be found in soliflucted streambank debris. This material is readily exposed in sub-outcrop by pitting the steeply-cut slope forming the southern stream bank.

Upper section

Nearly continuous exposure of hornblendite is present in the north-east headwater tributary of the Allt Cathair Bhan. The hornblendites contain minor albite and orthoclase. Apatite is developed in the less feldspathic variants of this rock type. Minor intrusions of irregular quartz-cored syenite veinlets occur locally. These are generally a few centimetres in width and locally contain traces of base-metal mineralisation in the form of galena. Galena and chalcopyrite are not seen as interstitial phases. Interstitial pyrite mineralisation also occurs within the hornblendites. In an adjacent tributary of the main stream [233280 912695] a xenolith of Lower Palaeozoic sediment, several tens of metres in length is exposed. The contacts between this xenolith and the adjacent pyroxenites are sharp but also somewhat sheared.

Sron Sgail area

The rocks of the Sron Sgaile ridge are of two principal types. Near the base of the ridge, poorly exposed and largely covered by drift, is hornblendite, similar in appearance to the upper Allt Cathair Bhan hornblendite. This passes through a sharp transition upwards into a lithology described by Phemister (1926) as being of 'epidioritic' nature. It is believed from Phemister's petrological and chemical descriptions of this rock that it bears similarities to the mafic syenites elsewhere in the Complex, but is best classified as being a transitional or hybrid type, with mixed mafic and syenitic mineral components. No detailed petrological work was carried out on the section due to the uniformly low PGE contents.

RECONNAISSANCE INVESTIGATIONS

Reconnaissance sampling was conducted to define areas for detailed study. Attention was mainly focused on the three ultramafic and mafic zones of the Complex, namely the Allt Cathair Bhan, Sron Sgaile and Upper Oykel. The locations of these bodies, taken from the published BGS 1:50000 Assynt sheet, are shown in Figure 2. Drainage sampling was carried out on streams draining these areas and from sites on the margins of the Complex in order to evaluate the potential for structurally-controlled hydrothermal PGE enrichment in these settings.

Evaluation of the three mafic-ultramafic bodies made during reconnaissance investigations indicated that, due to their relatively poor exposure and predominantly mafic compositions, the Upper Oykel and Sron Sgaile bodies were considered to be less prospective targets for the PGE than the Cathair Bhan pyroxenite.

Drainage sampling

Stream sediment and panned concentrate samples were collected from 42 sites. Sampling was undertaken according to the techniques described by Gunn (1989). To prevent undue disturbance and resultant loss of dense minerals from the sediment, sampling was conducted by careful digging using a concave-bladed shovel. Panned concentrate samples were collected by wet screening through a 2 mm nylon mesh in the field, followed by washing to remove clays and a final reduction by panning to a standard final volume. The standard reduction was from 4 litres down to 150 ml panned concentrate. Stream sediment samples were obtained by wet screening to -100 mesh. The sediment was allowed to settle prior to decanting into a Kraft bag.

Both sample types were analysed for a range of elements by XRF at BGS, Keyworth. Analysis for Pt, Pd, Rh and Au was conducted by lead fire assay with an ICP or AAS finish on 30 g samples by Acme Analytical of Vancouver. The lower limits of detection were 1 ppb for Pt and Au and 2 ppb for Pd and Rh in both sample types.

Panned concentrates

The distributions of Pt, V, Cr, Au and Cu in panned concentrate samples are illustrated in Figures 5 - 9. The legend employed for the geological and physiographic linework in these figures is the same as that used in Figure 2.

Summary statistics for panned concentrates (Table 1), show that mean levels for Pt and Pd are at or close to their minimum detection limits. Only five panned concentrate samples contain PGE levels in excess of 20 ppb. Pt levels are highest in the Allt Cathair Bhan catchment, with a maximum value of 82 ppb and slight enrichment occurs in the vicinity of Sron Sgaile (Figure 5). Only six samples contain Pd in excess of 5 ppb, with a maximum of 18 ppb. Four of these samples were derived from the Allt Cathair Bhan catchment and two in the Sron Sgaile area. Two samples collected from streams draining the north-east of the Complex, in the vicinity of Sron Sgaile, contain Rh slightly above the minimum detection limit, 5 and 6 ppb respectively.

Pt shows a strong statistical association with the siderophile elements Ca, V, Fe, Co and Ni, with all Spearman Rank correlations significant at the 99.9% confidence level. The geographical distribution patterns of this group of elements are similar to those of the PGE, with the highest levels occurring in the Allt Cathair Bhan catchment (Figure 6). In contrast to these elements, Cr shows a weaker spatial and statistical association with the PGE. It is probable that the high Cr levels determined over Lewisian rocks to the north-west of the Loch Ailsh Complex (Figure 7) are due to alluvial upgrading of locally-derived material. Lenses and bands of ultramafic and mafic material in the Lewisian gneisses are believed to be the sources of Cr-bearing detrital minerals. Pd displays a slightly closer association with the chalcophile elements than Pt, with Spearman Rank correlation coefficients of 0.63 and 0.60 for Zn and Cu respectively, although there are also significant correlations with Ca (0.64) and V (0.52).

The highest Au concentrations are found in the northern part of the Complex, within a zone between Sron Sgaile and Loch Sail an Ruathair (Figure 8). The maximum value of 523 ppb was from a stream draining Sron Sgaile. Only minor Au enrichment is present in the Cathair Bhan catchment, where a north-north-east draining tributary contains slightly enhanced levels at around 9 ppb. Cu also shows high values in the Sron Sgaile area (Figure 9) and in the lower Allt Cathair Bhan. There is also a close correlation between Au and Pb in the panned concentrate samples.

Stream sediments

The distributions of Pt, Pd and Au in stream sediments are illustrated in Figures 10 - 12. The legend employed for the geological and physiographic linework in these figures is the same as that used in Figure 2.

Summary statistics for stream sediments (Table 2) show that median PGE levels are close to their minimum detection limits and that maximum values are considerably higher than their panned concentrate equivalents. The Allt Cathair Bhan and Sron Sgail areas of the Complex both contain enhanced levels of Pt in stream sediments (Figure 10). The highest Pt values of 859 and 132 ppb were derived from the northern part of the Complex. These samples are not enriched in Pd, Au or base metals. There are no Spearman Rank correlation coefficients for Pt significant at the 99.9% level, although the Pt - Pd correlation of 0.45 is significant at the 99% confidence level.

Table 1 Summary statistics for panned concentrate samples
N=42 for all elements except Bi, Th and U (19). Values in ppm unless stated.

Variable	25%	Median	75%	90%	Minimum	Maximum
Au (ppb)	3	5	10	33	1	523
Pt (ppb)	1	2	4	14	1	82
Pd (ppb)	2	2	3	10	2	18
Rh (ppb)	2	2	2	2	2	6
Ca	17300	28300	55150	88020	2700	98800
Ti	4388	6500	10278	17252	2480	28860
V	89	138	199	361	34	854
Cr	221	292	511	876	118	1514
Mn	795	1350	1850	2355	240	2670
Fe	32975	41650	59325	114200	11200	228400
Co	9	16	25	36	4	41
Ni	20	39	92	140	8	261
Cu	10	15	33	55	3	163
Zn	35	55	74	89	11	109
Rb	12	19	24	48	1	61
Sr	263	487	657	815	60	1041
Y	11	17	26	48	6	118
Zr	243	412	801	1193	197	2246
Nb	7	13	18	26	4	40
Sb	<1	<1	<1	<1	<1	1
Ba	328	435	604	800	132	860
La	23	46	59	97	9	1171
Ce	38	73	128	182	17	1691
Pb	10	24	36	54	<1	116
Bi	<1	<1	<1	2	<1	3
Th	4	9	31	40	2	91
U	<1	<1	9	17	<1	30

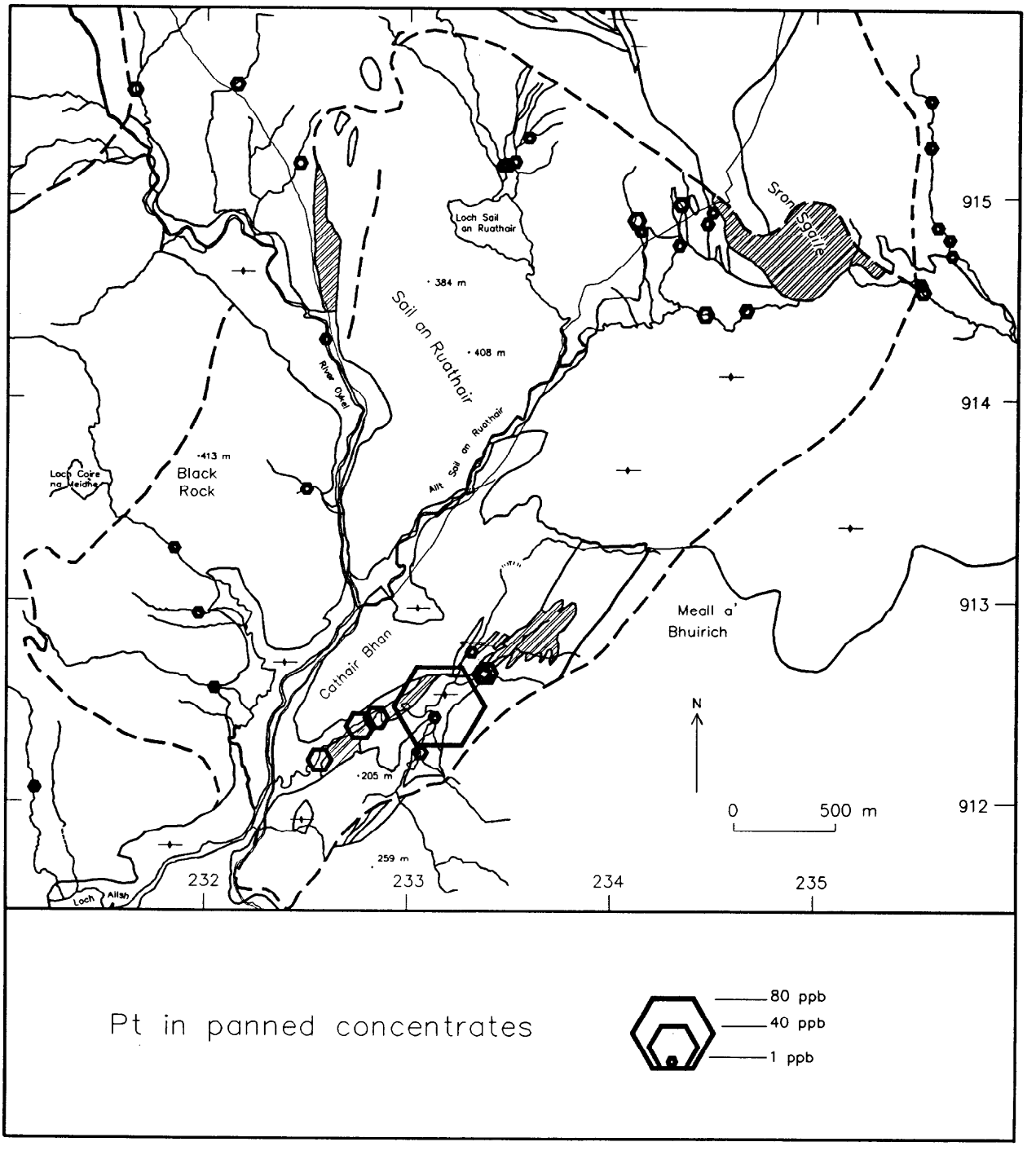

Figure 5 Distribution of platinum in panned concentrates

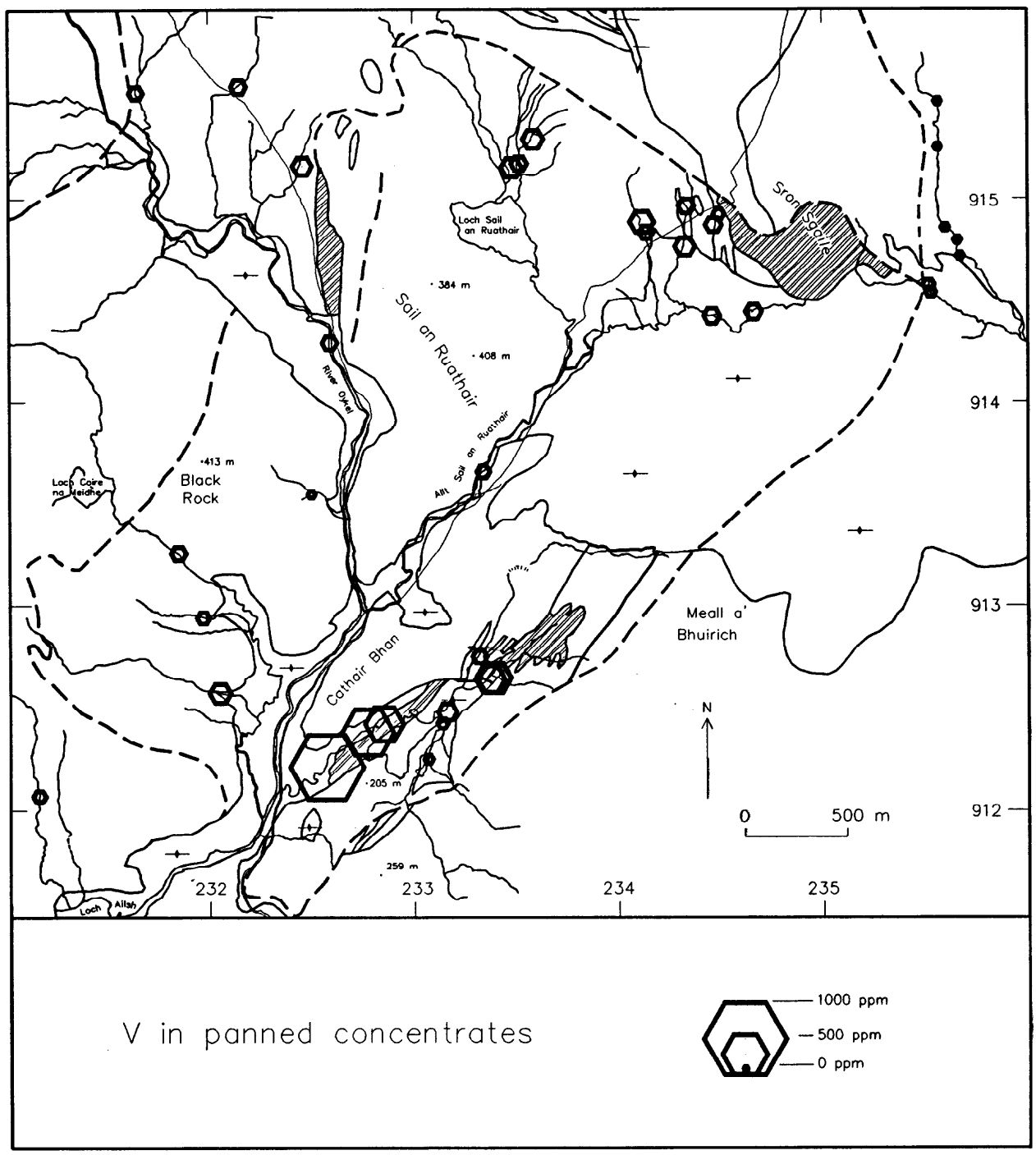

Figure 6 Distribution of vanadium in panned concentrates

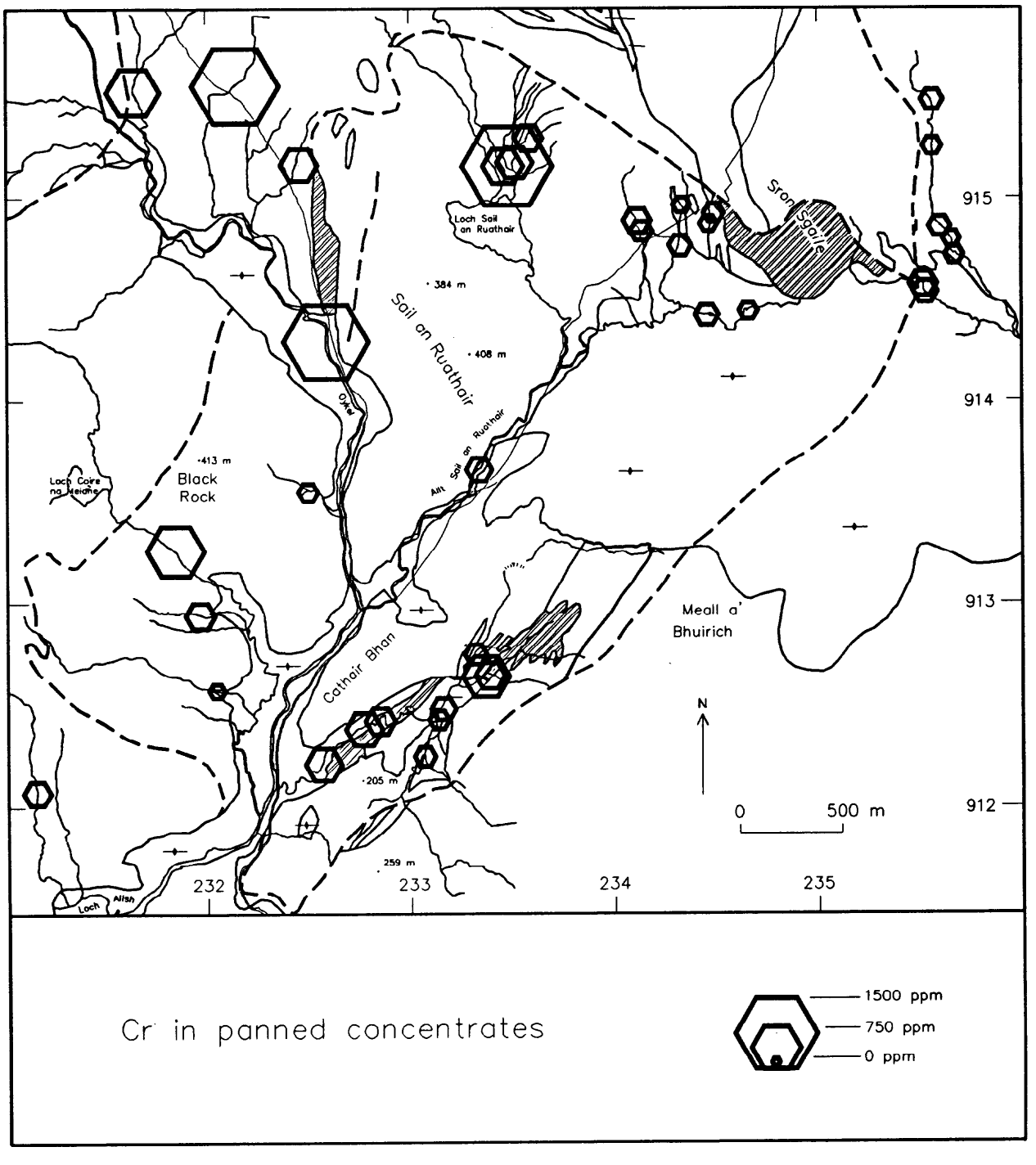

Figure 7 Distribution of chromium in panned concentrates

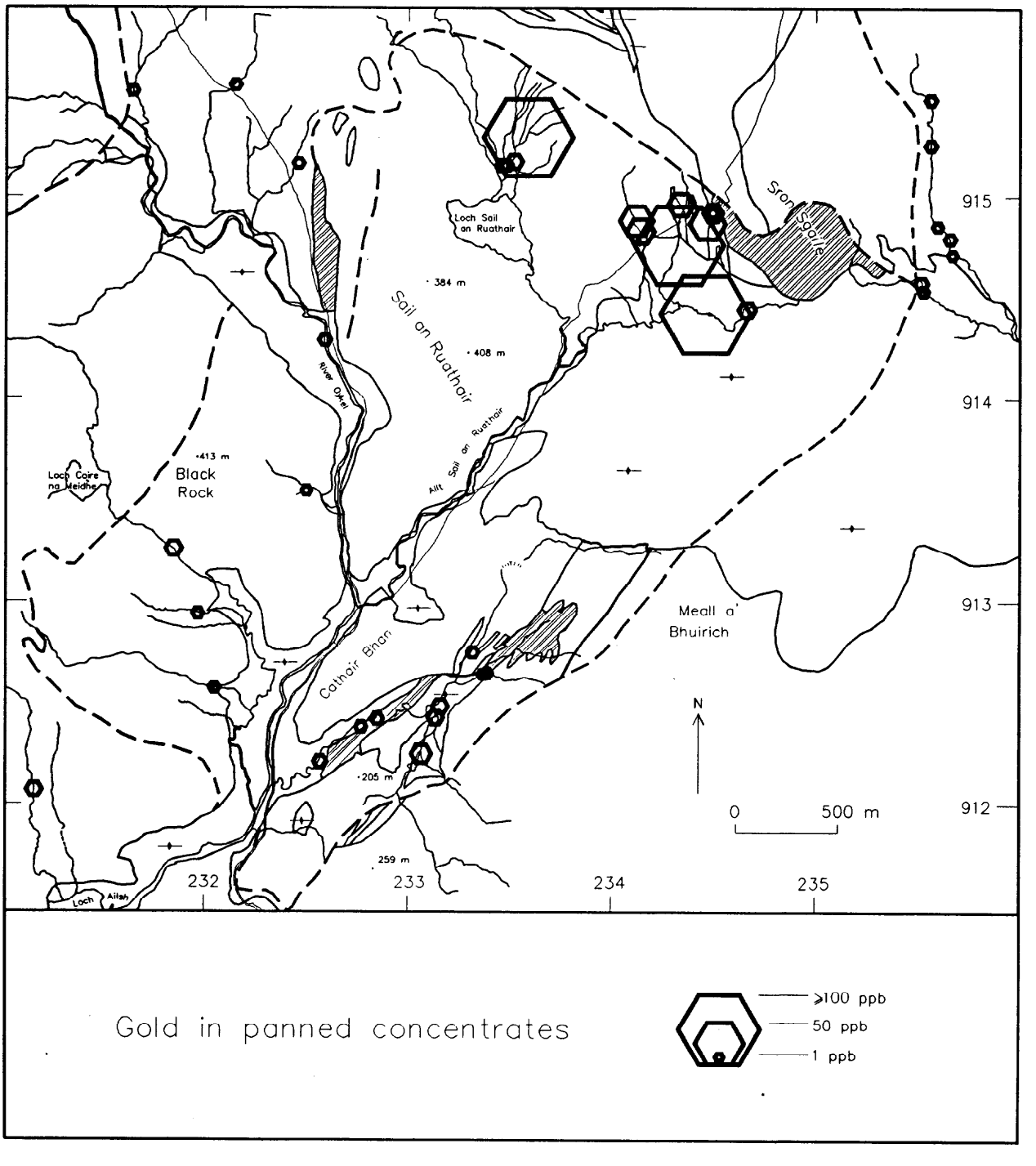

Figure 8 Distribution of gold in panned concentrates

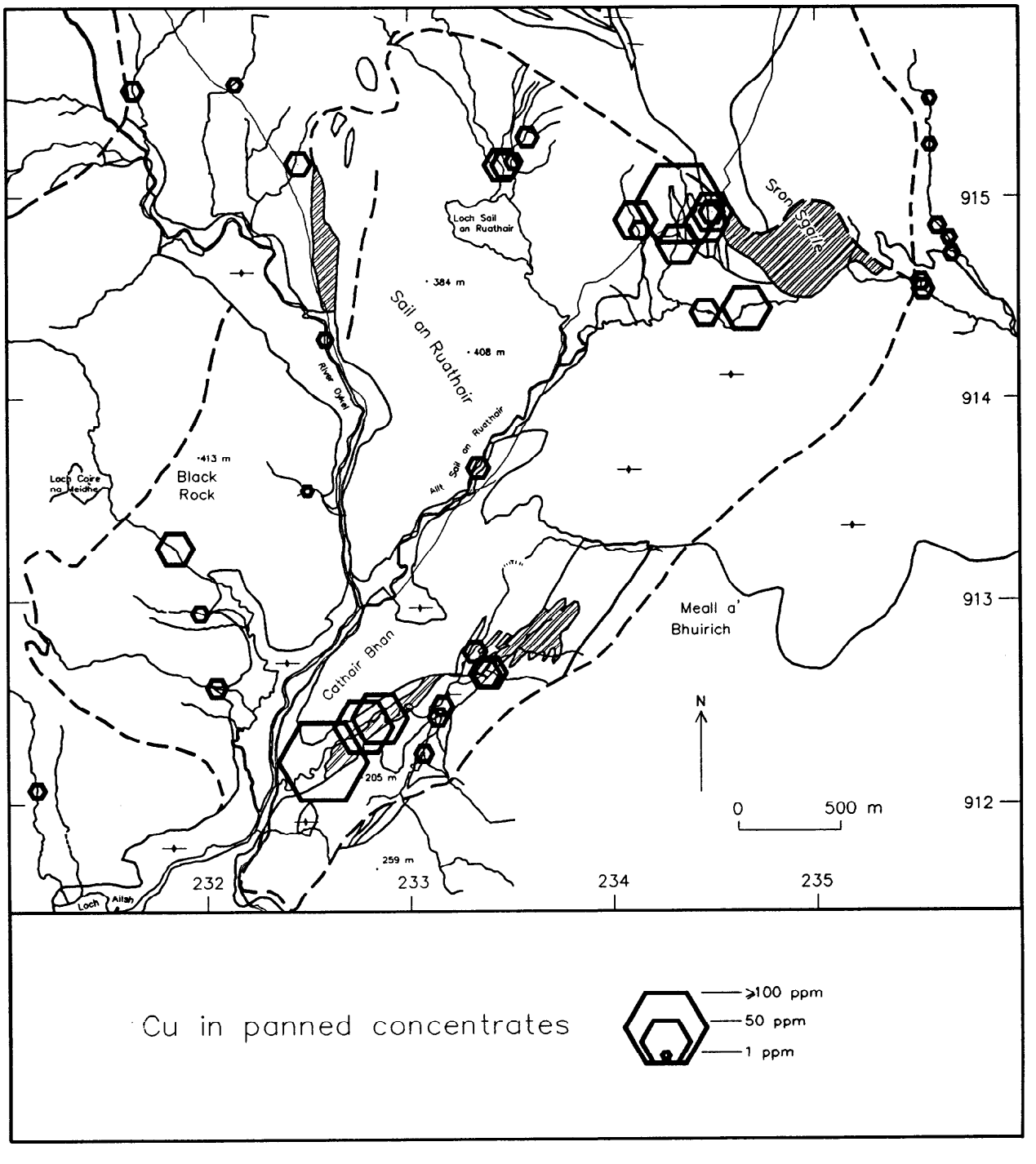

Figure 9 Distribution of copper in panned concentrates

Table 2 Summary statistics for stream sediment samples
N=42 for all elements except Bi, Th and U (19). Values in ppm unless stated.

Variable	25%	Median	75%	90%	Minimum	Maximum
Au (ppb)	14	30	75	319	2	553
Pt (ppb)	1	3	11	25	1	859
Pd (ppb)	2	3	5	12	2	43
Rh (ppb)	2	2	2	3	2	4
Ca	16300	27150	34075	54050	2900	63000
Ti	3485	4395	5598	6561	2400	9380
V	111	152	180	276	58	309
Cr	228	338	558	1335	73	2534
Mn	1610	2745	5140	12844	1110	24890
Fe	49200	63500	85775	101440	26500	133400
Co	20	32	44	56	13	84
Ni	28	52	118	166	13	473
Cu	16	40	78	155	6	874
Zn	62	103	140	199	29	285
Rb	20	26	44	85	10	119
Sr	285	445	595	703	136	868
Y	14	19	23	28	8	35
Zr	251	304	439	532	132	1175
Nb	8	12	15	17	6	21
Ag	<1	1	3	4	<1	6
Sb	<1	<1	<1	2	<1	4
Ba	431	533	766	1205	213	2386
La	31	47	71	87	19	850
Ce	48	78	126	165	20	1108
Pb	22	50	102	129	12	178
Bi	<1	3	2	2	<1	131
Th	7	10	15	16	5	22
U	<1	<1	10	26	<1	3

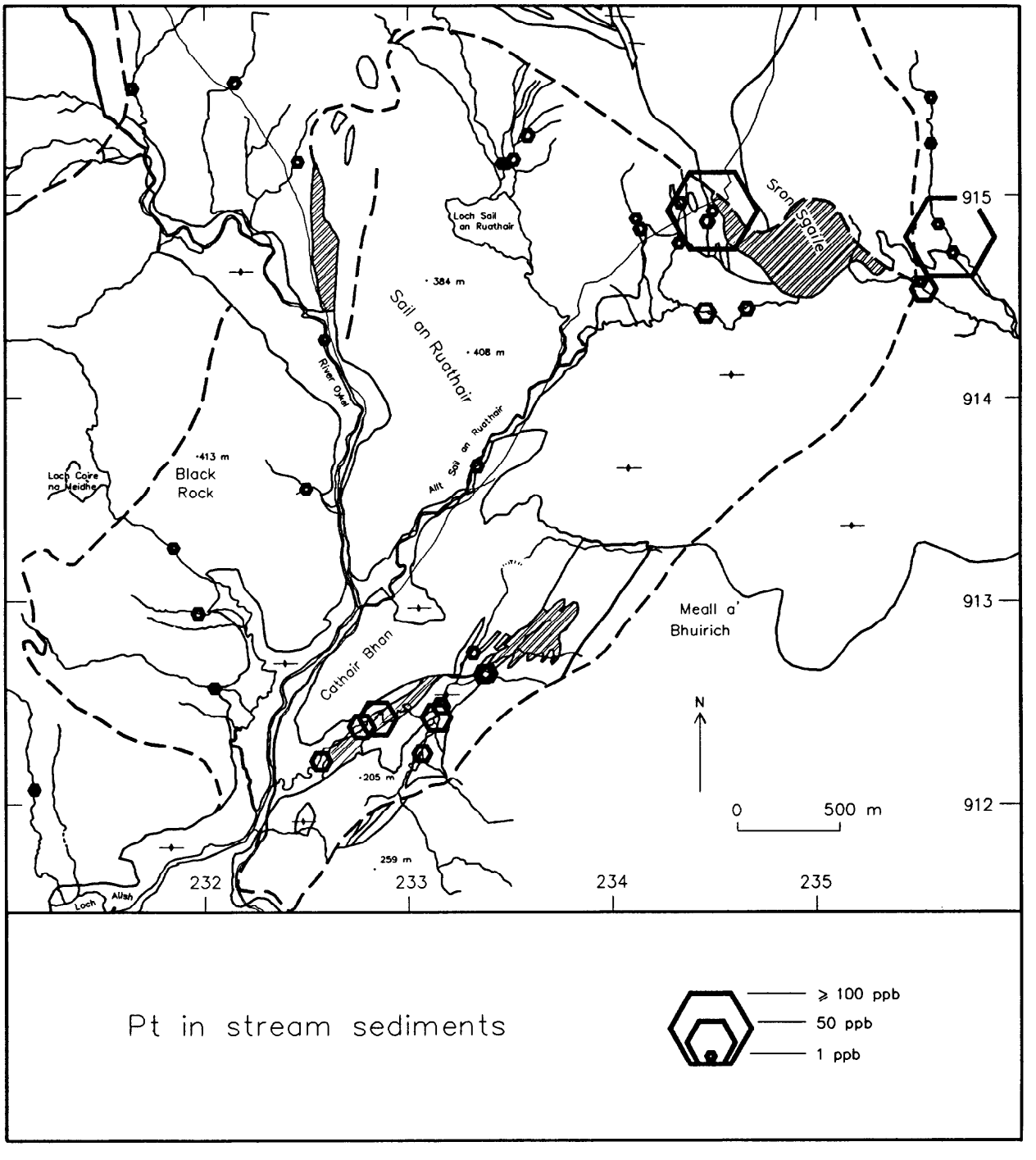

Figure 10 Distribution of platinum in stream sediments

The highest Pd value (Figure 11) was from the Cathair Bhan catchment (43 ppb), with attendant enrichment in Pt (36 ppb), Au (36 ppb) and Cu (874 ppm). The second highest Pd value (30 ppb) was from the Sron Sgaile area, which also contained enhanced Au (227 ppb) and slightly elevated Pt (13 ppb).

The strong chalcophile affinity of Pd is indicated by its correlation with Cu (0.59), significant at the 99.9% confidence level. There are also close correlations, significant at the 99.9% confidence level, between Pd and Ca (0.65), V (0.64), La (0.62) and Ce (0.63).

Nine of the twelve samples from the Allt Cathair Bhan catchment are enriched in Au, with concentrations between 20 and 507 ppb (Figure 12). Elevated Au levels also occur in two other parts of the Complex. Values of 553 ppb and 168 ppb were obtained from streams south of Black Rock [231 913], although these samples show no enrichment in the PGE. In the northern part of the Complex, elevated Au levels are found over an area stretching westwards from Sron Sgail (432 ppb) to the headwaters of Loch Sail an Ruathair (73 and 49 ppb). The samples from the second named locality show no significant enrichment in the PGE, and the area is outside any mapped mafic or ultramafic rocks.

Discussion

Levels of the PGE are generally higher in wet screened -100 mesh stream sediments than in panned concentrates. In both sample media there are highly significant Spearman Rank correlation coefficients between the PGE and Cu. The values suggest that Pd is more closely related to Cu than Pt.

In general Pt displays a stronger siderophile affinity than Pd. However, the close statistical association between Pd, Ca, V, La and Ce in stream sediments and Pd, Ca and V in panned concentrates may indicate an association between Pd and rocks rich in interstitial minerals such as apatite or magnetite. The association with the REE in the fine fraction suggests a possible association with REE-bearing carbonates or silicates.

The highest levels of Au occur in the northern part of the Complex, where 50% of the samples have values in excess of 50 ppb. Values for Pt and Pd in stream sediments and Cu in panned concentrates are also locally enhanced in this area, suggesting there may be a link between these elements. The area with elevated Au contents is more extensive than that of the Sron Sgaile mafic body.

DETAILED SAMPLING

Introduction

The main purpose of these investigations was to characterise the magnitude and extent of PGE anomalies over the Allt Cathair Bhan catchment. Additionally, ground geophysics was used to define

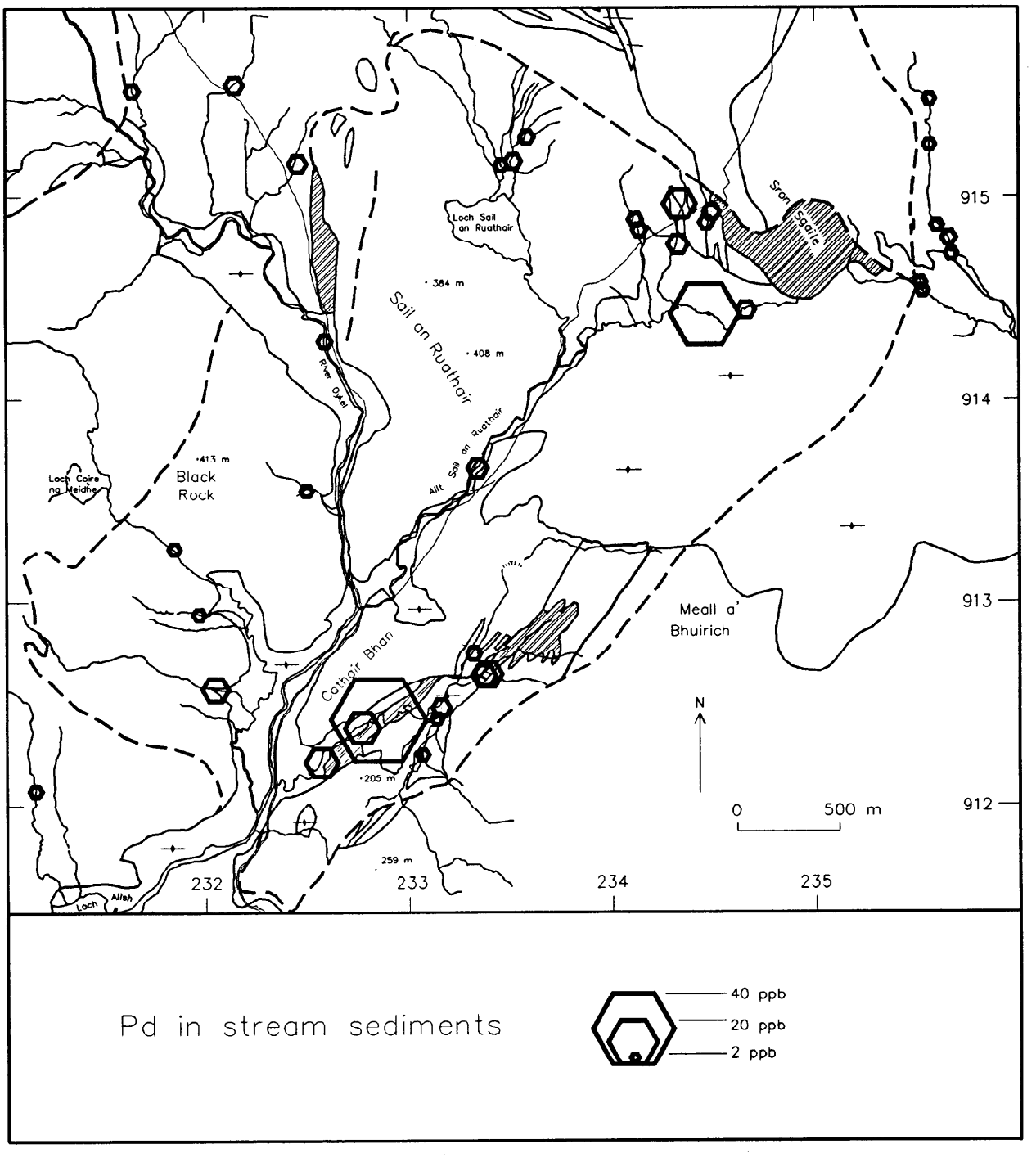

Figure 11 Distribution of palladium in stream sediments

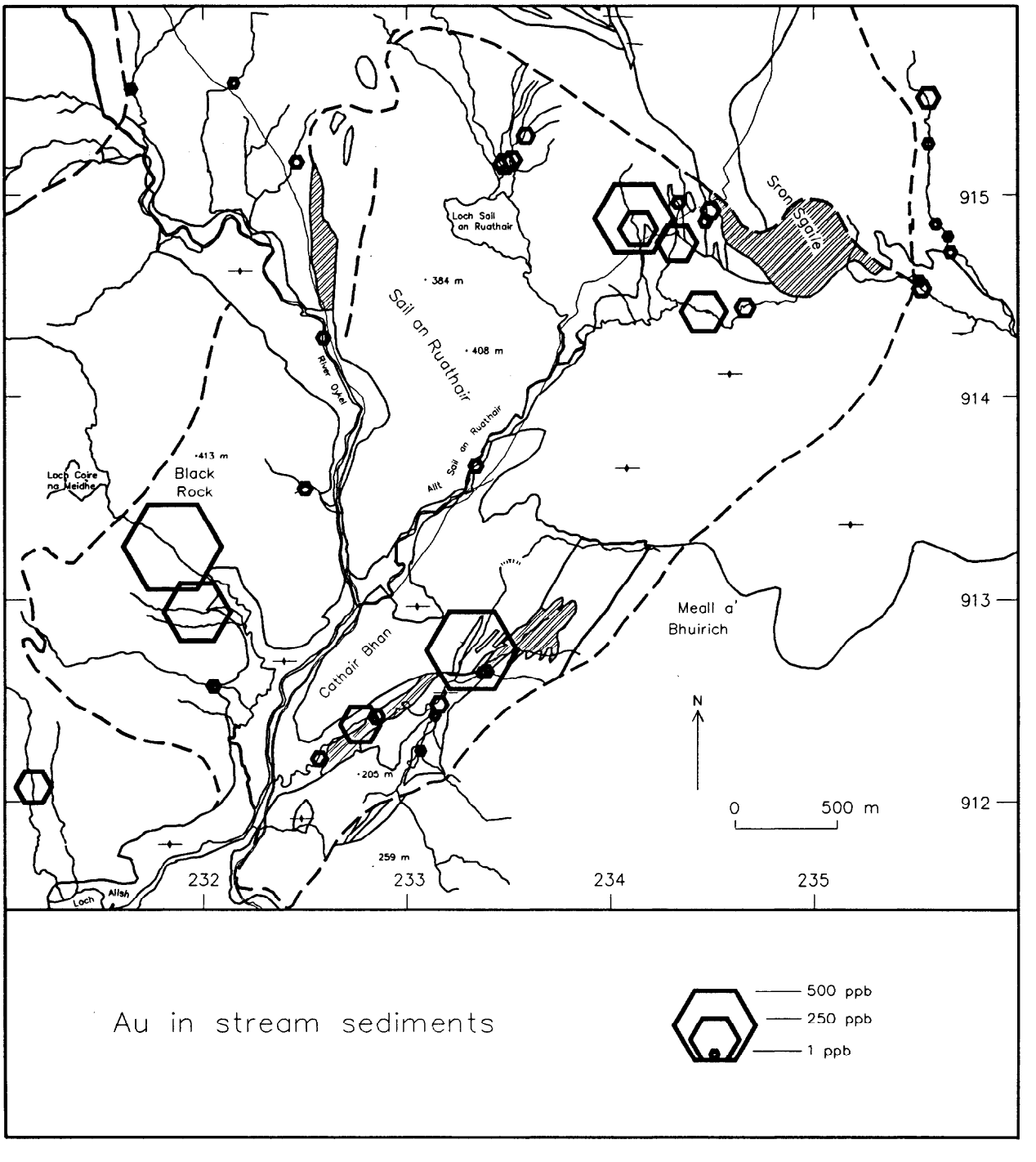

Figure 12 Distribution of gold in stream sediments

the extent and morphology of the Allt Cathair Bhan pyroxenites and to identify any geophysical anomalies which might indicate the presence of concealed PGE-bearing mineralisation.

In order to facilitate geophysical surveying and the accurate location of geochemical overburden sites, a survey grid was laid out using theodolite and tape. Survey traverses were checked by ground measurement to known mapped points. This verification was necessary because of the highly magnetic nature of the Allt Cathair Bhan pyroxenite which results in compass unreliability over much of the area of interest. Locations were marked with canes at 25 m intervals along traverses.

Overburden sampling

Following the discovery of enhanced PGE levels in drainage and bedrock samples during the reconnaissance phase, a detailed programme of overburden sampling was undertaken in the Allt Cathair Bhan catchment in order to investigate the distribution of these elements over the concealed parts of the body.

Sampling was undertaken using a Cobra percussion drill to explore to rockhead. The generally friable nature of the weathered pyroxenite bedrock facilitated collection of samples of high quality. To ensure consistency of sampling of rockhead material a probing tip was first used on the drill string to ascertain the thickness of the overburden. Sample collection utilised a standard through-flow tube, after first opening out the hole with the probing tool. To ensure collection of a representative sample of adequate size, three or four holes were drilled at each site within a 1 m radius and the samples combined for analysis.

A total of 182 samples was collected along 11 traverses, with the majority of sites spaced at 25 m intervals. Due to the relatively low values of the PGE in the upper Allt Cathair Bhan hornblendite bedrock, established from analyses of rocks collected during the first season of field work, it was decided to concentrate overburden sampling on the middle and lower Allt Cathair Bhan sections. The ground magnetic survey and observations of lithologies derived by Cobra sampling were used to determine the extent of the traverses. Closer-spaced sampling was carried out in an area of variable topography in one part of the lower Allt Cathair Bhan. Generally, overburden thicknesses varied from < 1 m on the ridges which flank the Allt Cathair Bhan valley to a mean of about 3 m over the lower ground. Locally the overburden thickness varies rapidly, reflecting the irregular rockhead surface within lithologically or structurally complex zones.

Penetration with the Cobra drill was restricted to a maximum of 6 m, with the sticky overburden significantly slowing retrieval at this depth. At some sites in the lower Allt Cathair Bhan section rockhead could not be reached and the samples are of uncertain provenance. At a few localities in the central section the presence of thick peat prevented the collection of any sample.

In the laboratory, samples were dried, disaggregated and sieved through 2 mm nylon mesh to remove coarser clasts which were mostly of quartz. In general, the pyroxenite bedrock 'plugs' were readily broken down by disaggregation, thereby producing high-quality samples for analysis. The sieved samples were then milled to -150 microns prior to sub-sampling for analysis.

Samples were analysed for trace elements by XRF on pressed powder pellets and for Pt, Pd, Rh and Au by Acme Analytical of Canada, using lead fire assay of 30 g samples followed by graphite furnace AAS or ICP determination.

Summary statistics for basal overburden samples are presented in Table 3 and Spearman Rank correlation coefficients in Table 4.

The maximum value for Pt of 110 ppb was obtained from a site adjacent the Allt Cathair Bhan. This sample shows minor enrichment in Pd, and a low level of Cu. However, elevated Ba (1455 ppm) and Sr (483 ppm) contents are present. A fragment of bedrock from 4.85 metres depth, incorporated in this sample, is a green-grey medium grained pyroxenite. This site is located at the south-western end of the main Pt overburden anomaly which trends for at least 300 m in a north-easterly direction through the middle Allt Cathair Bhan section (Figure 13). A second smaller group of high Pt values clusters at the south-western tip of the mapped lower Allt Cathair Bhan pyroxenite.

Ni displays a distribution pattern like that of Pt, with both elements generally higher in the central Allt Cathair Bhan section than in the lower section (Figure 13). Co and Fe have comparable distribution patterns, although the contrast between the central section and elsewhere is not as pronounced. The marked decline in Pt levels south of the Allt Cathair Bhan stream is reflected in a similar pattern for Ni, and is believed to mark the transition to limestone bedrock. The high Ni and low Pt levels in the central portion of the three most easterly traverses are consistent with a transition to upper Allt Cathair Bhan hornblendite, which as mentioned above is considered to have low PGE potential.

Supergene upgrading as a result of mineral entrainment is believed to have had little influence on basal overburden samples in the Allt Cathair Bhan catchment. This is indicated by the generally narrow range of analytical values for elements associated with detrital minerals such as zirconium. The interquartile range for Zr is between 115 and 178 ppm, roughly consistent with Zr levels found in pyroxenite bedrock (median value 87 ppm). The distribution pattern for Zr reflects the contrast between pyroxenite and syenite bedrock, with the highest values occurring over syenite at the northern ends of a number of traverses (Figure 14). Ba shows a highly variable distribution pattern in the lower Allt Cathair Bhan section and generally more consistent values in the middle section (Figure 14).

The elements Ti, V, Fe, Co and Ni show moderate positive Spearman Rank correlations with Pt, with correlation coefficients significant at the 99% confidence level. The correlation coefficients between Pt and these elements are all higher than their Pd equivalents, suggesting that Pt is more closely associated with the mafic silicates.

The highest values of Pd (70, 42 and 65 ppb) occur as a group to the north-west of the previousely mapped pyroxenite bodies (Figure 15). Pt levels for the same sites were 55, 13 and 32 ppb respectively and Au levels are also enhanced (19, 9 and 43 ppb). Levels of Cu in this zone are significantly higher than over the remainder of the central Allt Cathair Bhan section, with the highest level (381 ppm), coincident with the highest PGE value. The descriptions of Cobra bedrock plugs and magnetic data confirm the presence of ultramafic bedrock in this area.

Table 3 Summary statistics for basal overburden samples
N = 182 for all elements. Values in ppm unless stated.

Variable	25%	Median	75%	90%	Minimum	Maximum
Au (ppb)	6	9	17	37	1	269
Pt (ppb)	3	6	11	21	1	110
Pd (ppb)	3	6	10	17	2	70
Rh (ppb)	1	2	2	3	1	4
Ca	24800	49800	77250	99460	1100	246100
Ti	2773	3815	5520	7266	70	9920
V	114	163	241	319	5	409
Cr	168	259	392	561	5	2929
Mn	828	1135	1423	1688	140	16640
Fe	38825	50800	68425	83540	2800	109600
Co	20	31	43	54	1	84
Ni	53	82	150	237	<1	577
Cu	49	87	174	246	2	652
Zn	66	84	112	133	4	317
As	1	2	3	5	<1	16
Rb	23	33	45	65	<1	125
Sr	311	419	574	755	70	1557
Y	16	19	25	30	2	37
Zr	115	149	178	217	4	502
Nb	7	9	12	14	2	33
Sb	<1	<1	<1	2	<1	4
Ba	387	645	936	1322	18	4700
La	36	49	64	78	3	183
Ce	76	102	133	161	5	267
Pb	26	40	64	113	2	1724
Th	6	9	12	18	1	112
U	<1	1	3	6	<1	84

Table 4 Spearman Rank correlation coefficients for precious metals in basal overburden samples

Element	Au	Pt	Pd
Ca	-0.259	0.228	0.112
Ti	-0.032	0.435	0.363
V	-0.029	0.477	0.417
Cr	-0.015	0.272	-0.056
Mn	-0.108	0.275	0.139
Fe	-0.038	0.445	0.375
Co	-0.082	0.528	0.317
Ni	-0.074	0.428	0.126
Cu	0.314	0.136	0.544
Zn	0.022	0.388	0.449
As	0.004	-0.213	-0.120
Rb	0.110	0.022	0.086
Sr	0.178	-0.203	0.017
Y	0.061	0.271	0.218
Zr	0.179	-0.273	-0.177
Nb	0.139	0.049	-0.039
Ba	0.031	-0.003	-0.035
Sb	-0.094	-0.055	-0.097
La	0.088	0.105	0.194
Ce	0.045	0.226	0.248
Pb	0.250	-0.095	0.055
Th	0.167	-0.181	-0.190
U	0.026	0.118	0.045

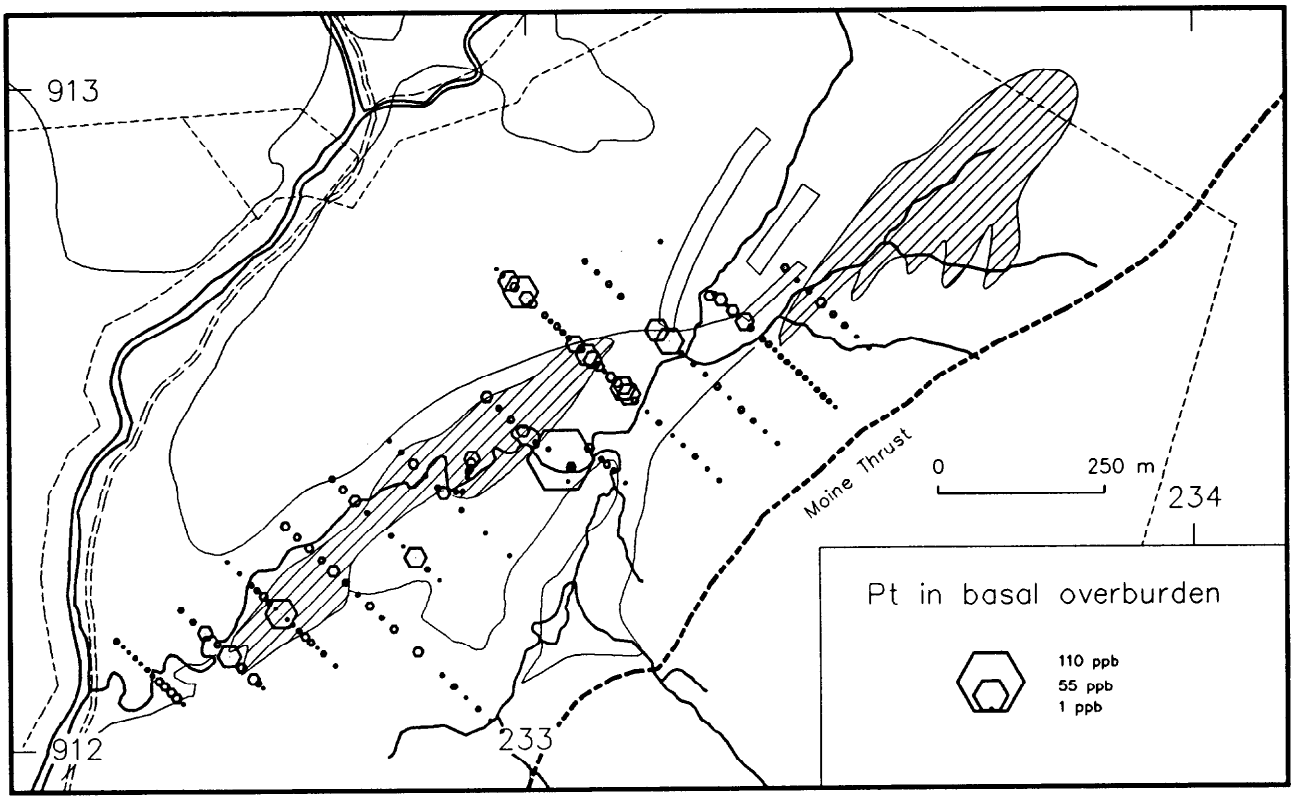

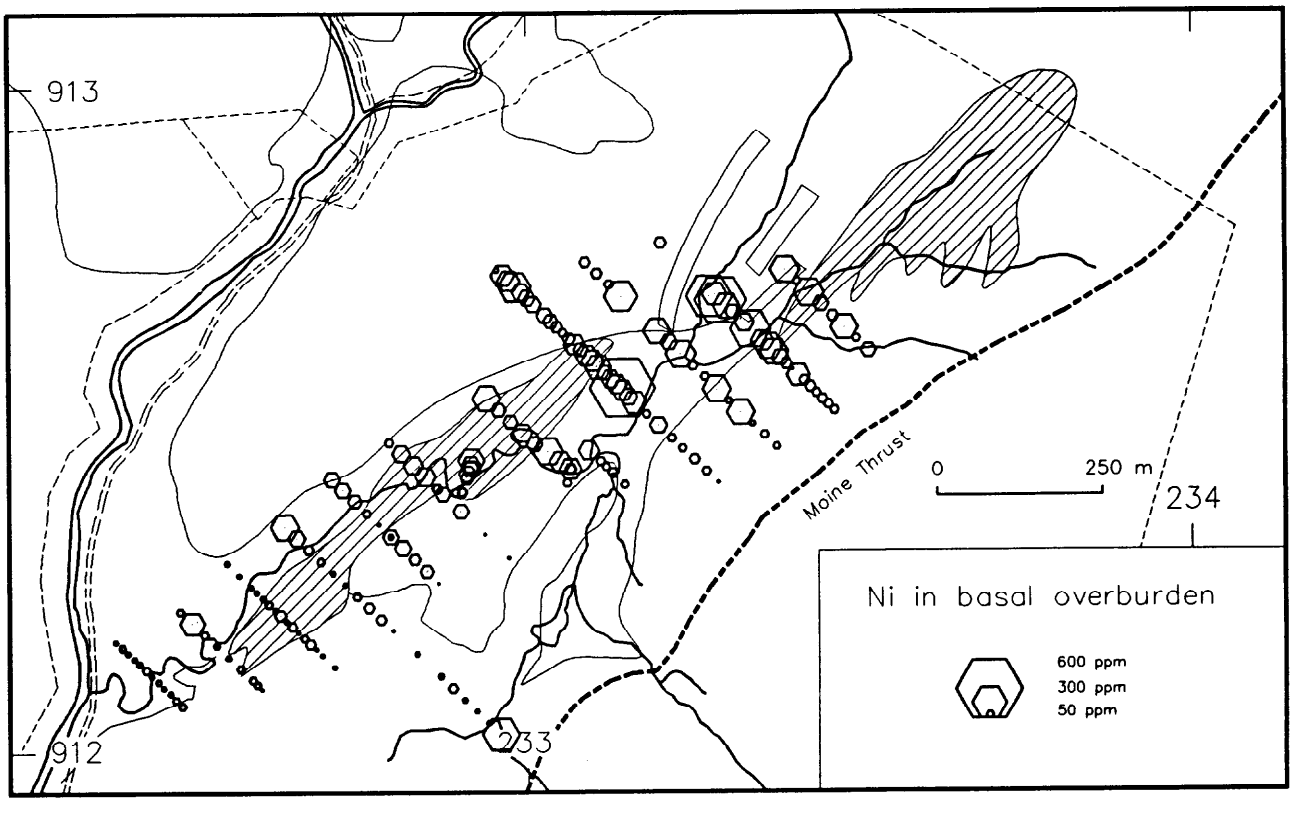

Figure 13 Distribution of platinum and nickel in basal overburden

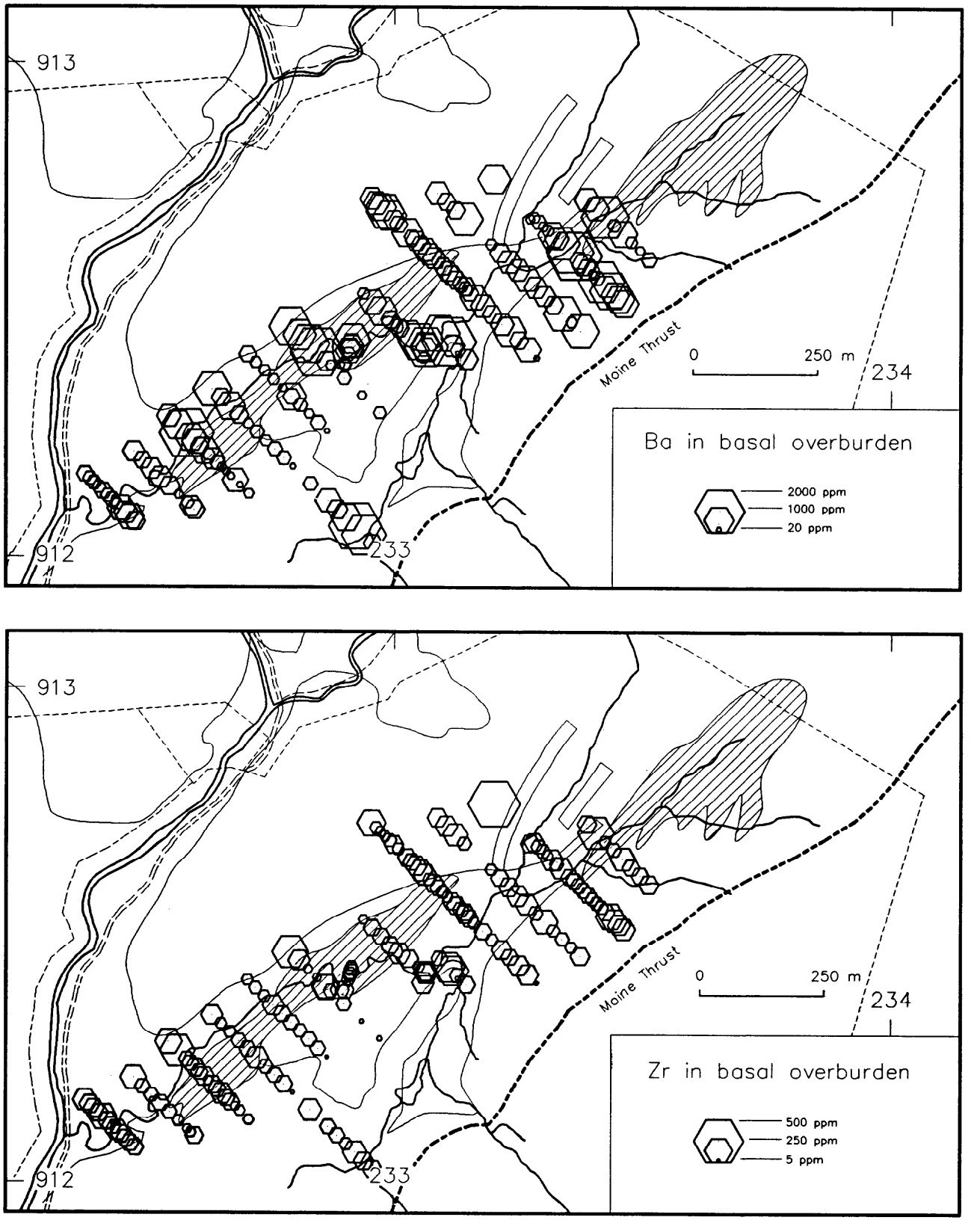

Figure 14 Distribution of barium and zirconium in basal overburden

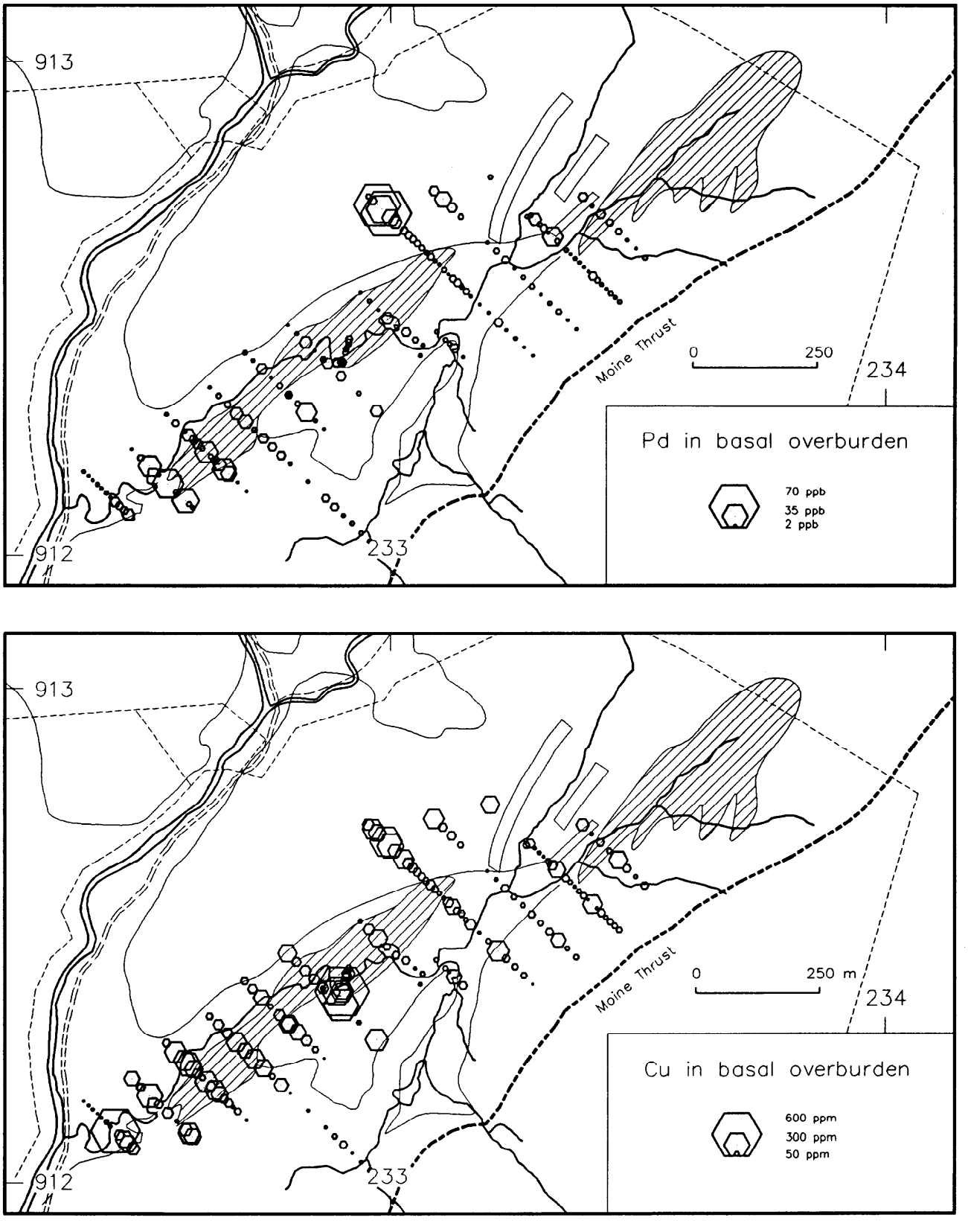

Figure 15 Distribution of palladium and copper in basal overburden

Enhanced levels of Pd occur sporadically throughout the lower Allt Cathair Bhan pyroxenite, with significantly lower values over the adjacent syenite and limestone lithologies. The pronounced cluster of enhanced Pd values at the south-west tip of the lower Allt Cathair Bhan pyroxenite coincides with the Pt anomaly described earlier. However, the broader spatial distribution of Pd in this zone appears to be more closely associated with Au than Pt.

A scatterplot of Pt v Pd indicates the presence of two anomalous groups with markedly different Pt/Pd ratios, shown as hatched and unhatched triangles in Figure 16. The locations of samples belonging to these groups and containing >10 ppb Pt are also shown in Figure 16. A clustering of samples enriched in Pt relative to Pd occurs in the central Allt Cathair Bhan section. By contrast, those samples enriched in Pd relative to Pt are located in the lower Allt Cathair Bhan section and in two zones marginal to the central Allt Cathair Bhan section. Due to the almost complete absence of exposure in the central Allt Cathair Bhan section it was not possible to characterise the bedrock in these zones.

Discussion

The patterns of PGE distribution in basal overburden in the Allt Cathair Bhan catchment reflect variations in the underlying bedrock. Distribution patterns of other elements indicate that only a minimal degree of mineral entrainment has occurred at or near the bedrock interface and that basal overburden samples are representative of the underlying bedrock.

The distribution patterns of the siderophile elements suggests a geochemical zonation of the pyroxenite which could represent horizontal layering. Alternatively, these patterns may reflect zonal rather than layered separation of these elements. The pattern of PGE distribution provided by Pt/Pd ratios indicates that the central Allt Cathair Bhan section contains a zone of enrichment in Pt relative to Pd, approximately 250 m x 100 m in extent.

Two zones containing enhanced Pd, sometimes with Pt, Au and Cu, occur at the south-west margin of the lower Allt Cathair Bhan section and on the northern flank of the central Allt Cathair Bhan section. It is believed from this association that localised upgrading of the PGE has occurred as a result of hydrothermal reworking, possibly along the structurally-controlled margins of the pyroxenite.

Au shows a concentration within the Allt Cathair Bhan section slightly displaced from the main Pt anomaly. The cluster of high values occurs within a linear zone containing intercalated Cambrian sediments and intrusives. The south-west trending stream course dividing the central Allt Cathair Bhan section is believed to define the line of a fault passing through this zone. This fault may have acted as a conduit for Au-bearing fluids.

Rock sampling

Rock samples were collected from 198 localities throughout the Complex. The principal targets were the pyroxenites of the Allt Cathair Bhan catchment and adjacent syenitic lithologies. A number of other rock types were also sampled, notably mylonite zones in pyroxenites, syenite and limestone, skarn rocks of ultramafic origin and a small suite Lower Palaeozoic lithologies, predominantly limestones. Representative rocks from other parts of the Complex were also collected.

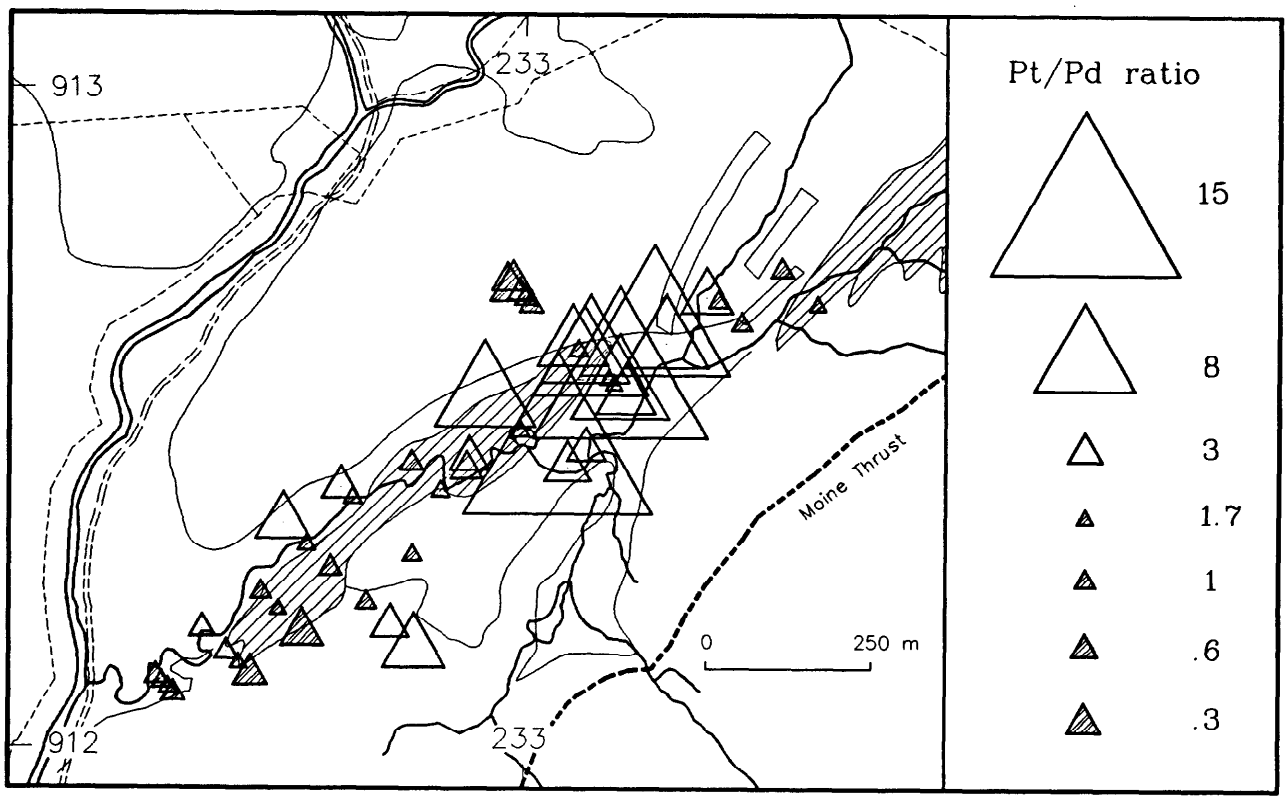

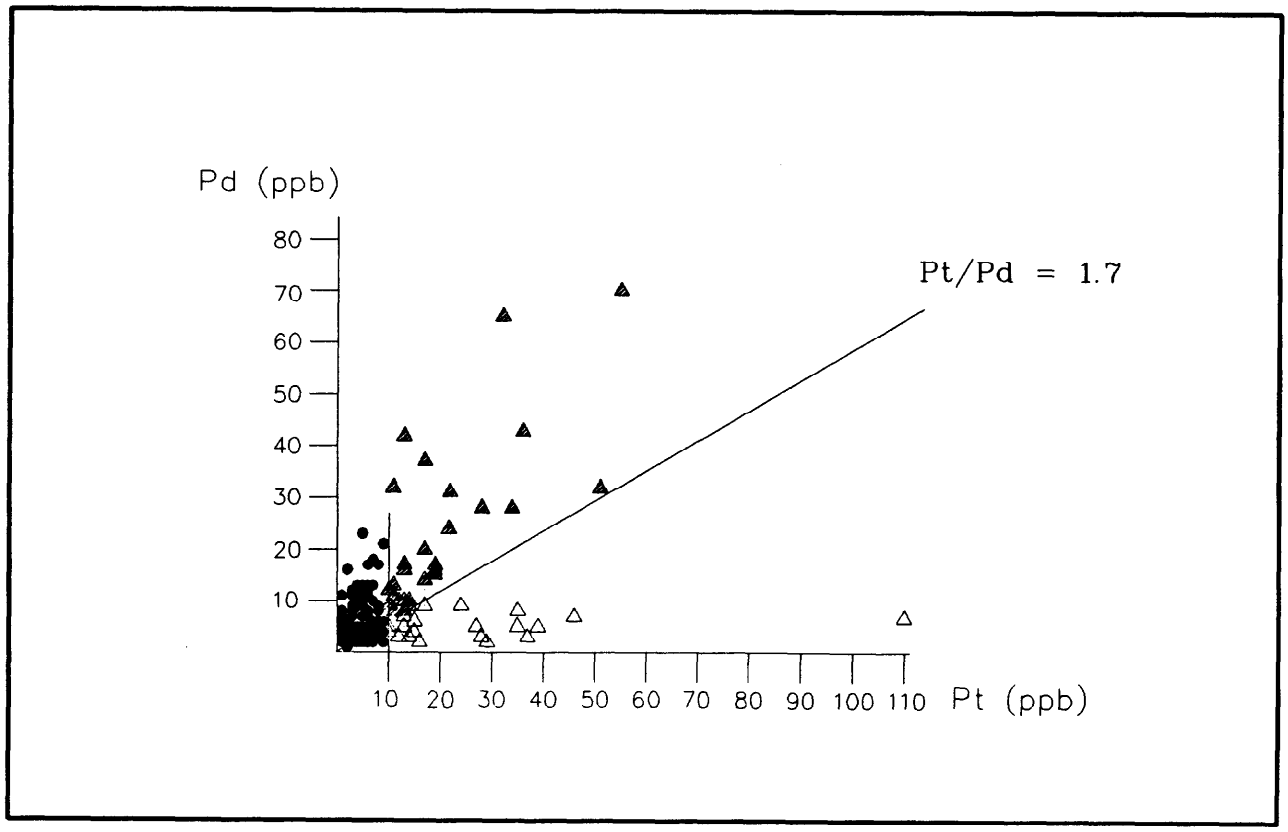

Figure 16 Plot showing Pt/Pd ratios in basal overburden samples

In order to obtain a representative sample for analysis from each outcrop, samples comprised 2-4 kg of unweathered rock taken from several points on a single outcrop. Rock samples were also collected from bedrock exposed by manual pitting.

Analysis was conducted for a range of trace and major elements by BGS and for Pt, Pd, Rh and Au using fire assay and ICP or AAS finish on 30 g samples at Acme, Vancouver.

The results for the main rock types, classified according to lithology, are shown in Tables 5 to 8.

Pyroxenites and hornblendites

Pt and Pd levels are significantly higher in the pyroxenites of the lower Allt Cathair Bhan than in the upper section hornblendites. The highest PGE value from the upper section lithology was 29 ppb. The widespread uniform enrichment in Pt and Pd in pyroxenites is indicated by the comparatively high 25 percentile values for these elements (Table 5).

The maximum values of 130 ppb Pt and 170 ppb Pd were recorded in a foliated biotite pyroxenite from the lower section of the Allt Cathair Bhan [232590 912270]. This sample also contained elevated Ba (2302 ppm) and Sr (791 ppm), with minor enrichment in Sb (2 ppm) and Bi (2 ppm). Low concentrations of Au (10 ppb) and Cu (241 ppm) were reported in this sample. The second highest Pt + Pd value (218 ppb) was derived from a sample with relatively low levels of Ba, Sr, Sb anb Bi, but significantly enriched in Cu. A second sample from the same site (188 ppb Pt + Pd) also has high Cu content.

The concentrations of Pt in the ultramafic rocks correlate in general with those of Pd, but those in the lower section are relatively enriched in Pt and the upper-section in Pd. Pt and Pd show a close correlation with V, Cu and Zn, while Ba is also enriched in several samples containing high Pd.

The highest Au level in a lower Allt Cathair Bhan pyroxenite sample is 65 ppb, and is associated with enhanced Pt (37 ppb), Pd (63 ppb), Cu (1136 ppm) and Sr (6649 ppm). A number of Au-enriched pyroxenites also contain enhanced Cu.

Syenites and pyroxene syenites

The table of summary statistics indicates that median levels of Pt and Pd are close to their lower detection limits (Table 6). Only two syenite samples show significant enrichment >40 ppb Pt+Pd.

The highest combined Pt+Pd value in a syenite is from the River Oykel, 500 m upstream of its confluence with the Allt Cathair Bhan. In this area the S3 type xenocrystic syenite has been mylonitised due to the influence of thrusting at the base of the Cathair Bhan ridge. The analytical results for this sample are 21 ppb Pt, 91 ppb Pd, 33 ppb Au and 1286 ppm Cu. Along with other samples from this zone, there is a pronounced enrichment in Ba (1700 ppm) and Sr (1118 ppm).

The second highest Pt+Pd sample (30 ppb and 13 ppb respectively) was collected from a 30 cm wide, north-south trending vein within the Allt Cathair Bhan pyroxenite [232590 912270]. The sample is a leucosyenite, containing disseminated chalcopyrite up to 0.5 mm in size and coarser blebs of galena, sometimes haloed with chalcopyrite, on joint surfaces. This sample was also enriched in Au, Bi and Cu (52 ppb, 15 ppm and 3390 ppm respectively).

Table 5 Summary statistics for pyroxenite and hornblendite samples
N=68 for all elements except Y and Pb (67) and Bi (44). Values in ppm unless stated.

Variable	25%	Median	75%	90%	Minimum	Maximum
Au (ppb)	3	6	11	23	1	65
Pt (ppb)	7	13	28	79	2	135
Pd (ppb)	8	15	34	67	2	170
Rh (ppb)	2	2	2	3	2	7
Ca	73000	90050	101550	112200	24000	119400
Ti	4745	6215	8305	9230	1920	11960
V	259	327	397	441	88	1186
Cr	98	187	323	611	32	1028
Mn	1300	1495	1635	1890	810	4350
Fe	71750	81750	99100	104600	36600	121500
Co	42	49	58	62	17	75
Ni	98	134	182	309	13	505
Cu	62	191	434	1455	<1	3370
Zn	105	125	152	171	44	588
As	<1	<1	1	2	<1	3
Rb	19	41	53	75	1	116
Sr	218	316	452	782	37	1807
Y	15	21	30	38	7	65
Zr	61	80	108	142	6	247
Nb	6	9	13	16	2	30
Mo	<1	2	3	5	<1	193
Sb	<1	<1	<1	1	<1	2
Ba	361	558	1143	2154	70	6649
La	38	67	113	183	6	860
Ce	80	152	229	342	6	1456
Pb	10	22	55	141	<1	15261
Bi	<1	1	1	2	<1	63
Th	4	6	12	18	1	83
U	2	3	7	10	<1	51

Table 6 Summary statistics for syenites and pyroxene syenite samples
N=78 for all elements except Bi (62). Values in ppm unless stated.

Element	25%	Median	75%	90%	Minimum	Maximum
Au (ppb)	2	4	14	42	1	287
Pt (ppb)	1	2	4	7	1	30
Pd (ppb)	2	2	4	8	2	91
Rh (ppb)	2	2	2	2	2	4
Ca	2800	9300	18600	41900	100	63900
Ti	700	1050	2000	3400	280	6530
V	44	65	143	208	9	373
Cr	95	127	183	346	41	783
Mn	220	410	880	1170	40	1740
Fe	12400	15450	26300	48000	4800	93600
Co	2	4	8	25	<1	52
Ni	2	5	12	49	<1	252
Cu	24	77	196	523	<1	4794
Zn	20	33	57	86	2	135
As	<1	1	2	3	<1	8
Rb	25	39	52	69	<1	262
Sr	369	578	1036	1512	73	3214
Y	8	12	17	24	2	97
Zr	131	231	352	814	22	1356
Nb	12	17	22	33	4	70
Mo	3	5	7	13	<1	221
Sb	<1	<1	1	2	<1	3
Ba	738	1211	1804	2776	140	6047
La	25	41	79	154	7	3239
Ce	56	88	152	245	11	3956
Pb	21	51	109	205	4	3625
Bi	1	1	2	4	<1	61
Th	15	30	45	94	1	244
U	3	9	17	46	<1	175

The element most commonly associated with the PGE in the syenite samples collected is Cu. The correlation of 0.43 between Cu and Pt is significant at the 99% confidence level. Field observations and analytical suggest that the PGE are frequently associated with base-metal sulphides and Au in structurally controlled settings.

Mylonites

Mylonite zones occur in a variety of lithologies, including pyroxenite, syenite and limestone. This is reflected in the wide range of values for most major and trace elements (Table 7). From a total of 13 samples analysed, eight have an undoubted ultramafic affinity. They show variable enrichment in the PGE, up to maximum levels of 26 ppb Pt and 28 ppb Pd. The three highest PGE samples were collected from one locality [232620 912270], and were enriched in Pb (2417 - 3090 ppb), Mo (98 - 125 ppm), Ba (12064 - 32138 ppm) and Bi (33 - 52 ppm).

Most of the mylonite samples show enrichment in Au. Ten samples have Au contents in excess of 10 ppb, with a maximum of 53 ppb.

Galena and chalcopyrite were identified in a number of mylonite samples, although Cu levels are generally low. Two samples containing more than 500 ppm Cu show no significant enrichment in the PGE or Au.

Skarns

A total of 18 skarn samples was collected. Due to their propensity for weathering, the skarns are not exposed, but were identified during basal overburden sampling. They occur in two principal zones - along the northern margin of the Durness Limestone plateau and as sub-outcrop on the southern bank of the Allt Cathair Bhan in its middle section.

The skarns form a mineralogically and geochemically varied suite. Remnant igneous textures may be observed in some samples, whereas others are dominated by the hydrosilicates epidote, chlorite and tremolite. Two skarn samples contained Ca in excess of 135000 ppm, suggesting that assimilation of limestone has occurred locally. Highly variable levels of Fe (16600 - 59600 ppm), V (17 - 249 ppm), Rb (0 - 96 ppm) and Sr (62 - 1319 ppm), are indicative of the variable chemistry of these rocks and suggest a strong influence of magmatic fluids in their formation.

The maximum Pt value reported in skarns was 13 ppb with a median level of 3 ppb (Table 8). Pd levels are slightly higher than Pt, with four values in excess of 12 ppb, and a maximum value of 66 ppb. There is no clear correlation between the PGE and other elements.

A marked enrichment in Au is present in most skarn samples, with nearly 70% containing in excess of 10 ppb. The samples with the highest Au content show an association with Cu, up to a maximum of 1130 ppm. As levels in these samples are also slightly enhanced.

Durness limestone (marble)

Six samples of limestone collected from the Cathair Bhan area contain Ca levels in the range 18 to 26%. These rocks show few signs of sulphide mineralisation, with only one sample slightly enriched in Cu (76 ppm). Two limestone samples show slight enrichment in Pd, with values of 5 and 6 ppb,

Table 7 Summary statistics for mylonite samples
N=13 for all elements except Zr (12) and Bi (10). Values in ppm unless stated.

Variable	25%	Median	75%	90%	Minimum	Maximum
Au (ppb)	1	16	23	40	1	53
Pt (ppb)	1	4	6	19	1	26
Pd (ppb)	2	3	9	28	2	28
Rh (ppb)	2	2	2	2	2	3
Ca	52200	90400	97700	166700	900	320300
Ti	1000	3230	3970	5150	240	7590
V	76	239	324	394	13	408
Cr	60	122	151	410	4	482
Mn	1040	1550	2110	2280	140	2310
Fe	19100	42000	45900	74500	7300	76500
Co	3	18	26	46	2	49
Ni	10	27	62	148	<1	197
Cu	39	59	191	544	5	611
Zn	46	106	121	132	23	154
As	<1	1	2	3	<1	3
Rb	24	46	60	88	7	188
Sr	521	930	2181	3587	141	5332
Y	17	34	43	58	3	66
Zr	43	120	199	246	<1	268
Nb	12	18	21	31	2	57
Mo	4	12	124	132	1	1086
Sb	<1	<1	<1	1	<1	1
Ba	616	2040	12064	32138	314	38529
La	55	146	240	455	26	709
Ce	106	234	570	778	65	1210
Pb	47	682	2417	3090	19	6504
Bi	1	8	33	47	<1	52
Th	9	23	34	48	5	112
U	3	12	17	25	1	41

Table 8 Summary statistics for skarn samples
N = 18 for all elements except Bi (17). Values in ppm unless stated.

Variable	25%	Median	75%	90%	Minimum	Maximum
Au (ppb)	6	19	57	114	1	179
Pt (ppb)	1	3	7	11	1	13
Pd (ppb)	2	5	9	15	2	66
Rh (ppb)	2	2	2	2	2	2
Ca	38600	65050	97100	135900	8700	155200
Ti	1060	1625	4220	5740	210	5900
V	38	72	144	188	17	249
Cr	20	53	96	230	6	545
Mn	770	940	1140	1500	270	1690
Fe	20400	30950	50600	59600	16600	62000
Co	11	16	24	32	7	43
Ni	6	11	28	72	2	227
Cu	72	123	195	538	34	1130
Zn	58	82	102	147	12	284
As	1	3	4	4	<1	8
Rb	4	12	27	86	<1	96
Sr	166	445	630	906	62	1319
Y	7	10	15	26	<1	34
Zr	100	124	192	203	10	211
Nb	5	7	10	11	3	14
Mo	<1	<1	2	4	<1	7
Sb	<1	<1	1	1	<1	2
Ba	390	554	1064	1391	89	1773
La	12	25	35	48	<1	80
Ce	21	51	65	109	5	195
Pb	7	15	26	115	1	133
Bi	<1	<1	1	2	<1	3
Th	2	7	8	16	1	22
U	<1	1	2	5	<1	5

and none contain enhanced levels of Pt. Au contents are close to the minimum detection limit, with a maximum of 4 ppb.

Other Au occurrences

Four samples of epidiorite collected from outcrop in the Sron Sgail body showed no significant enrichment in the PGE or Au. However, a boulder of shonkinite from the adjacent peat-covered low ground [23423 91482], containing abundant pyrite in coarse interstitial aggregates and on joint surfaces, contained elevated Au (287 ppb) and was also slightly enriched in Pt and Pd (7 and 11 ppb). The bedrock source of this sample was not discovered, nor was the source of Pd enrichment in stream sediments from the same area.

Rock samples collected from the Black Rock area show Au concentrations up to 228 ppb. Enrichment occurs within both hybrid rocks [231840 913190] and S3 syenites [232050 912570], in association with interstitial pyrite occurring as blebs up to 1 mm diameter.

Discussion

The pyroxenites of the lower Allt Cathair Bhan section show a uniform low tenor enrichment in the PGE, which may be explained in terms of primary magmatic processes. Higher levels of the PGE are frequently associated with enhanced Au, Cu, Bi, Ba and Sr in various rock types. In contrast, syenites and pyroxene syenites have low median contents of PGE and Au.

The chalcopyrite mineralisation apparent on joint surfaces and within brittle and ductile shears in these rocks is clearly post-magmatic. It is considered that this mineralisation and accompanying elevated precious metal levels are the products of hydrothermal processes.

The elevated Au contents present in shonkinite float in the Sron Sgaile area confirm those found in drainage sampling.

GEOPHYSICS

Introduction

The main geophysical techniques employed at Loch Ailsh were magnetic, VLF magnetic field and induced polarisation (IP).

Within the remit of MRP investigations the main geophysical aspects of the work were the identification of the main structural elements, the definition of the magnetic structure within the Allt Cathair Bhan pyroxenite zone and the examination of an unclosed IP anomaly identified in earlier commercial surveys.

During 1989 an integrated IP-VLF-MAG survey was made over ground north of Loch Ailsh and south-east of the River Oykel, centred around the Allt Cathair Bhan catchment. The preliminary surveys were based on a theodolite-surveyed rectangular grid with an origin at [232852 912962] and a baseline orientation of 050° magnetic (044° grid).

Much of the ground south and east of the grid origin is forested with conifers about 10 years old, leading to considerable problems surveying by line of sight. Furthermore, local compass deviation due to the localised presence of magnetite-rich pyroxenites compounded the surveying problems. In order to bypass these problems lines were surveyed by a combination of theodolite and tape, and caned at intervals of 50 m.

In 1990 the survey area was extended, with the same origin but a profile orientation of 044° grid over the Sron Sgaile area. Additional magnetic and VLF data were collected across this area. Further induced polarisation surveys were made across the ground east of the confluence of the Allt Sail an Ruathair and the River Oykel to help resolve earlier IP results.

Previous investigations

Regional aeromagnetic data across the Loch Ailsh area were collected for BGS in analogue form in 1964, along east-west flight lines spaced approximately 2 km apart. Inspection of these data show a pronounced local anomaly, with values 500 nT above the UK reference field (along a flight line passing through BNG intersection [233 912]).

Parsons (1965a) examined the eastern side of the Loch Ailsh intrusion using detailed magnetic traverses and identified ground anomalies of up to 5000 nT over the pyroxenites in the upper part of the Allt Cathair Bhan catchment.

As part of a base-metal exploration programme, commercial contractors carried out a pole-dipole IP survey on behalf of Noranda Exploration (UK) Ltd across two grids. In the northern grid, lines had been surveyed at a spacing of 800 or 400 feet (metric equivalent: 243 or 122 m). The potential electrode separation P1P2 was maintained at 200 feet (60 m) and data were collected with C1P1 of 600 and 800 feet (182 and 243 m). With these array dimensions depth penetration is nominally about 90 and 120 m respectively. The data were collected with a Scintrex IPR-7 system and the survey identified an IP anomaly across several of these lines. The commercial IP work had also suggested that there was an unclosed IP anomaly trending ENE through [233 913] towards sites in the River Oykel where minor galena and chalcopyrite mineralisation were recorded.

Survey methods

The ground magnetic data (Figure 17) were collected with a Scintrex IGS-2 system configured to observe total magnetic field and the VLF magnetic field sequentially. Magnetic observations were made at paced intervals of 5 or 10 m along surveyed traverse lines flagged every 50 m. Total field observations were made using the backpack-mounted bottle for convenience with the concurrent VLF measurements. This is less accurate than a pole-mounted system but since anomalies were of the order of 5000 nT this was not considered important. All total field magnetic data were related to base station observations made at several sites. The base stations were linked together and corrections for diurnal change have been applied. All corrected observations are related to the minimum observed total magnetic intensity observed at base station 1.

The total field magnetic observations made as part of the current MRP work differ from those made by Parsons (1963) by over 500 nT, as a consequence of the change in the earth's magnetic field. The

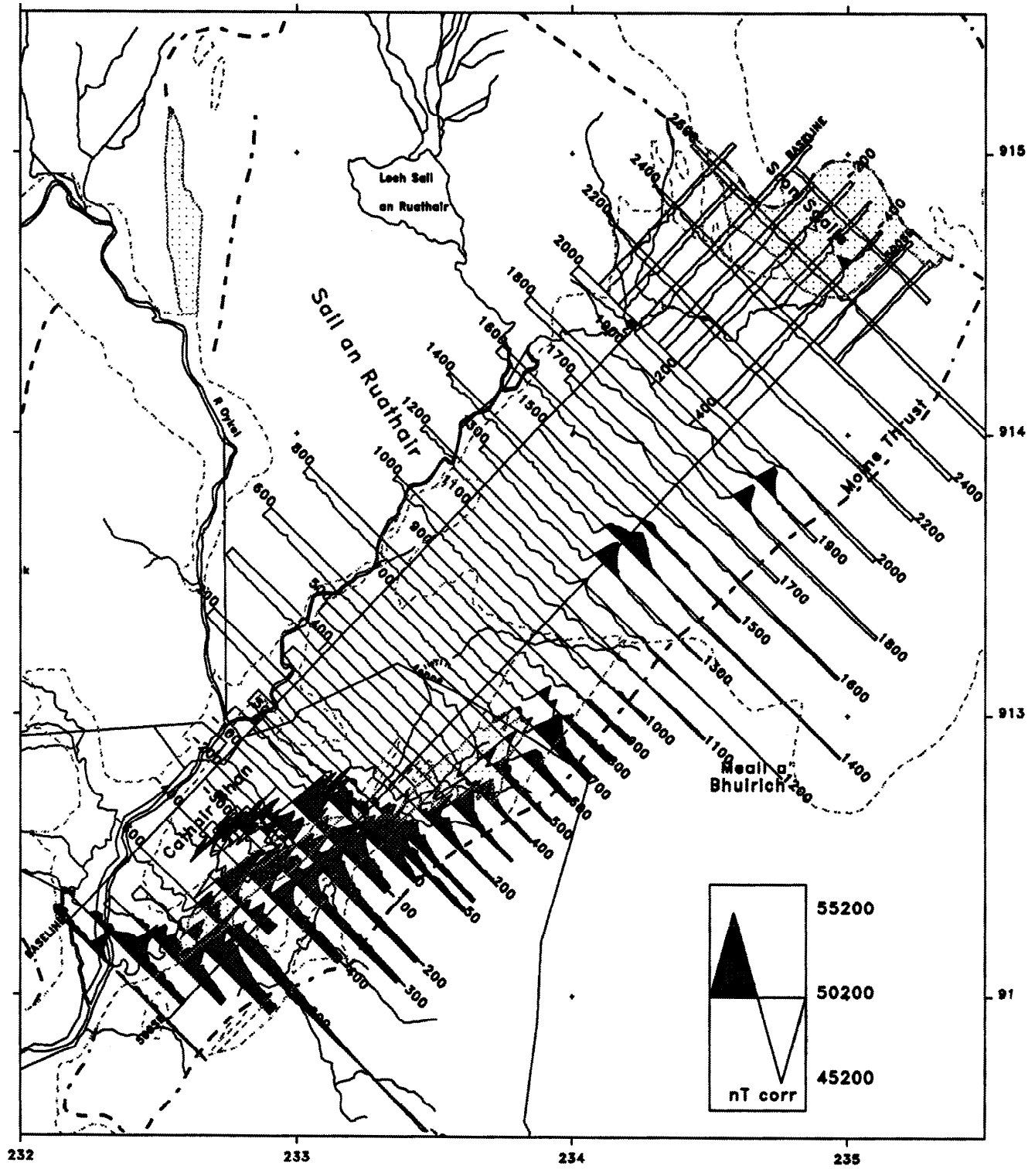

Figure 17 Total field magnetic data, Loch Ailsh. All data corrected for diurnal change and referenced to the minimum field observed at base station 1

calculated field strengths for the BNG point 230 km E, 910 km N for the epochs 1963 and 1989 are 49208 and 49886 nT respectively.

VLF magnetic field data were collected sequentially with the total field magnetic data using the transmitters at either Bordeaux FUO (15.1 kHz) or Rugby GBR (16.0 kHz). Both these stations have similar orientations to the traverse lines so that data collected with either station can be compiled together. All VLF measurements were made using a back-mounted receiver coil and facing towards the transmitter stations.

Magnetic results

Susceptibility measurements were made at several sites for the present survey. Figure 18 shows the locations of sites in the Allt Cathair Bhan catchment, together with an indication of the amplitude of the mean site value. Figure 19 shows a simple histogram of the mean site susceptibility data for the area. A significant percentage of the population has a mean susceptibility above 0.060 SI. The maximum mean measured susceptibility was 0.18 SI.

The magnitude and orientation of the main anomalies is shown in the amplitude trace plot of the magnetic data, relative to a datum of 50200 nT (Figure 17). Total field anomalies range between 48000 and 55000 nT, with recognisable magnetic structures traceable across several lines. The Allt Cathair Bhan pyroxenite is defined by prominent anomalies between lines 980S and 800N. These anomalies can be related to the mapped zones of pyroxenites in the upper and lower Allt Cathair Bhan catchment and to thin bands of pyroxenite along the east side of the Cathair Bhan ridge.

In the lower Allt Cathair Bhan catchment (Figure 20) maximum amplitudes are associated with the south-east edge of the mapped pyroxenite immediately adjacent to the Durness Limestone and in the poorly exposed middle section of the Cathair Bhan valley. Anomaly values in both areas locally exceed 55200 nT. The anomaly extends south-east of the margin of the Lower Palaeozoic rocks. The general zone of higher total magnetic field extends from the outcrop of the lower to the upper pyroxenites with no significant areas of non-magnetic rocks. Across the upper pyroxenite, local magnetic highs occur at the south-east margin of the pyroxenites but the maximum anomaly is usually over Lower Palaeozoic rocks. In simple terms there appear to be two sub-parallel zones of very magnetic pyroxenites. These are more clearly separated in the central part of the Allt Cathair Bhan, along lines 0N and 100S, than to the north or south.

Total field values are generally much higher over the Durness Limestone and Moinian rocks than over the syenite, often by over 1000 nT. This suggests that these rocks are underlain by magnetite-rich pyroxenites for a considerable distance south-east of the surface exposures. Line 600S was extended to about 1400E to examine the shape of the long wavelength anomaly, and indicated a steady fall in anomaly values to the south-east.

The ground magnetic data along the lines 1200N, 1300N, 1400N and 1500N to the south-east of Sail an Ruathair (Figure 21) suggest a discontinuous lens of magnetic material beneath shallow drift. These anomalies of magnitude greater than 1500 nT are likely to be lenses of pyroxenite. Across Sron Sgaile, the magnetic data collected along the secondary grid show amplitudes which are much

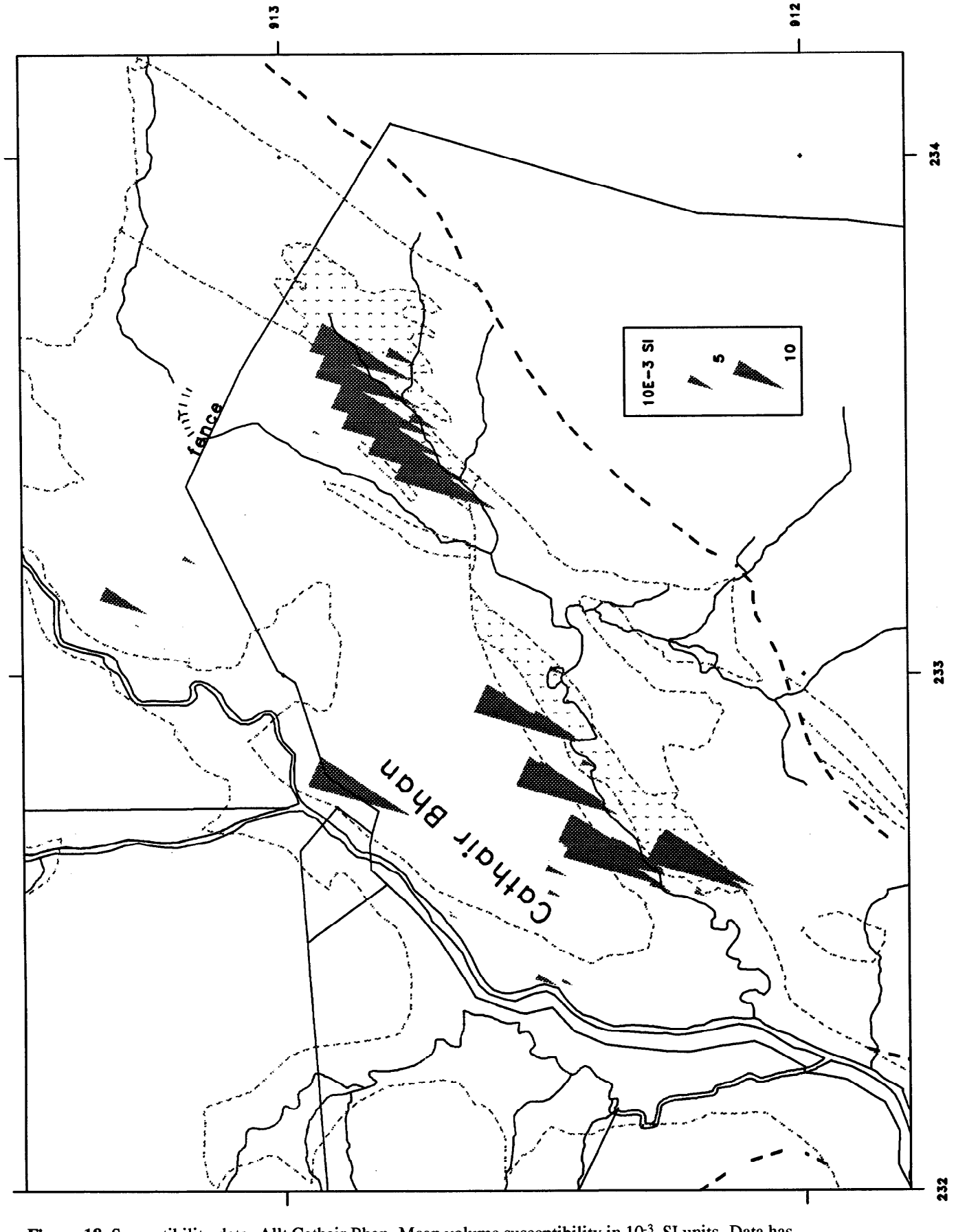

Figure 18 Susceptibility data, Allt Cathair Bhan. Mean volume susceptibility in 10^{-3} SI units. Data has been truncated at 0.020 SI

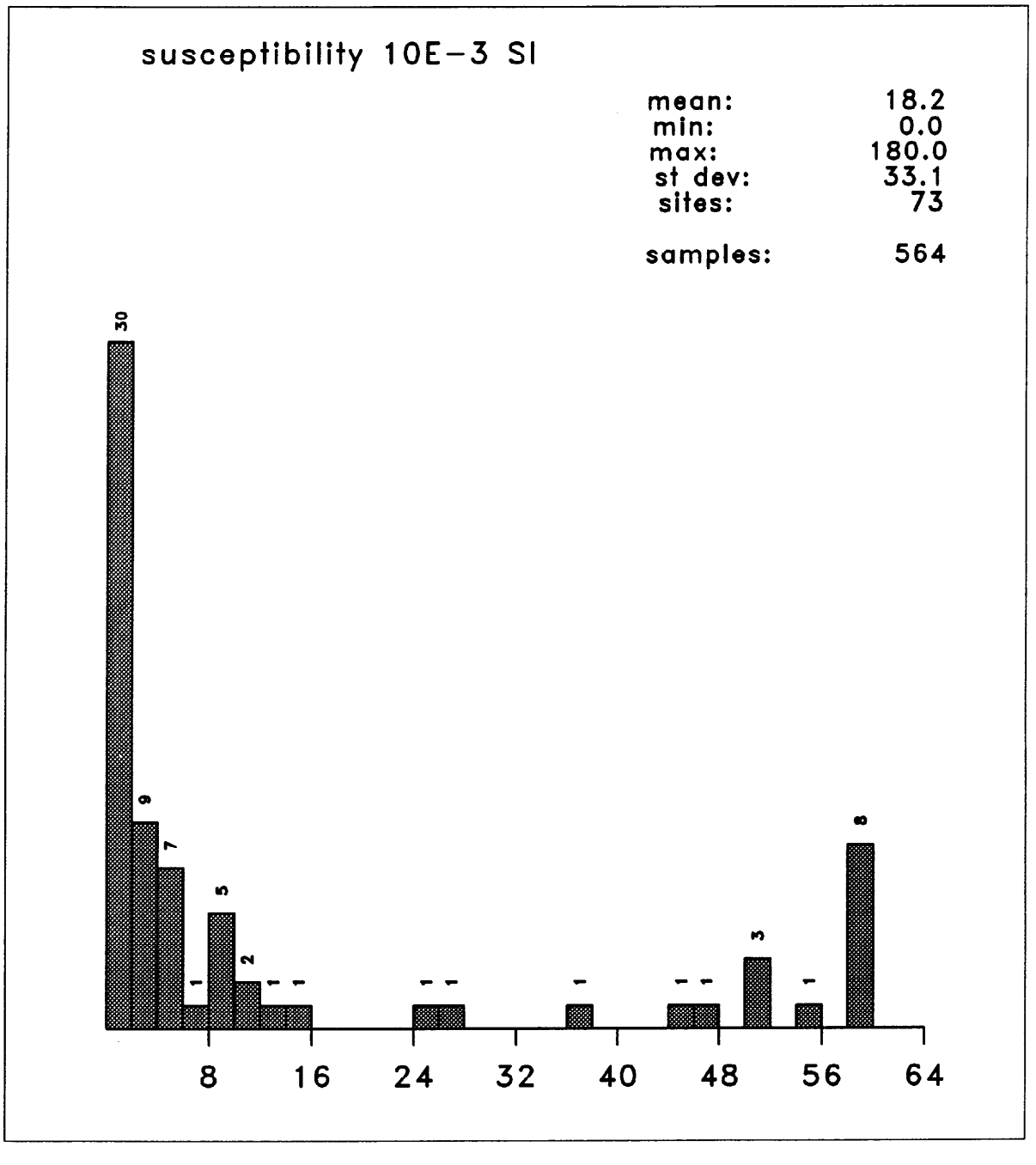

Figure 19 Histogram of magnetic susceptibility, Allt Cathair Bhan. Data truncated at 0.06 SI

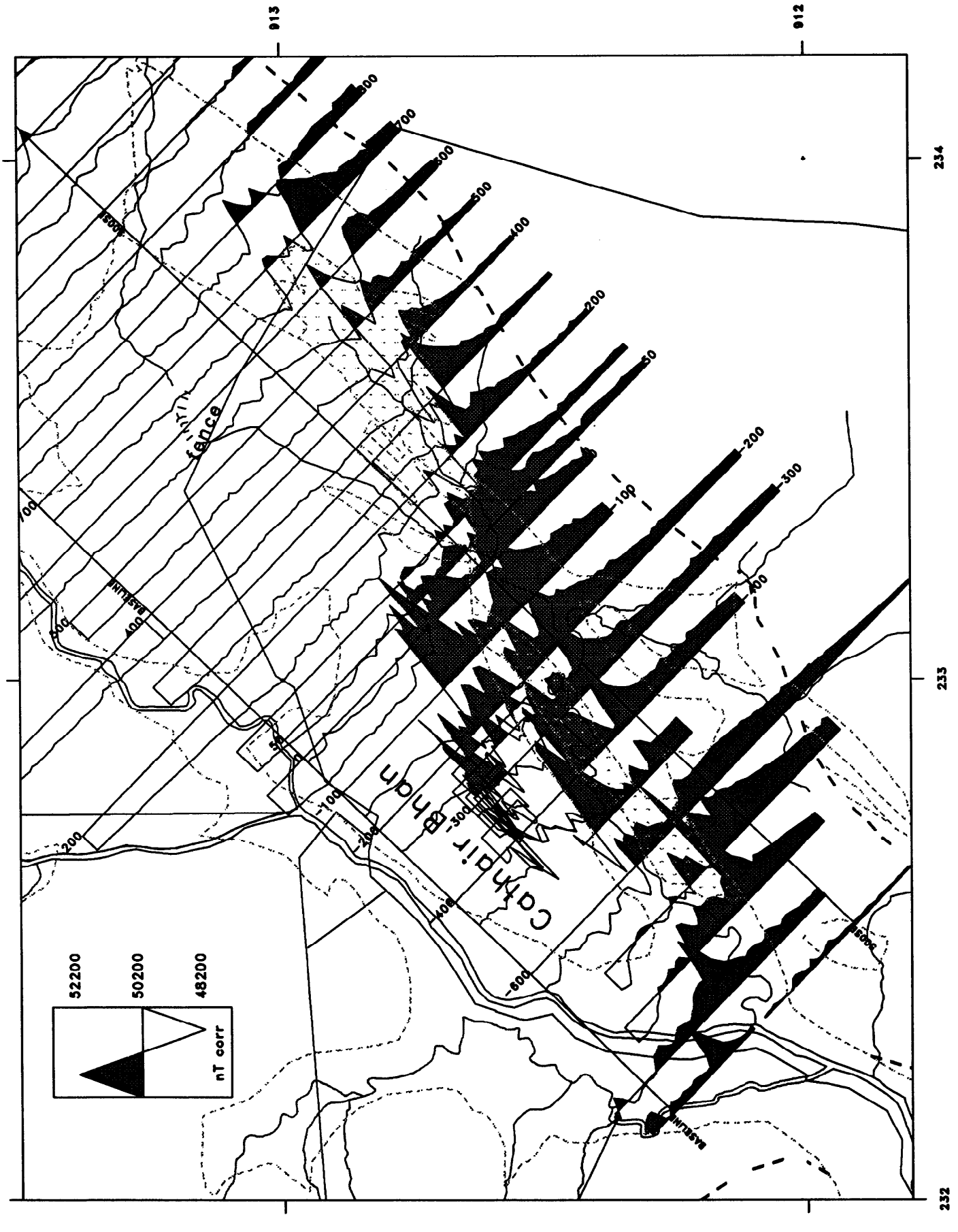

Figure 20 Total field magnetic data, Allt Cathair Bhan. All data corrected for diurnal change and referenced to the minimum field observed at base station 1

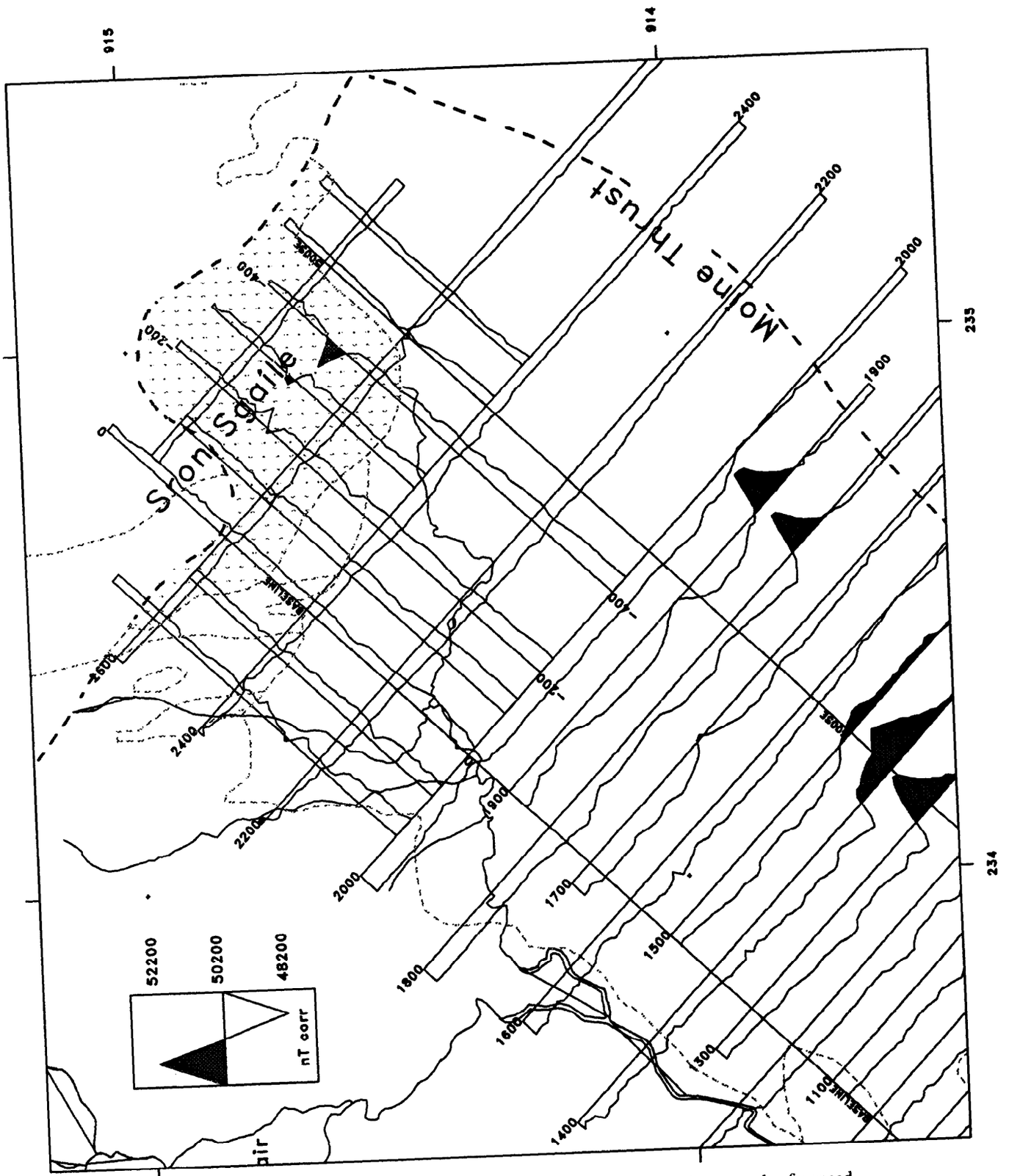

Figure 21 Total field magnetic data, Sron Sgaile. All data corrected for diurnal change and referenced to the minimum field observed at base station 1

lower, with only a few zones with values above 50200 nT. The Sron Sgaile intrusion would appear to be significantly less magnetic than the Allt Cathair Bhan pyroxenites.

Several lines of ground magnetic data have been interpreted using the GRAVMAG package (Pedley, 1991), which is an interactive combined gravity and magnetic modelling program in 2.5D. The lines selected were 600S, 400S, 300N and 700N. The models (Figures 22-25) attempt to show the possible structure and disposition of the main magnetic sources in the sub-surface. Ground magnetic profiles were modelled after diurnal correction and after subtraction of a constant regional field of 49900 nT. This is approximately the International Geomagnetic Reference Field (IGRF) for the point 232 km E, 912 km N for 1990. The observed anomalies can be approximated by sheets of magnetic pyroxenites dipping at about 60-80° to the south-east and up to about 800 m thick. Table 9 lists the properties of the polygons shown in the model profiles.

On line 600S (Figure 22) observed anomalies are lower than on adjacent lines but a long wavelength anomaly with an amplitude above 1000 nT and a maximum over the Durness Limestone has to be modelled as magnetic pyroxenites at depth. Local gradients were occasionally too large (above 5000 nT/m) to be measured using the IGS2-MP4 magnetometer. Such zones indicate extremely magnetic rocks at or very close to the ground surface. Several of the features of the ground profiles require mean volume susceptibilities above 0.1 SI. The apparent dip of structures is estimated at 60-75° to the south-east. The magnetic structures are modelled to depths of about 800 m below Ordnance Datum (OD) although the calculated solution is not very sensitive to the depth of the base of the model.

Line 400S (Figure 23) includes three main zones of magnetic material: a thin zone of pyroxenite within syenite at about 170E, a strong anomaly of amplitude 400 nT between 350-450E and a second strong anomaly at about 500E. These anomalies are all modelled using assuming induced magnetisation and a series of pyroxenites with apparent dips to the south-east of about 80°. Locally, susceptibility must be above 0.15 SI to explain the observed anomalies. Magnetic rocks must occur up to and beneath the Moine Thrust to explain the observed anomalies.

On line 300N (Figure 24) the two main anomalies can be modelled as two lenses of pyroxenite with a mean susceptibility of about 0.1 SI, dipping south east at about 75° and extending to depths of about 800 m. The disposition of these anomalies is consistent with the pyroxenites being included in a thrust sheet beneath the Moine Thrust.

Line 700N (Figure 25) indicates essentially three magnetic anomalies which can be directly modelled as three pyroxenite-rich zones with susceptibilities up to 0.1 SI dipping at about 60° to the south-east.

VLF data

The VLF data are shown in Figure 26 after manual editing of most of the cultural noise. Sections of some lines, with serious cultural interference due to power lines and fences have been removed. The main feature of the VLF data is a large positive in-phase anomaly extending from about line 400N to line 2600N and trending approximately 020°. Figure 27 shows the Fraser filter operator applied to

Table 9 Magnetic susceptibility used in the GRAVMAG model profiles

Polygon No.	Magnetic susceptibility SI			
	600S Fig. 22	400S Fig. 23	300N Fig. 24	700N Fig. 25
1	0.050	0.000	0.000	0.100
2	0.000	0.040	0.050	0.000
3	0.000	0.120	0.100	0.010
4	0.040	0.100	0.100	
5	0.060	0.180	0.005	
6	0.090	0.120	0.100	
7	0.010	0.080	0.050	
8	0.100	0.040	0.005	
9	0.040	0.050		
10	0.010	0.000		
11	0.025			
12	0.130			

All polygons have an assumed half strike length of 10000 km and induced magnetisation in an earth field of 38.5 A/m.

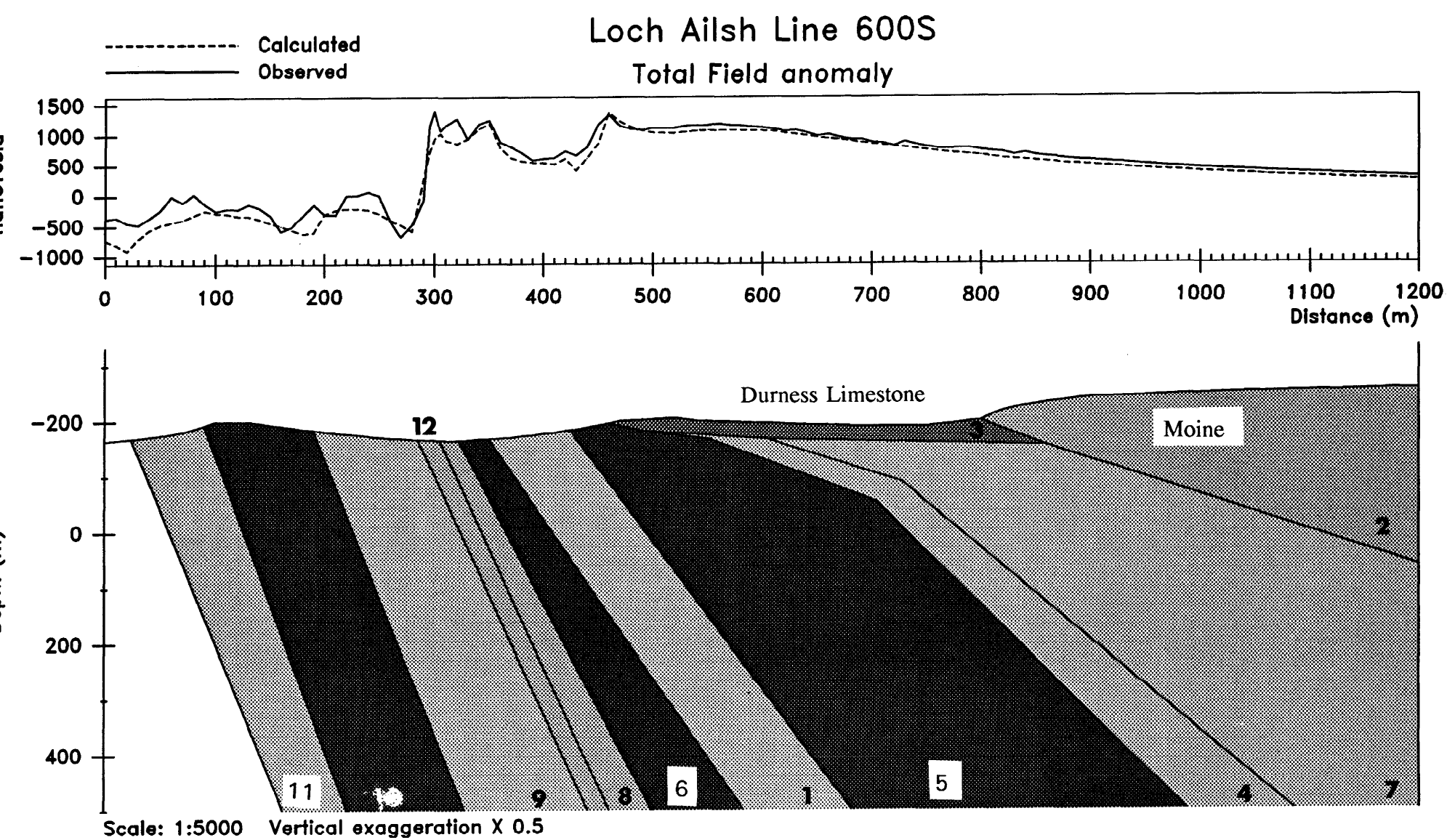

Figure 22 GRAVMAG model of magnetic data Line 600S. Regional datum of 49900 nT removed. Polygon properties listed in Table 9

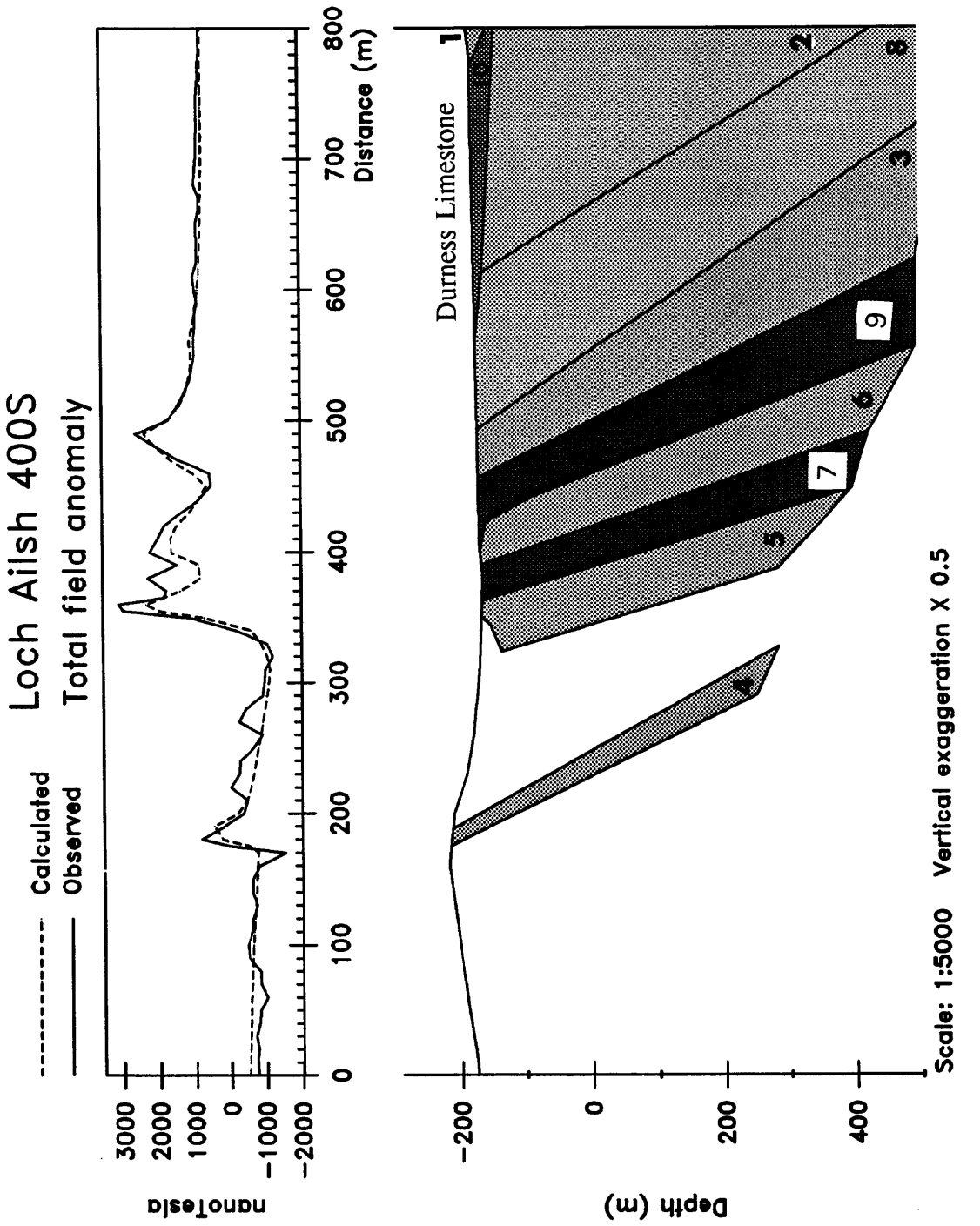

Figure 23 GRAVMAG model of magnetic data Line 400S. Regional datum of 49900 nT removed. Polygon properties listed in Table 9

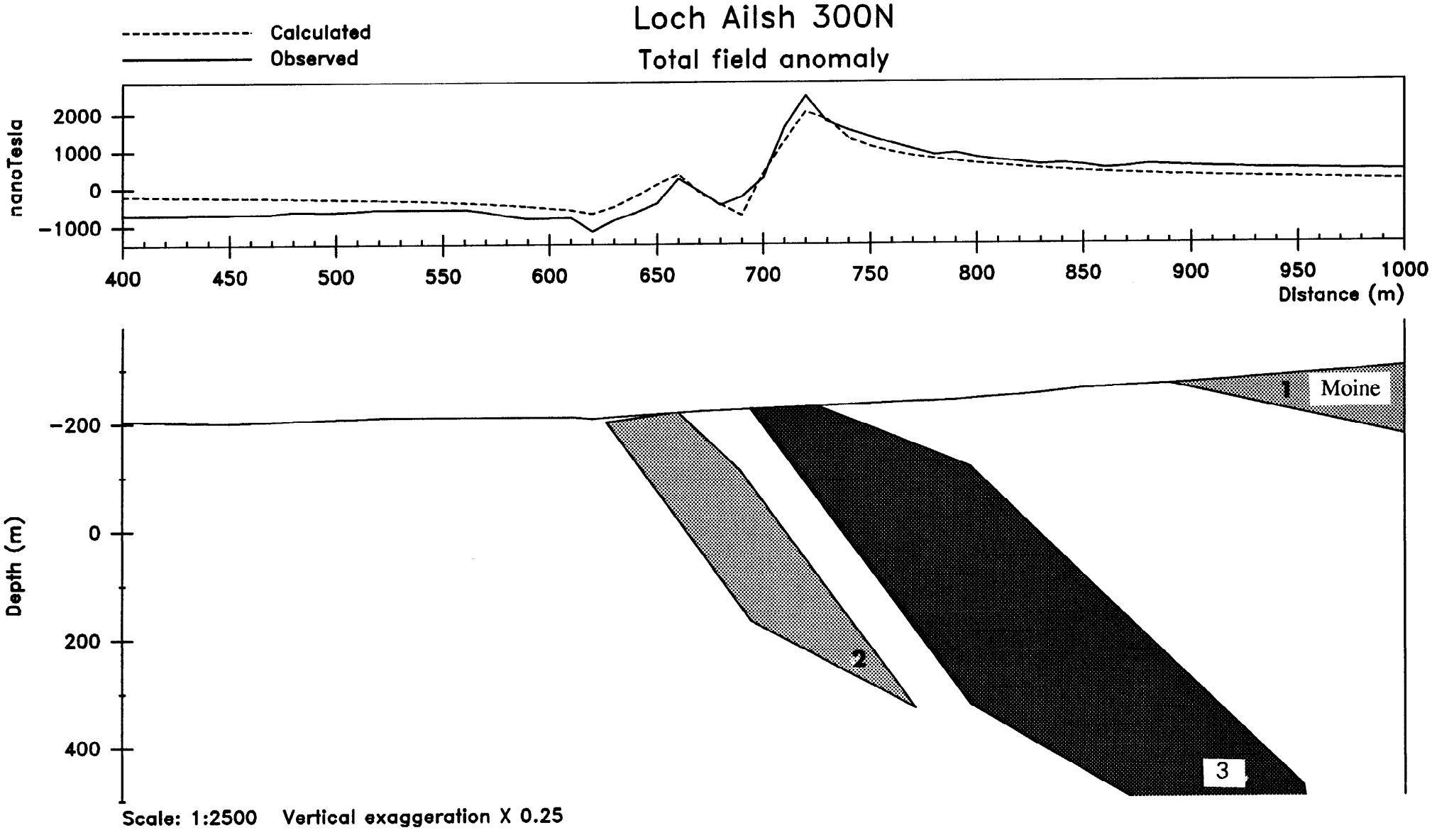

Figure 24 GRAVMAG model of magnetic data Line 300N. Regional datum of 49900 nT removed. Polygon properties listed in Table 9

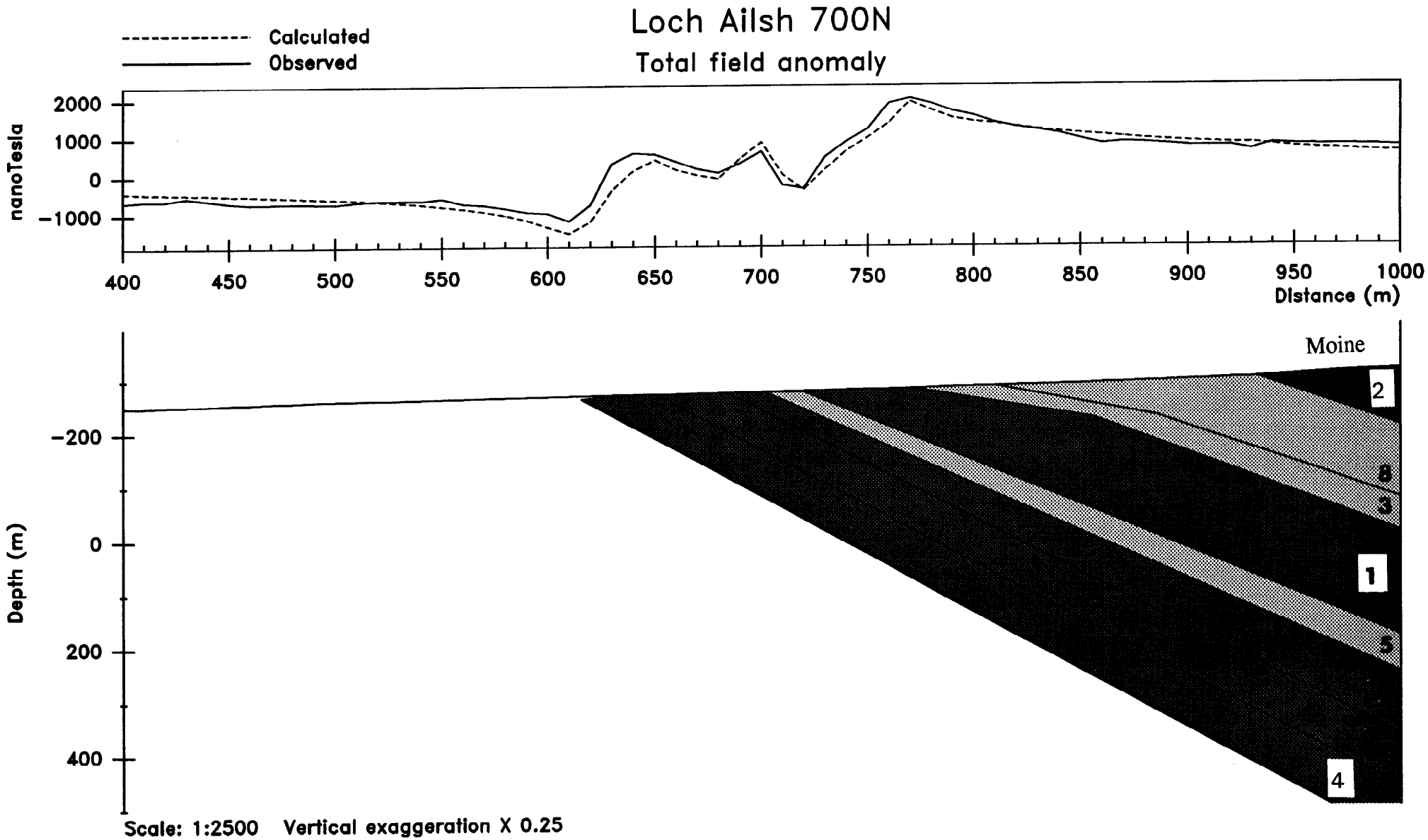

Figure 25 GRAVMAG model of magnetic data Line 700N. Regional datum of 49900 nT removed. Polygon properties listed in Table 9

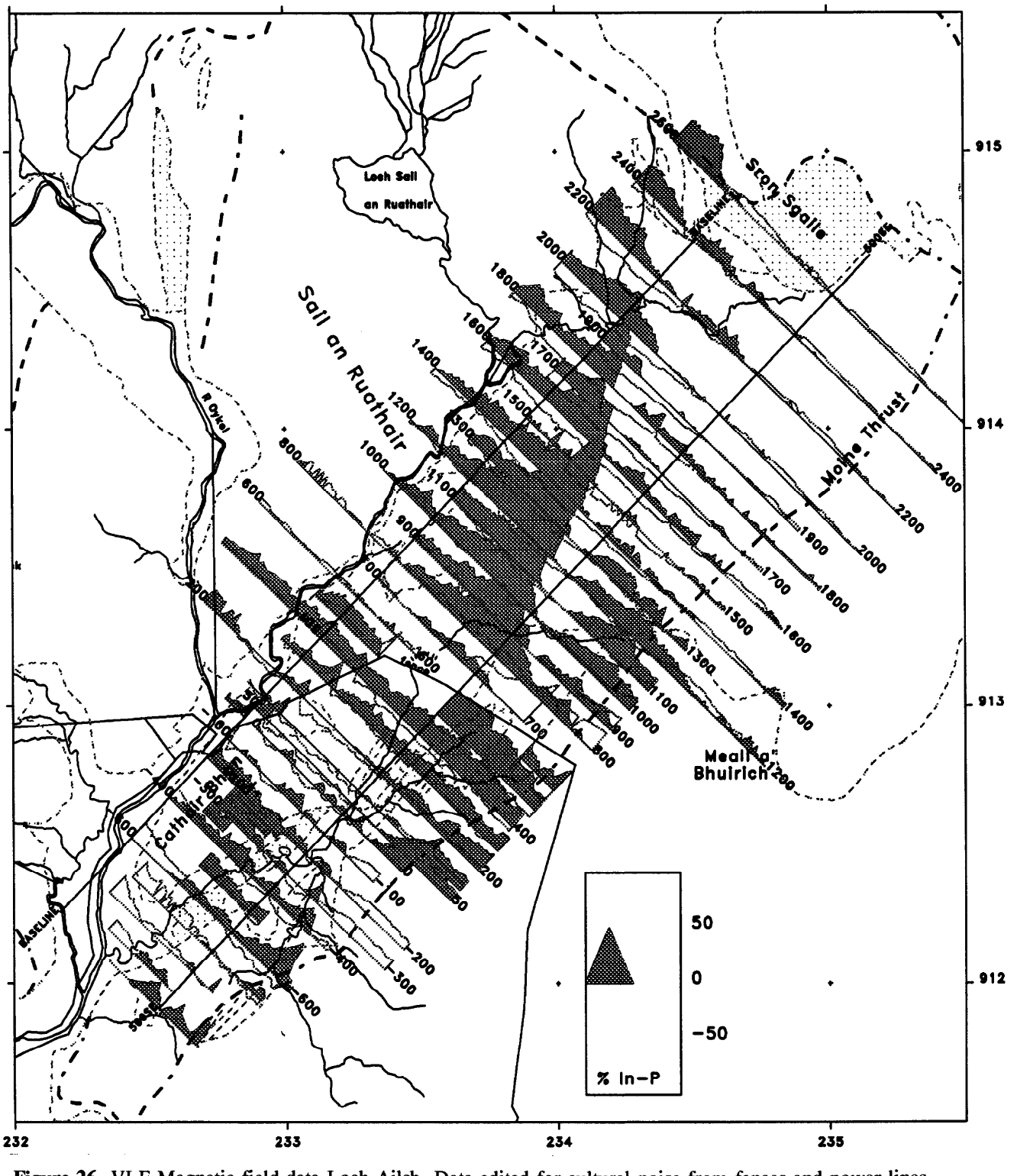

Figure 26 VLF Magnetic-field data Loch Ailsh. Data edited for cultural noise from fences and power lines. VLF frequencies 15.1 and 16. kHz. In-phase component shaded, out-of-phase component line trace

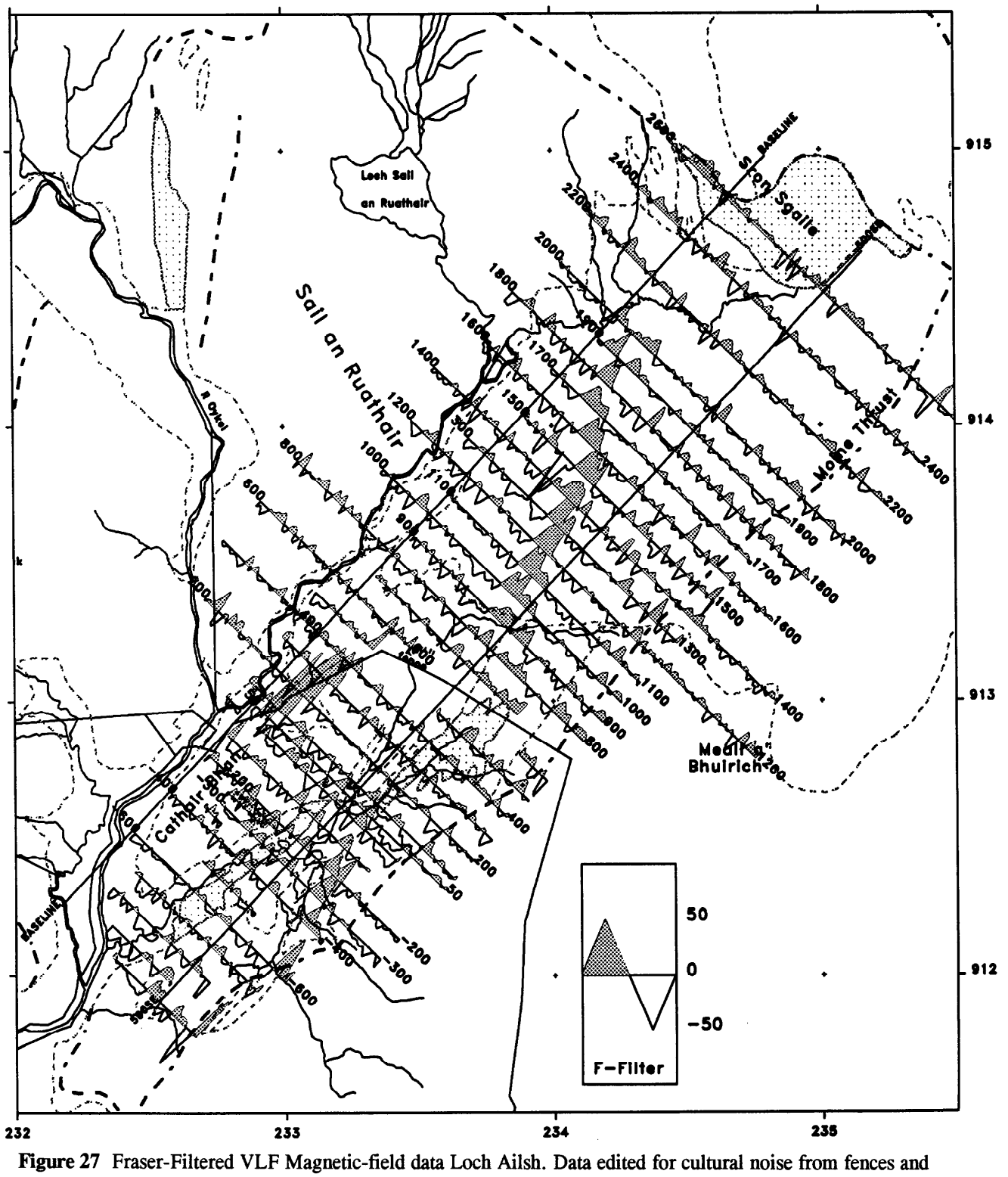

Figure 27 Fraser-Filtered VLF Magnetic-field data Loch Ailsh. Data edited for cultural noise from fences and power lines. VLF frequencies 15.1 and 16 kHz. Filter from in-phase component

the in-phase VLF data after editing the cultural noise. The location of the main conductivity boundary is more clearly identified.

The detail of the edited VLF data and the VLF Fraser filtered data for the south-east part of the grid in the Allt Cathair Bhan are shown in Figures 28 and 29. A strong positive in-phase anomaly with a prominent cross-over feature is traceable across 6 lines north of line 600S and trends 020°. This feature corresponds to an area of peat-covered ground adjacent to the Moine thrust plane. The actual anomaly lies just south-east of the spur of Durness Limestone which is crossed by lines 400S, 300S and 200S. This may represent a fault through the Lower Palaeozoic rocks but cannot be easily distinguished north of line 0N.

The Moine Thrust appears to have a small recognisable anomaly on lines 100, 200 and 300N but is less clear on the more northern lines. The main feature across the north-east part of the grid is the very strong positive in-phase VLF anomaly with amplitudes generally above 40%. The form of the anomaly, with a minor dip in the out-of-phase component and very little negative component, is typical of a major conductivity boundary, possibly a thrust horizon. South of line 700N this VLF anomaly appears to align with the margin of the syenite adjacent to the Durness Limestone. Furthermore, lines 2000N, 2200N and 2600N in the north indicate that the main VLF anomaly aligns with the mapped boundary between syenite and Lower Palaeozoic rocks west of the Sron Sgaile basic rocks. It is therefore considered to represent the unexposed south-east margin of the syenite adjacent to Lower Palaeozoic rocks, the latter locally including lenses of pyroxenite.

Apparent current density modelling of the VLF in-phase component for several lines across the main VLF anomaly, calculated using a cosine filter, indicates a major zone of enhanced current density associated with the main VLF anomaly (e.g. Figure 30). This zone is interpreted as the margin of the syenite against Lower Palaeozoic rocks.

Induced Polarisation (IP) data

Initial IP observations were made using a dipole-dipole array with a dipole length of 50 m. Huntec Mark 3 time-domain equipment was used with a cycle time of 8 seconds and a duty ratio of unity. Chargeabilities were measured over the period 120 - 1080 milliseconds after switch off of a 2 second polarising pulse. Input current was generally 100 or 200 mA. Background chargeabilities using this system were in the range 0-15 milliseconds. Background apparent resistivities are up to 10000 ohm metres in the syenite and less than 1000 ohm metres over the Durness Limestone and Moine schists.

The preliminary IP survey was conducted between lines 0N and 800N. The dipole-dipole IP results for lines 200, 400, 600, 800N are displayed as pseudosections of chargeability and apparent resistivity in Figures 31-34. The sections show significant chargeability and resistivity anomalies on all lines and especially on lines 200N and 600N. Most of the lines show significant zones of higher apparent resistivity, especially on lines 600N and 800N. Chargeabilities exceed 70 milliseconds and resistivities are locally less than 400 ohm metres. These features are frequently associated with a 2 m high deer fence across the north part of the grid. More specifically, along lines 200N and 600N one of the potential or current electrode stations for the strongest anomaly is within 5 m of the fence. The proximity of the fence to electrodes was therefore considered as the likely cause of the large anomalies on these lines. Contoured maps of chargeability, clearly indicate the effect of the fence

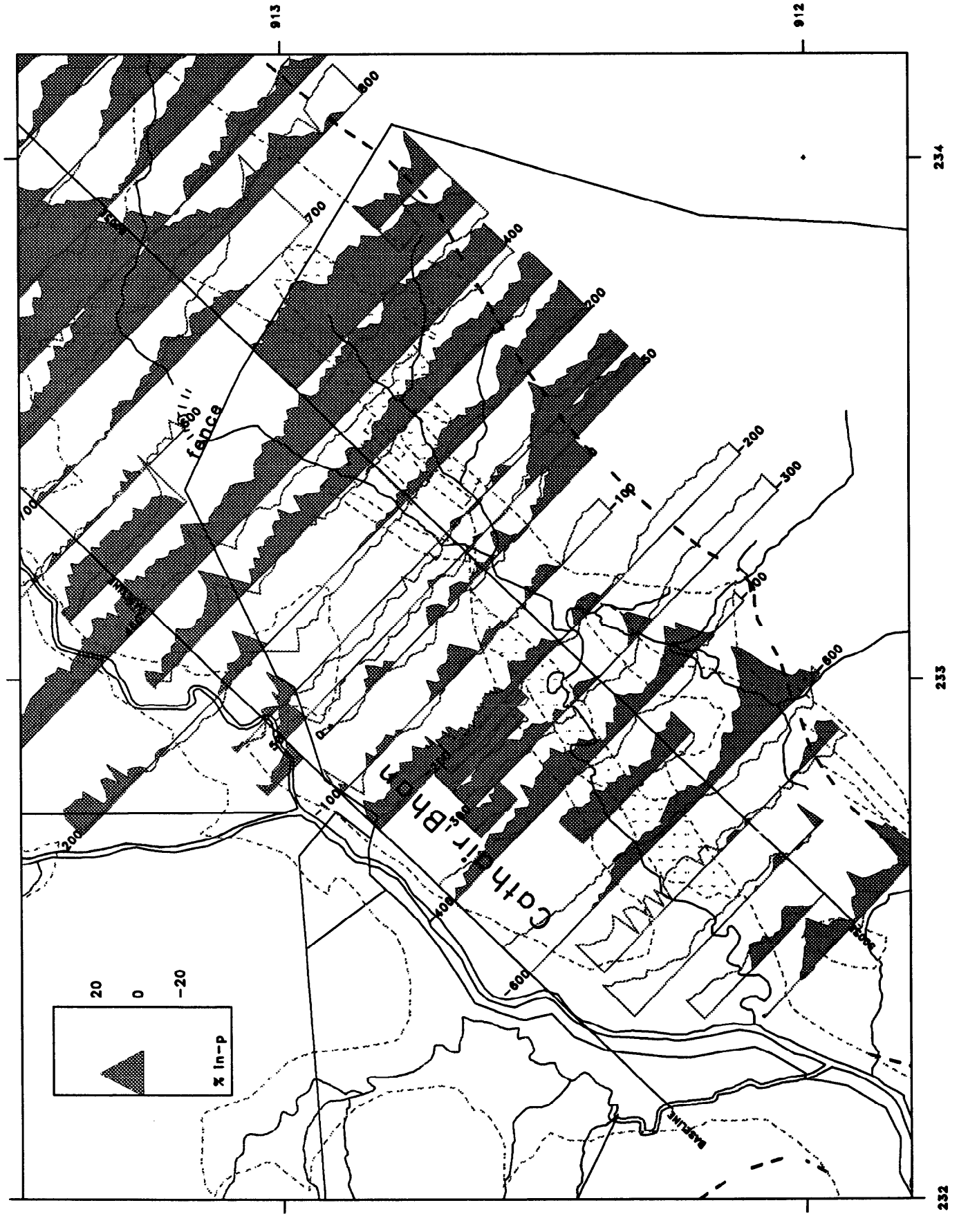

Figure 28 Detail of the VLF Magnetic-field data in the Allt Cathair Bhan. Data edited for cultural noise from fences and power lines. VLF frequencies 15.1 and 16 kHz. In-phase component shaded, out-of-phase component line trace

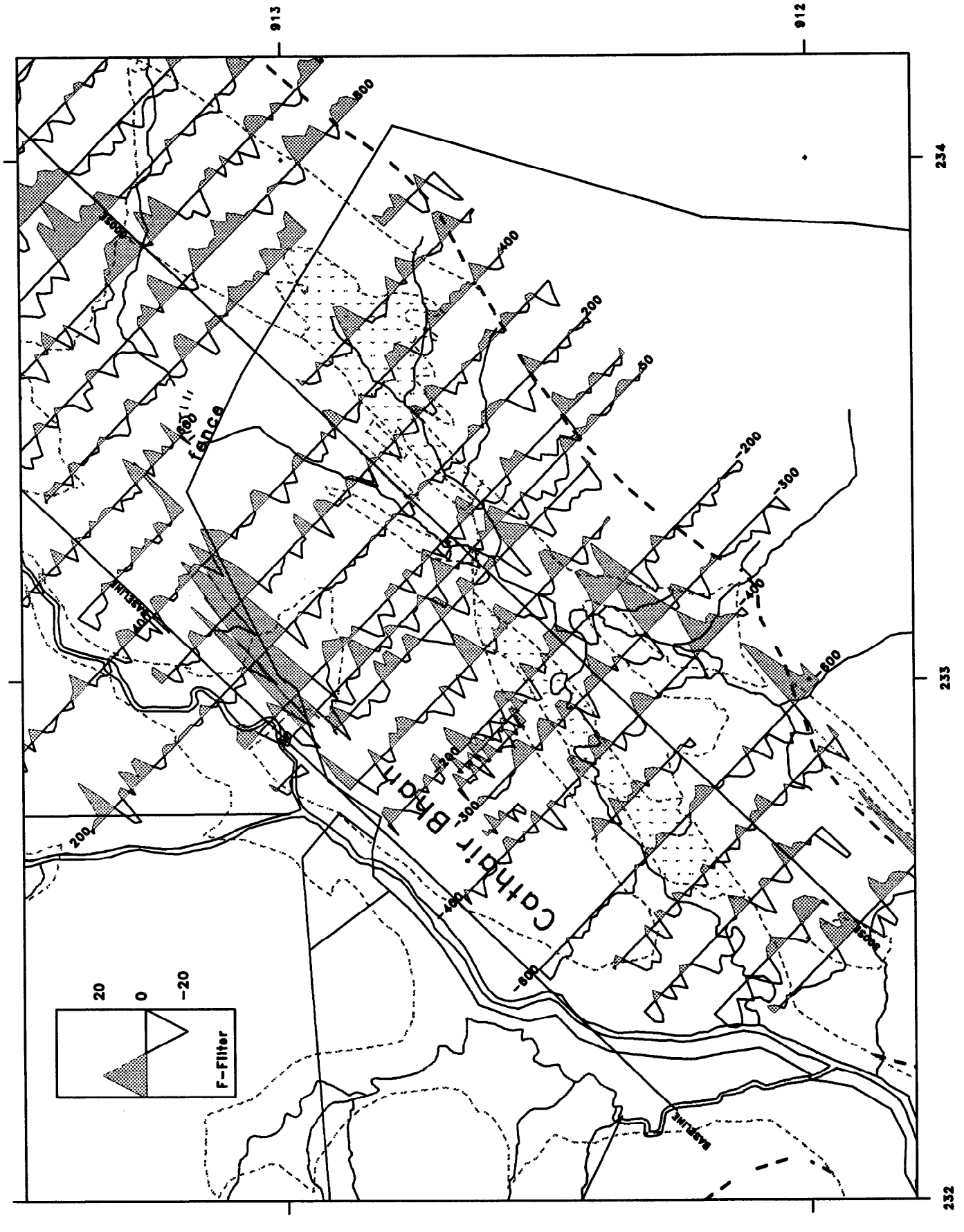

Figure 29 Detail of the Fraser-Filtered VLF Magnetic-field data in the Allt Cathair Bhan. Data edited for cultural noise from fences and power lines. VLF frequencies 15.1 and 16 kHz. Filter from in-phase component

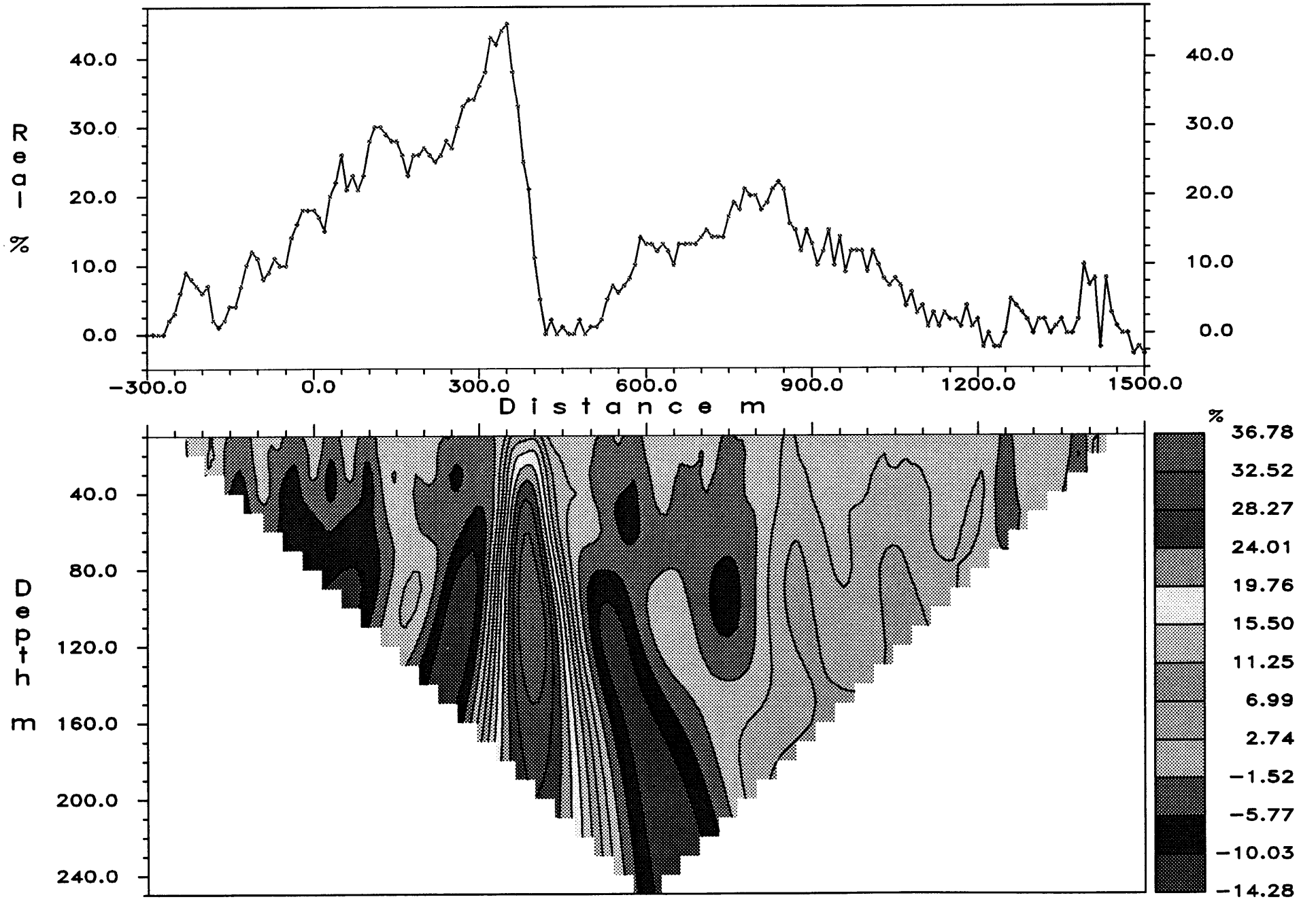

Figure 30 VLF Apparent current density distribution for Line 1200N derived using a cosine filter

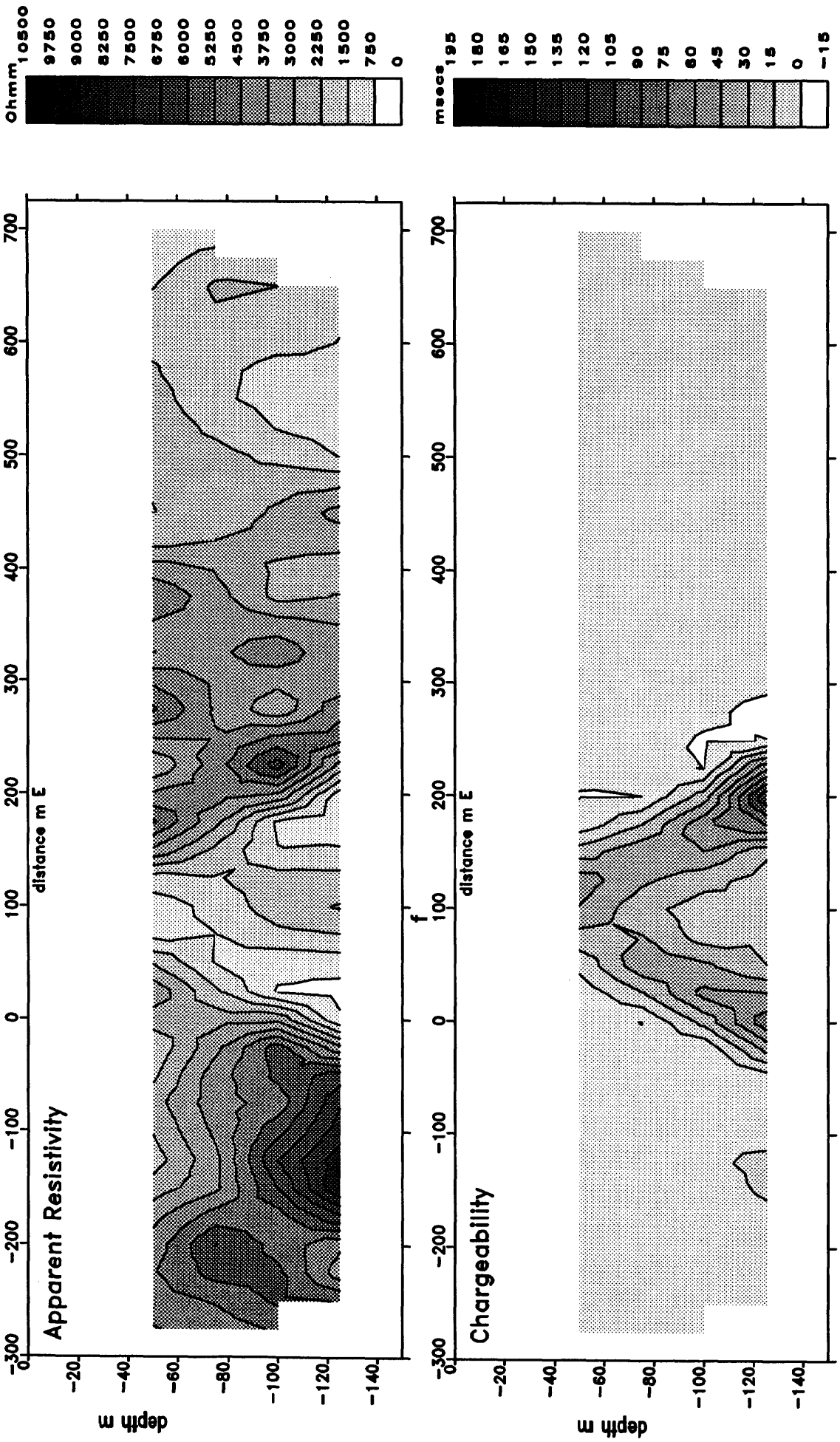

Figure 31 Dipole-dipole IP Data Line 200N. Pseudosections of apparent resistivity and chargeability

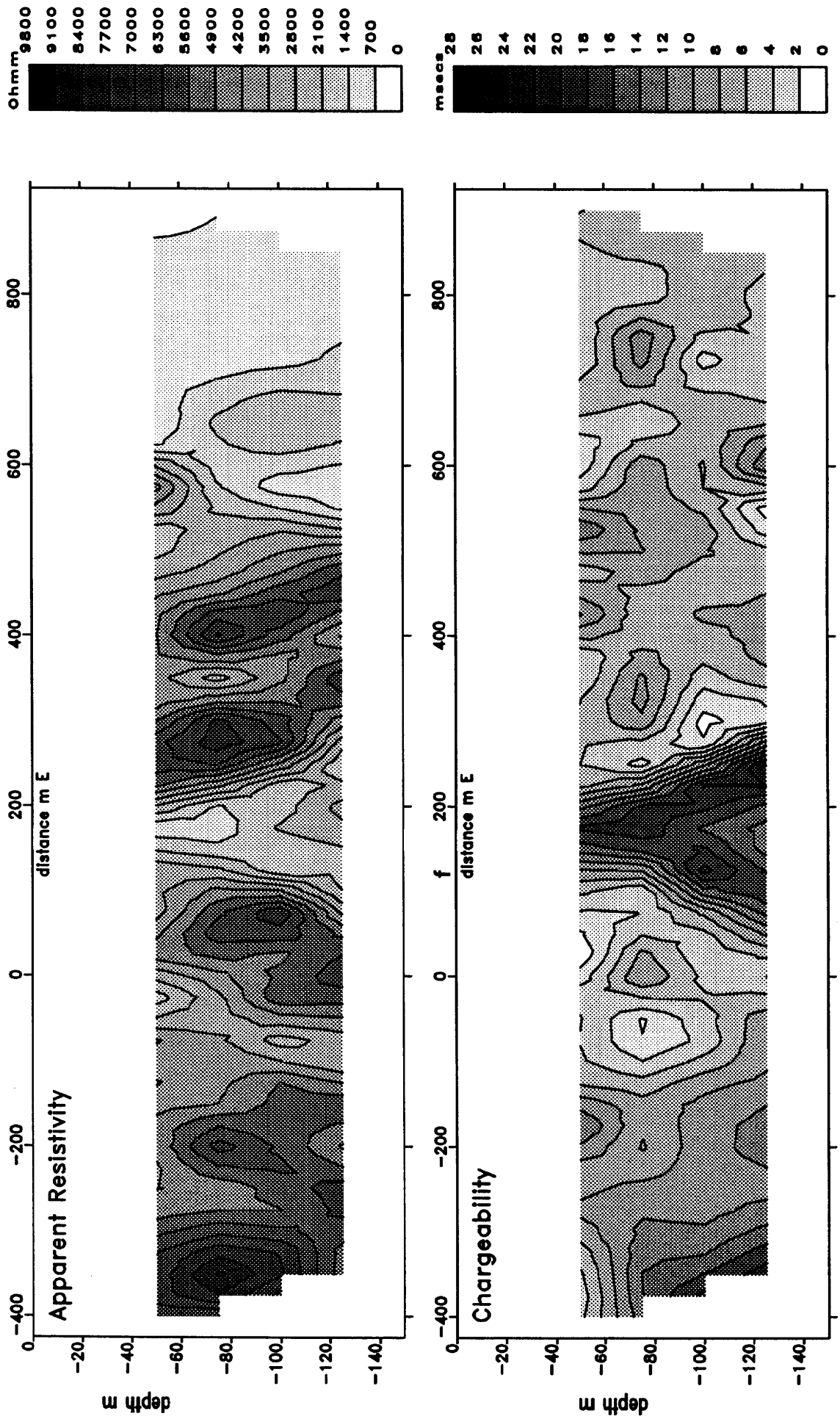

Figure 32 Dipole-dipole IP Data Line 400N. Pseudosections of apparent resistivity and chargeability

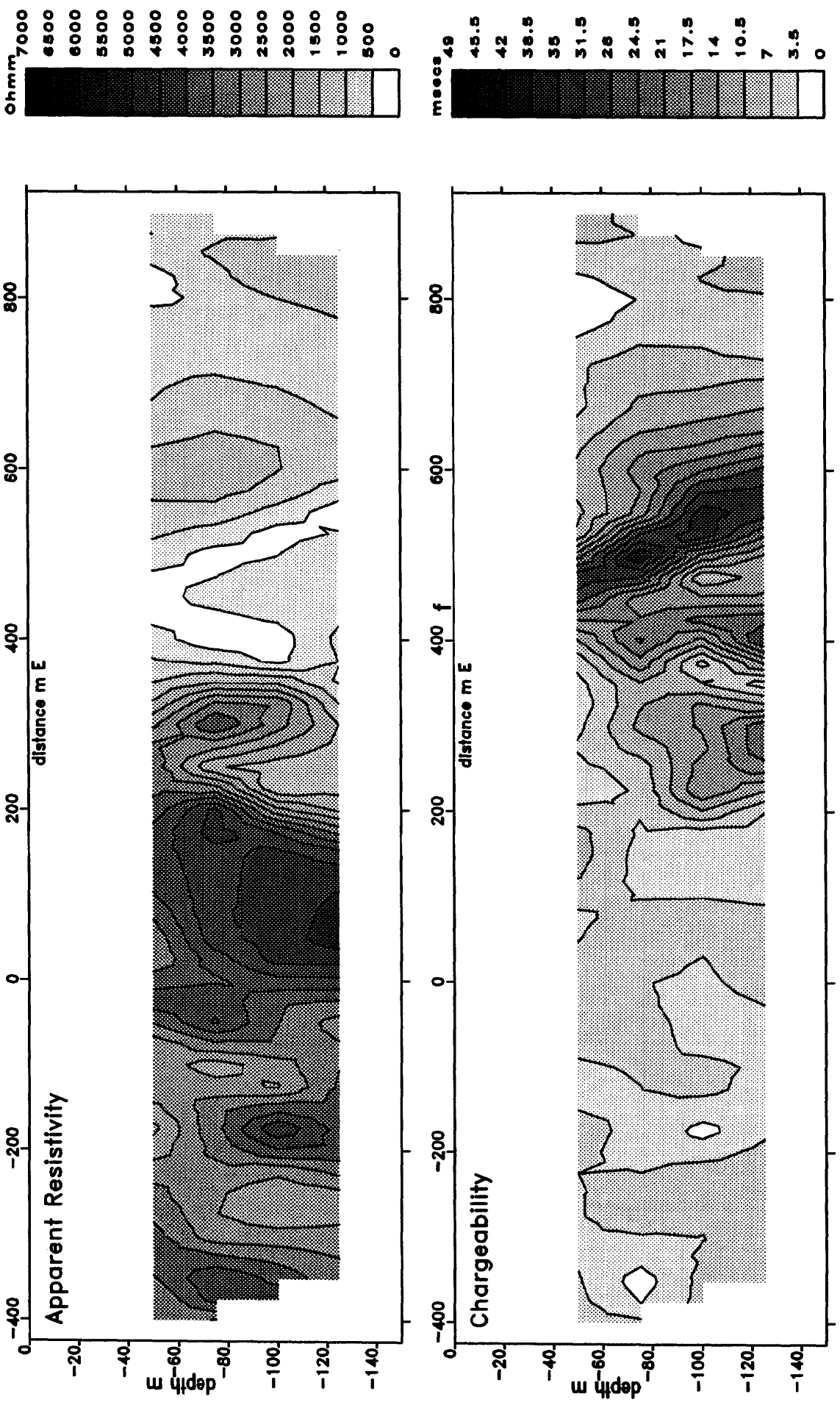

Figure 33 Dipole-dipole IP Data Line 600N. Pseudosections of apparent resistivity and chargeability

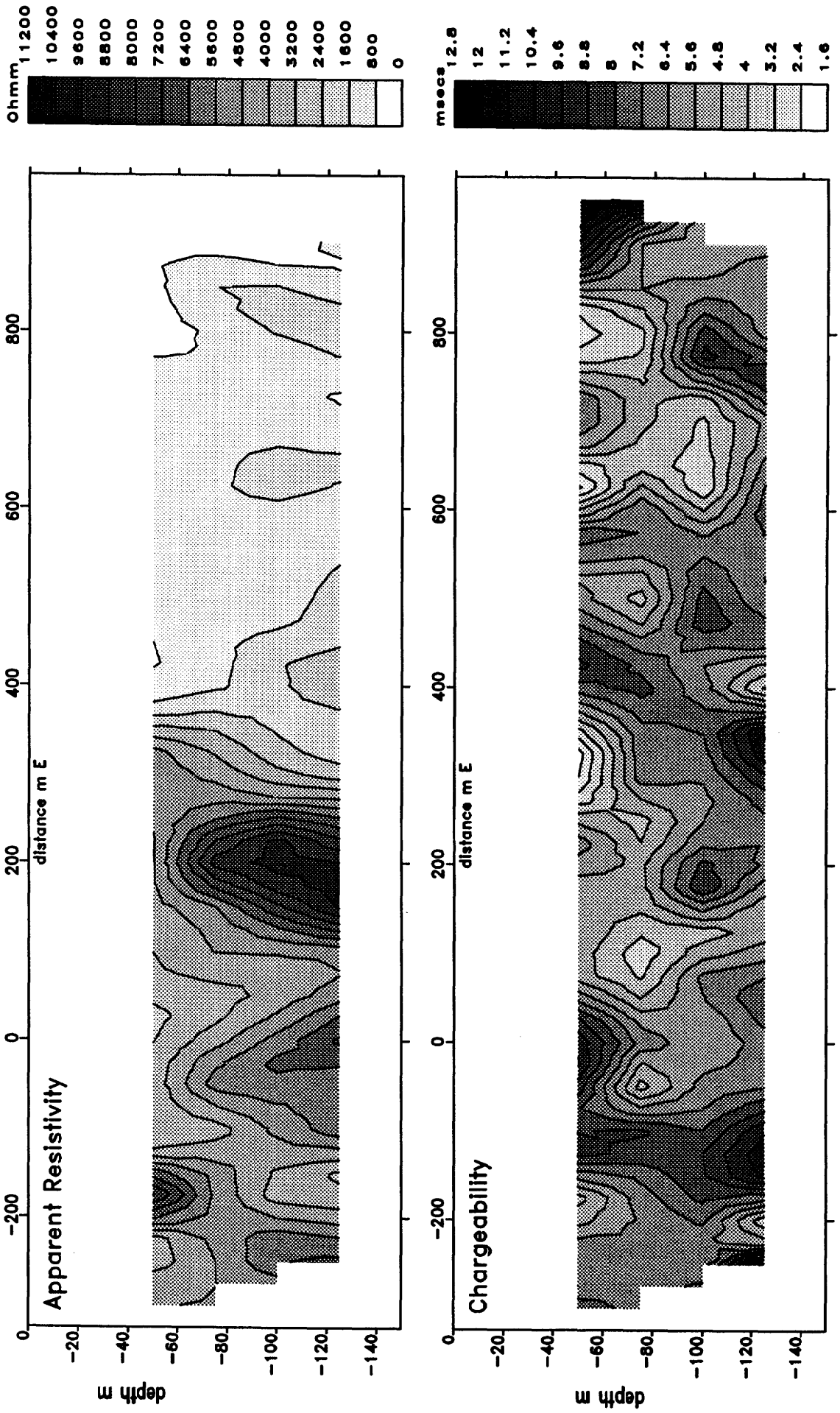

Figure 34 Dipole-dipole IP Data Line 800N. Pseudosections of apparent resistivity and chargeability

(Figure 35 for values of n=2) although a north-east trend to the anomaly appears to align with the geological contact between Lower Palaeozoic rocks and pyroxenites.

The pseudosection for line 800 N (Figure 34) indicates a strong resistivity anomaly over the south-east part of the syenite with a small chargeability anomaly further to the south-east. Since this line is north of the fence a geological cause of the IP anomaly is possible.

The early dipole-dipole IP work therefore suggested that the IP anomaly described in the commercial report seems less significant than the plan or text of the report suggests. The new data did identify a strong localised anomaly which appeared in part to be caused by a relatively new 2 m deer fence. The only suggestion of enhanced chargeabilities significantly away from the fence is at the western end of line 400 N.

As part of the second phase of work, additional IP observations were made using a Schlumberger array with a potential electrode spacing of 25 m along a number of lines. Figures 36 and 37 show the amplitude trace plots of apparent resistivity and chargeability for the Schlumberger array IP data.

A positive apparent resistivity anomaly trends 060° across the lines. The strong resistivity anomaly on line 700N, with an associated chargeability anomaly to the south-east, is not a feature of cultural origin. Maximum chargeability on line 100N occurs in peaty ground south-east of the forestry fence and on lines 200N and 600N close to the forestry fence, with a strong resistivity maximum to the north-west. A detailed gradient array survey near the fence around line 400N, using a potential electrode spacing of 10 m, indicated that the source of the IP anomaly occurred in the ground to the south-east of the fence. Significantly, a number of the gradient array lines indicated that the maximum chargeabilities were not at the potential electrode positions which straddled the fence. Furthermore, the local IP anomaly close to the fence on line 100N appears to be related to a geological feature associated with a peat-filled topographic hollow. Shallow digging and trenching identified mineralised gossan in a thin zone within syenite, a few metres south of the fence.

Discussion

A summary of the main geophysical results is shown in Figure 38. High-amplitude, high-frequency total-field magnetic anomalies are associated with the Allt Cathair Bhan pyroxenites, and significant localised anomalies occur further north-east in drift-covered ground. Quantitative modelling of the ground magnetic-profile data suggest that magnetic pyroxenites with susceptibilities up to about 0.1 SI dip at steep angles (60-80°) to the south-east beneath the Lower Palaeozoic Durness Limestone.

The magnetic structure across the northern part of the grid is less complex. A change in pattern of the profiles occurs between 00N and 200 N. A local magnetic anomaly centred on line 1400N is considered to be due to shallow pyroxenite. The absence of any significant magnetic anomalies over the Sron Sgaile outcrop indicates an essentially different suite of lithologies.

A strong VLF anomaly with a positive in-phase component locally in excess of 50% occurs north-west of the mapped Moine Thrust and trends north-north-east across the survey grid. The form of the anomaly suggests a significant resistivity boundary and the feature aligns with the mapped contact

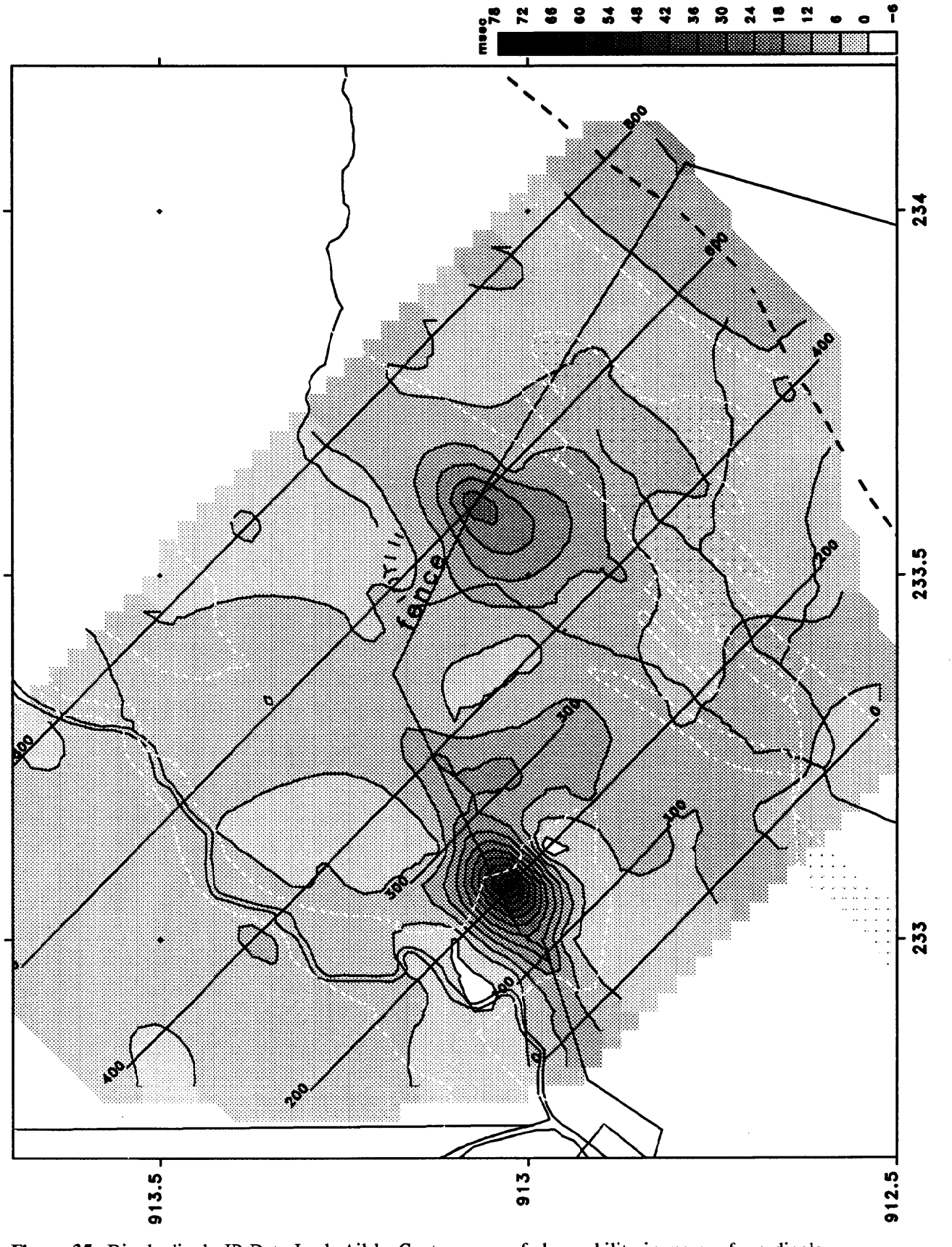

Figure 35 Dipole-dipole IP Data Loch Ailsh. Contour map of chargeability in msecs. for a dipole separation of n=2

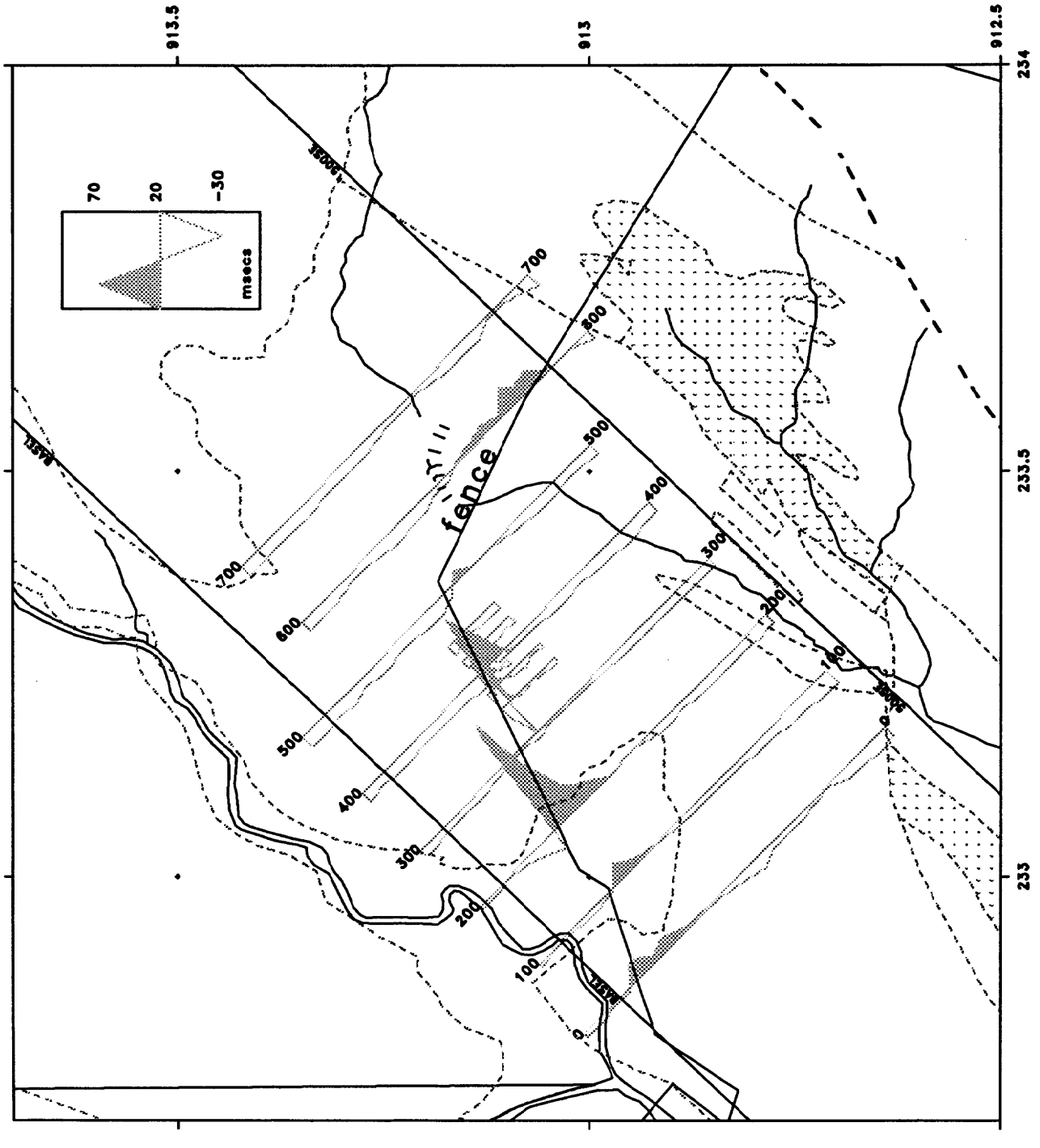

Figure 36 Schlumberger and gradient array IP data, Loch Ailsh. Chargeability results in msecs.

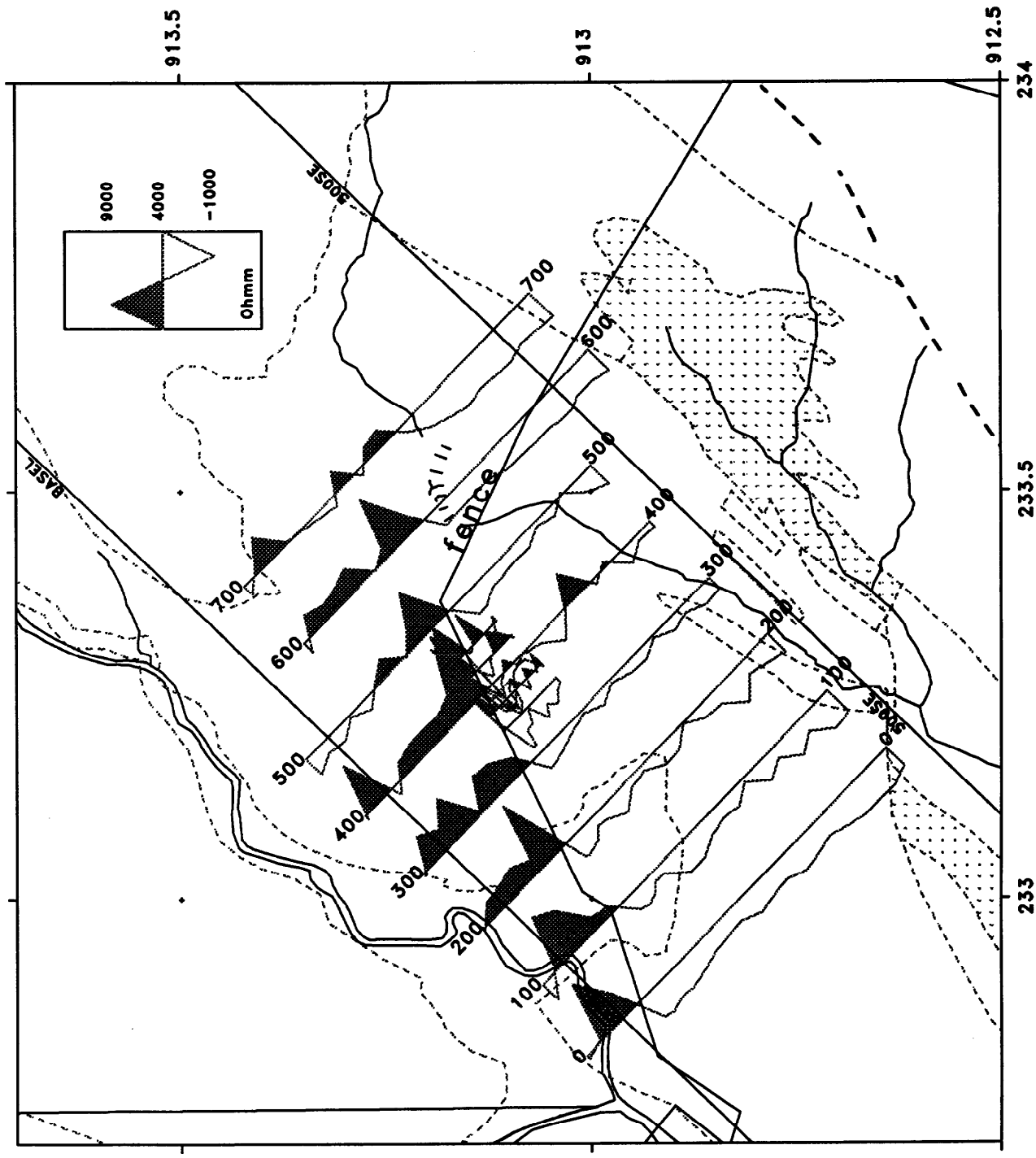

Figure 37 Schlumberger and gradient array IP data, Loch Ailsh. Apparent resistivity results in Ohm metre

Figure 38 Summary of geophysical results, Loch Ailsh. Hatch filled trace is the total magnetic field profile where this exceeds 50800 nT

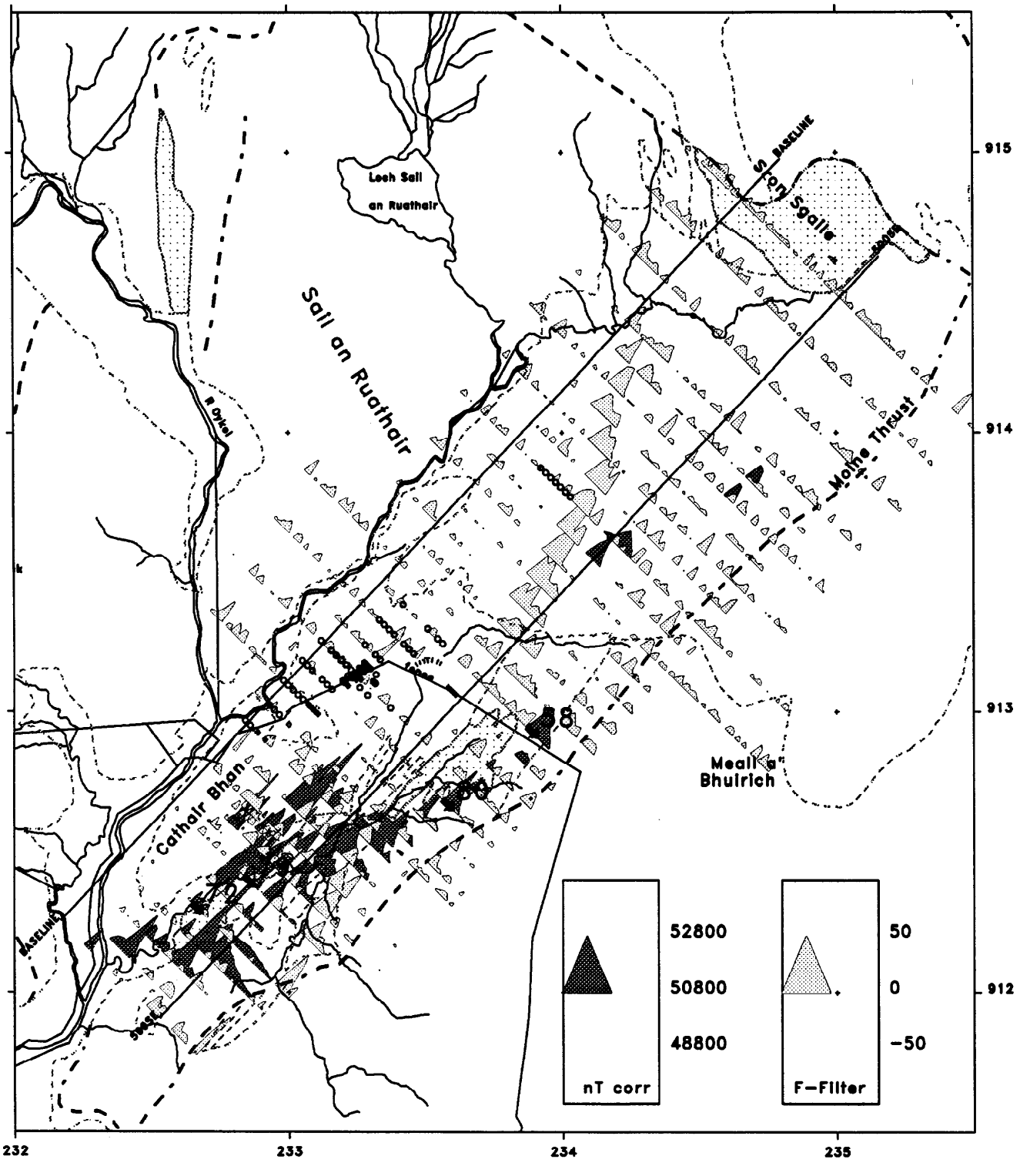

Stipple trace is the Fraser-filter VLF in-phase component after editing of cultural noise. Open circle symbols are sites where the Schlumberger resistivity is greater than 5000 Ohmm, diamond symbols where the chargeability exceeds 30 msecs. Dip arrows are the apparent dip solutions of the magnetic pyroxenite derived from 2.5D modelling. Outline geology as in Figure 2, mafic rocks stippled.

between syenite and Lower Palaeozoic rocks. This suggests that the area mapped as extensive drift is underlain by large area of Lower Palaeozoic rocks.

IP resistivity profiles indicate that the cause of the strong VLF anomaly is a resistive zone close to the south-east margin of the syenite, with a zone of enhanced chargeability slightly to the south-east of this. An IP anomaly, close to a 2 m high metal deer fence, occurs on several lines especially 100N, 200N and 400N, and coincides with gossanous horizons within the syenite.

MINERALOGY

Introduction

On the basis of lithogeochemical results and the presence of base-metal mineralisation, a suite of 21 samples was selected for mineralogical study. In order to elucidate the nature of the Pt and Pd enrichment a search for PGE-bearing phases was carried out using an automated searching technique on the automated electron microprobe.

The samples selected are listed in Table 10. A petrographic summary and identification of all the samples studied is given in Open File Report WG/93/7 (Styles, 1993).

Petrology

The main rock type studied is the ultramafic clinopyroxenite. The least-altered samples show that it was originally coarse grained with lath-shaped pyroxene grains around 5 mm in size. Interstitial phases are biotite, magnetite, apatite, and minor felsic material. Several samples show high-temperature recrystallisation to give a granular polygonal texture. Large brown poikilitic amphiboles frequently include and replace finer clinopyroxenes and appear to be a late magmatic phase. Biotite is also a late phase and is associated with abundant sphene in some sections. These minerals appear to have formed at about the same time, at a late magmatic stage, probably from volatile-rich residual magmas or fluids.

Several samples are cut by thin felsic veins which are composed largely of albite with minor quartz and a little K-feldspar. These veins also show evidence of deformation, with subgrain formation along shears. Some alteration of the pyroxenite is connected with these veins, particularly the alteration of clinopyroxene to a green hornblende and in rare cases a bluish amphibole. In many rocks alteration of clinopyroxene to amphibole is very limited away from these veins, though some that are cut by shears show extensive amphibolitisation.

Carbonate veins cutting across many samples are associated with shears and generally also possess a strong fabric. The carbonate veins is often accompanied by chlorite or pale tremolitic amphibole and minor sulphide mineralisation.

Silicate mineral chemistry

The composition of the main rock-forming minerals from two samples of pyroxenite was determined by electron microprobe, using an energy-dispersive analyser on a Cambridge Instruments Microscan

Table 10 - Thin section descriptions

Scottish Thin Section Number	MRP Number	Brief description	Rock name
S94910	PGR8081	Extensively altered coarse clinopyroxenite, cut by carbonate veins and shears, with minor fine pyrite and chalcopyrite.	Amphibolitised clinopyroxenite
S94911	PGR8082	Fine clinopyroxenite with interstitial biotite and magnetite. Chalcopyrite, scattered and along fractures.	Recrystallised clinopyroxenite
S94912	PGR8087	Medium grained quartz and feldspar with K-feldspar phenocrysts, cut by shear zones.	Sheared syenite
S94913	PGR8103	Extensively recrystallised albite, K-feldspar, quartz, minor biotite and magnetite, little pyrite and chalcopyrite	?Quartz syenite
S94914	PGR8108	Medium grained clinopyroxenite cut by syenite veins. Extensive amphibolitisation adjacent to veins. Abundant chalcopyrite associated with syenite. Later carbonate veins	Clinopyroxenite with syenite veins
S94915	PGR8124	Coarse clinopyroxenite with interstitial magnetite, apatite and felsic material. Large plates of brown amphibole replacing clinopyroxene. Few small chalcopyrite grains.	Amphibole clinopyroxenite
S94916	PGR8141	Coarse pyroxenite. More biotite and slight foliation	Amphibole clinopyroxenite
S94917	PGR8147	Medium-grained hornblende-feldspar rock with epidote and opaque minerals. Patches and veins of epidote, late carbonate and chlorite veins. Brownish sulphide, ?pyrrhotite.	Epidotised amphibolite
S94918	PGR8156	Fragmental rock with clasts of quartz and feldspar (0.5mm) in foliated matrix of carbonate with fine graphite. Cross-cutting ferruginous carbonate veins.	Calcite-quartz schist Metamorphosed calcareous sandstone
S94919	PGR8166	Coarse clinopyroxenite with interstitial biotite, magnetite, apatite and little felsic material.	Clinopyroxenite
S94920	PGR8167	Granular clinopyroxenite with abundant interstitial biotite apatite and magnetite. Large plates of brown amphibole. Abundant chalcopyrite along fractures.	Biotite clinopyroxenite
S94921	PGR8168	Granular clinopyroxenite. Interstitial sphene with biotite. Carbonate veins with minor chalcopyrite and pyrite.	Clinopyroxenite
S94922	PGR8181	Coarse K-feldspar perthites and albite cut by fracture zones. Little pyrite and chalcopyrite.	Feldspar pegmatite

S94923	PGR8183	Medium-coarse clinopyroxenite with interstitial biotite and magnetite, cut by felsic vein with amphibolitisation along vein margin. Abundant chalcopyrite in fractures and associated with shears.	Clinopyroxenite with felsic veins.
S94924	PGR8186	Medium-coarse clinopyroxenite with interstitial biotite and magnetite. Minor scattered chalcopyrite	Clinopyroxenite with felsic veins
S94925	PGR8195	Coarse, strained, K-feldspar cut by numerous fine shear zones. Carbonate and pyrite in recrystallised areas.	K-feldspar pegmatite
S94926	PGR8196	Coarse textured mafic rock with aggregates of fine hornblende after mafic minerals; and muscovite and epidote after feldspar; and sphene after ilmenite. Scattered fine chalcopyrite.	Very altered
S94927	PGR8239	Section very poor. Large tremolitic amphibole surrounded by chlorite, ?talc, little pyrite.	Amphibolitised clinopyroxenite
S94928	PGR8123	Coarse clinopyroxenite with interstitial biotite and magnetite. Few large brown amphiboles replacing clinopyroxene. Chalcopyrite associated with fractures.	Clinopyroxenite
S94929	PGR8162	Schistose talc with patches of serpentine and chlorite.	Talc schist
S94930	PGR8191	Fine grained, strongly schistose with mylonitic fabric. Recognisable larger clasts mostly K-feldspar.	Very altered ultramafic Mylonite - possibly originally granite

5. The results from the two samples were very similar. Typical analyses from specimen S94920 are given in Table 11.

The clinopyroxenes (analyses 1-3) are magnesian calcic augites with Mg' (Mg/[Mg+Fe]) around 0.8. They also have relatively high Al and Ti contents which is typical of ultramafic rocks with alkaline affinities. The large brown amphiboles (analyses 4 and 5), are titanian pargasite, with Mg' around 0.7. The high Ti content of 3 wt % causes the dark brown colour. This contrasts with the green amphibole, formed by hydration of clinopyroxene (analysis 6), which has much less Ti (0.65 wt %), but a similar Mg'. The micas, (analyses 7 and 8), are titanian phlogopites, with Mg' around 0.73, similar to the amphiboles, with the high Ti content again causing a brown colour. The high-Ti amphiboles and micas are more Fe-rich than the pyroxenes suggesting that they formed from later more fractionated fluid-rich magma, consistent with their interstitial habit and occurrence with magnetite and sphene.

Ore mineralogy

The most abundant opaque mineral in the clinopyroxenite is magnetite, which occurs interstitially to the pyroxenes and was formed during magmatic crystallisation. Sulphides and other ore minerals that are of definite magmatic origin are rare. A few samples contain small aggregates of chalcopyrite, pyrrhotite and pentlandite included in clinopyroxene that are probably the result of unmixing of a high-temperature sulphide during cooling. By far the most abundant sulphide in the samples is chalcopyrite that occurs as thin veins and grains up to 1-2 mm in size. The mode of occurrence of the chalcopyrite varies: some finer grains are randomly scattered through the rock whilst most, and particularly the larger grains, occur along fractures and shears, many associated with the thin syenite veins but also along fractures through the pyroxenite. Pyrite occurs in several rocks, mostly as fine grains associated with carbonate veins and shears. Small amounts of galena and sphalerite have also been found, in a similar mode of occurrence to the chalcopyrite and pyrite The mode of mineralisation for most of the base metals is clearly post-magmatic, associated with brittle fractures. The association with the felsic veins is possibly because these contain abundant fractures for the later mineralising fluids.

A few analyses of the sulphides were made by electron microprobe, using an energy-dispersive analyser, to check the optical identifications. These showed that the sulphides were simple stoichiometric compounds with no detectable impurities apart from a possible trace of As in the chalcopyrite.

Automated electron microprobe searching for PGM

Platinum group minerals (PGM) were not observed during optical petrographic examination. In view of the relatively low PGE assay values in the samples selected this was not surprising. The six samples with the highest assay PGE contents were selected for automated searching by electron microprobe using the "TurboScan" software developed at Imperial College London with support from MIRO and the EEC. This method had been successfully used to locate PGM in ultrabasic rocks from Aberdeenshire (Gunn et al., 1990). This technique uses the sophisticated computer control of the Cameca SX50 electron microprobe to make a search of the sample on a 1 micron grid. Each point is checked for a high atomic number using the backscattered electron signal and when dense phases are encountered the composition is checked for the presence of three elements, in this case Pt, Pd and

Table 11 **Electron microprobe analyses of clinopyroxenes, amphiboles and micas in pyroxenite sample S94920**

	1	2	3	4	5	6
SiO2	52.091	50.622	50.645	41.1123	40.744	40.742
TiO2	0.576	0.7	0.894	2.72	3.033	0.642
Al2O3	1.988	3.197	3.444	11.52	11.49	11.65
Cr2O3	0	0	0	0	0	0
FeO	5.118	6.884	6.857	11.176	11.262	13.806
MnO	0.248	0	0	0	0	0
MgO	14.899	14.296	13.6	13.667	13.127	12.642
CaO	23.64	22.735	22.899	12.03	11.953	11.667
Na2O	0.375	0.56	0.675	2.651	2.531	2.777
K2O				1.411	1.502	1.182
	98.94	**98.99**	**99.01**	**96.29**	**95.64**	**95.11**
	Ionic formula					
Si	1.942	1.899	1.900	6.186	6.182	6.220
Al IV				1.814	1.818	1.780
Al VI	0.016	0.020	0.025	0.229	0.238	0.316
Ti	0.087	0.141	0.152	0.308	0.346	0.074
Cr	0.000	0.000	0.000	0.000	0.000	0.000
Fe3+	0.000	0.000	0.000	0.028	0.000	0.388
Fe2+	0.160	0.216	0.215	1.378	1.429	1.375
Mn	0.008	0.000	0.000	0.000	0.000	0.000
Mg	0.828	0.800	0.761	3.065	2.969	2.877
Ca	0.944	0.914	0.921	1.939	1.943	1.908
Na	0.027	0.041	0.049	0.775	0.746	0.823
K				0.271	0.291	0.230
Mg/Mg+Fe	0.838	0.787	0.780	0.690	0.675	0.677
Fe/Fe+Mg+	0.083	0.112	0.113			
Mg/Fe+Mg+	0.429	0.414	0.401			
Ca+Fe+Mg+	0.489	0.474	0.485			

1-3 Clinopyroxenes
4-6 Amphiboles
7-8 Micas

Au. If the X-ray counts for any of these elements exceeds the preset threshold value the location of the point is stored for further investigation.

The searching technique located PGM in two of the six samples examined (S93924 and S94920). These were studied in detail as described in the following section. An interesting spin-off from this searching technique is that X-ray spectrum interferences can reveal the presence of previously unrecognised minerals. In this case several of the samples were found to contain small amounts of baryte, presumably related to the late base-metal mineralisation.

The automated searching showed that PGM were present in three areas on sample S94924 and one area on S94920. All the grains were small, less than 10 microns, and preliminary examination showed that most were complex multiphase grains. Past experience has shown that the best way to study these fine intergrowths is by fine-scale X-ray mapping to reveal the chemical variation within the grains. This is done by making X-ray measurements on a grid, in this case with a 0.1 micron spacing, and presenting the data as a microchemical map. In these maps increasing concentration is related to the colour plotted, with maximum values in red.

Sample S94924 - microchemical mapping

PGM were found in three areas on this section, the first two are very similar, being single complex grains, and the third area consisted of a cluster of four grains.

Backscattered electron photomicrographs of the PGM grains were produced. One photomicrograph showed an elongate grain about 10 microns in size occuring along the grain boundary between two clinopyroxene grains. The grain is slightly darker in the central region, indicating a different composition with lower mean atomic number. The microchemical maps (Plate 1a) show that most of the grain is PtAs (sperrylite) and that the central part is Pd+Sb with a minor amount of As, which proved to be isomertieite.

A second similar grain is also around 10 microns in size and occurs along the boundary between biotite and apatite grains (Plate 1b). In this case the larger part of the grain is the Pd+Sb+As mineral, isomertieite, and the smaller part sperrylite.

A third area has a cluster of PGM with four grains around 5 microns in size and several smaller grains. They occur in and along the edge of a vein of sphene at the boundary between two clinopyroxene grains. Preliminary checks showed that the lower two grains were sperrylite while the upper two were complex. Microchemical maps were made to show the fine variation in the area containing the two upper grains. These showed that the grains were very complex in composition (Plate 2a and b). The larger grain was similar to those elsewhere in the section, composed of sperrylite and isomertieite. The second largest grain, to the right hand side, consisted largely of Pd+Sb+As with a small particle of PtAs on the top right side. There are also several other elements present within this grain, shown by the contents of Ag, Te and Bi. From the maps on Plate 2 it is clear that there is a good correlation between Pd and Ag but a less clear one between Pd and Te or Bi. The image processing capability of the system was used to check the exact location of the various elements.

A threshold can be set on the multicolour maps so that for each element all points above a certain value are shown as a single colour. New images can then be made by adding together these single colour thresholded images so that new colours are formed where two elements occur at above the threshold level in the same place. Plate 3 shows such thresholded images for the area covered by Plate 2. Plate 3a shows high levels of Pd in light blue and, where Pd occurs with higher levels of Ag, the addition is shown as bright green. This shows that the Ag-rich grain is in the centre of the right hand isomertieite grain. Plate 3b shows the relationship between Pd and Te where Pd is again shown in light blue and Te in dark blue. Where the two elements occur together it is green. The areas where they occur together are in the small grain below the left hand isomertieite and on the right hand side of the right hand isomertieite. The fact that the overlap is cocentric on the first grain suggests that this is a Pd telluride. However it is off-centre on the latter grain suggesting that the elements are not actually in the same phase. The partial overlap may be caused by edge effects, since very small grains (less than two microns) tend to have a halo (rainbow) effect around their edges as the electron beam spreads out in the specimen to a diameter around 1 micron. Consequently, when the step size of the maps is very small, in this case about 0.1 microns, the spatial resolution is impaired and blurring of the edges occurs.

The relations between Te and Bi are shown on Plate 3c, which shows two telluride particles, but only the one to the right is a Bi telluride. The other grain in addition to Pd contains Pb (Plate 3d). There are also very small Pd-, Pb- and Ag-bearing grains extending upwards from the larger isomertieite grain, and at least one of these is a telluride.

In summary, microchemical mapping has shown that within an area 20 microns square there are nine PGM grains consisting of two sperrylites, two isomertieites, one Pd+Ag telluride, one Bi telluride and at least three Pb+Pd+Ag tellurides.

Sample S94924 - quantitative analysis

High-quality quantitative analysis of very small PGM grains is very difficult because of problems of spatial resolution of the electron beam. Analyses are made at 30 kv to excite the required X-ray lines which means that the beam penetrates and spreads in the sample and generates X-rays from a volume well over a micron in depth. As a result, X-rays are often generated from more than one mineral phase which results in mixed analyses and greater errors in the matrix corrections. The information from the chemical maps can be used to remove known contaminants and the remainder normalised to give an approximation to the original pure analysis.

The sperrylite grains from all areas give reasonably good analyses which show that they are essentially stoichiometric PtAs with a little Fe (Table 12). The larger Pd minerals also give good analyses (Table 13, columns 1-3) which show that they are isomertieite which has an ideal formula $Pd_{11}Sb_2As_2$. There is a substitution of Cu and Ag for Pd in these grains. An attempt was made to analyse the small grain in area 3 where the isomertieite occurs in association with the various tellurides described above (Table 13, col. 4). The results however indicate a mixture of constituents from which individual phases could not be distinguished.

Sample S94920 - microchemical mapping

One PGM grain about 15 microns in size was found in sample S94920. It occurs along a fracture through a clinopyroxene grain and is largely enclosed by later chalcopyrite. A backscattered electron

Table 12 Electron microprobe analyses of sperrylite grains in pyroxenite sample S94924

	1	2	2	4
Pt	50.11	51.46	54.37	51.06
Fe	0.86	0.97	1.02	0.77
As	40.96	39.33	42.83	43.02
S	0.20	0.35	0.91	0.12
Total	92.13	92.11	99.13	94.97

Number of atoms on basis of 2 As+Sb

Pt	0.93	0.98	0.93	0.91
Fe	0.06	0.06	0.06	0.05
As	1.98	1.96	1.91	1.99
S	0.02	0.04	0.09	0.01

1	Area1
2	Area 2
3 & 4	Area 3

Table 13 **Electron microprobe analyses of Pb-rich grains in pyroxenite sample S94924**

	1	2	3	4
Pd	66.69	69.32	63.84	31.06
Ag	1.70	1.71	0.48	5.42
Bi	0.20	0.00	0.00	6.88
Pb	0.00	0.00	0.00	0.06
Cu	4.12	3.94	2.53	0.85
Sb	16.14	16.78	14.43	5.43
As	8.98	8.41	8.81	9.07
Se	0.00	0.00	0.00	0.00
S	0.00	0.03	0.11	0.14
Te	0.00	0.00	0.00	16.67
	97.83	100.19	90.20	75.58
recalculated to totals of 100%				
Pd	68.17	69.19	70.78	41.10
Ag	1.74	1.71	0.53	7.17
Bi	0.20	0.00	0.00	9.10
Pb	0.00	0.00	0.00	0.08
Cu	4.21	3.93	2.80	1.12
Sb	16.50	16.75	16.00	7.18
As	9.18	8.39	9.77	12.00
Se	0.00	0.00	0.00	0.00
S	0.00	0.03	0.12	0.19
Te	0.00	0.00	0.00	22.06
number of atoms on the basis of X Sb+As+Se+Te+S				
Pd	9.97	10.42	10.06	9.75
Ag	0.25	0.25	0.07	1.67
Bi	0.02	0.00	0.00	1.09
Pb	0.00	0.00	0.00	0.01
Cu	1.03	0.99	0.67	0.45
Sb	2.10	2.20	1.98	1.48
As	1.90	1.79	1.96	4.03
Se	0.00	0.00	0.00	0.00
S	0.00	0.01	0.06	0.15
Te	0.00	0.00	0.00	4.34
X	4.00	4.00	4.00	10.00

1 and 2: large grains of isomertieite in Area 2
3: large grain of sperrylite in Area 3
4: small grain of an unidentified mineral in Area 3

micrograph showed that it has complex internal variation. A series of microchemical maps were made to investigate this grain in detail.

The maps (Plate 4) show that the grain is largely telluride with the right-hand part largely Pd telluride with minor Bi. Bismuth is more abundant around the rim of the grain. The map for sulphur shows the position of the enclosing chalcopyrite and also indicates that there are no sulphide phases within the PGM. The principal elements in the left hand end of the grain is shown in Plate 4b. It consists of Ag telluride, both adjacent to the Pd telluride forming the main part of the grain and as a rim around the left hand part of the grain. This rim of Ag telluride encloses an area of Pb selenide. These overgrowths of telluride and selenide are very thin, around 1 micron in thickness.

Sample S94920 - quantitative analysis

Similar problems were encountered to those described for the previous sample. However some data of reasonable quality were obtained (Table 14). The main part of the grain is composed of a Pd+Bi telluride (col. 1) which corresponds to a formula Pd_6BiTe_4. It has not been possible to match this to any known PGM. The analysis of the rim of the grain is "contaminated" by chalcopyrite and, after removing this, the rim composition is have an approximate formula Pd_2BiTe, which again cannot be matched with known minerals.

The Ag+Te and Pb+Se minerals in the rim are so intimately intergrown they cannot be separated (columns 3-5). The two phases can be easily be recalculated from the mixed analyses (Table 15) which shows that the minerals are Ag_4Te and PbSe. The latter is the mineral claustalite but the Ag telluride has not been identified.

Discussion

Study of the ore mineralogy shows that there are several phases of mineralisation. The magmatic phase is characterised by minor base-metal sulphides, chalcopyrite, pyrrhotite and pentlandite. There is also a distinct, very late, phase of base-metal sulphide mineralisation, related to brittle fracture; the dominant mineral is chalcopyrite, with subordinate pyrite, galena and sphalerite. The PGM mineralisation does not appear to be related to either phase of sulphide mineralisation and is dominated by arsenides, antimonides, tellurides and selenides. The textural evidence shows that the PGM occur along grain boundaries and minor fractures, often associated with sphene. In several rocks sphene is associated with late interstitial Ti-rich phlogopite and it is suggested that the PGM crystallised from the volatile-rich magma in the final stages of consolidation.

The presence of small amounts of selenides with the PGM in rocks rich in sulphides also suggests that they must have formed from a separate phase of mineralisation. If selenides had formed at the same time as the sulphides the selenium would have gone into solid solution in sulphide minerals rather than forming separate selenide phases.

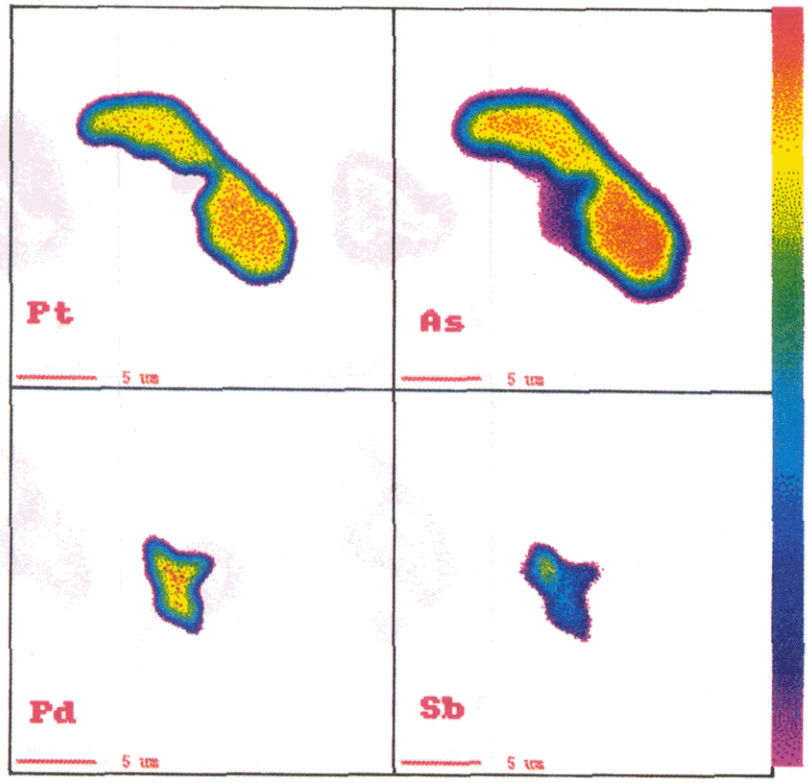

1a (S94924 area 1) Microchemical maps showing intergrown sperrylite, isomertieite and other Pd minerals

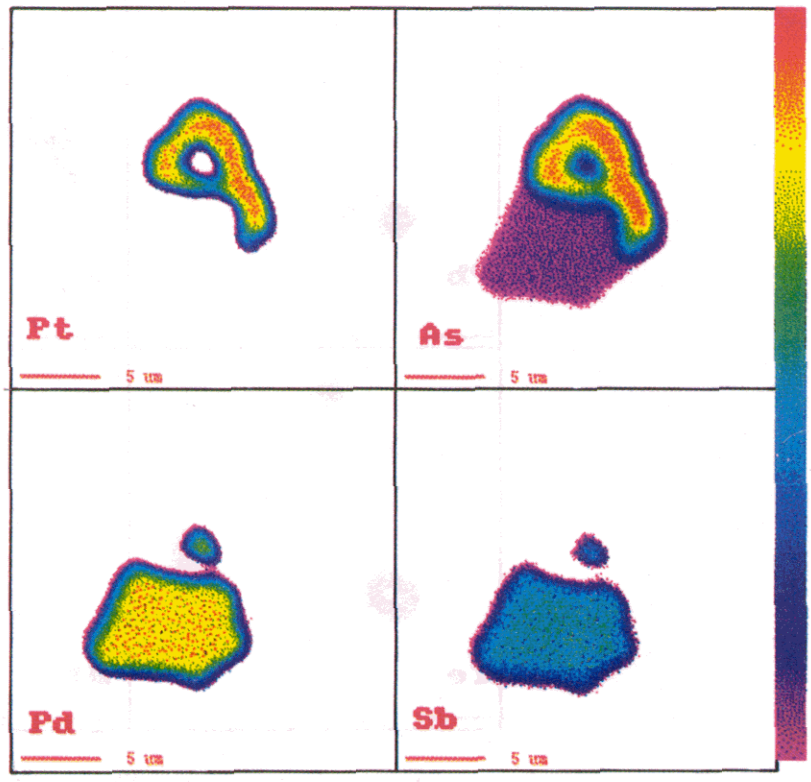

1b (S94924 area 2) Microchemical maps showing intergrown sperrylite and isomertieite

Plate 2

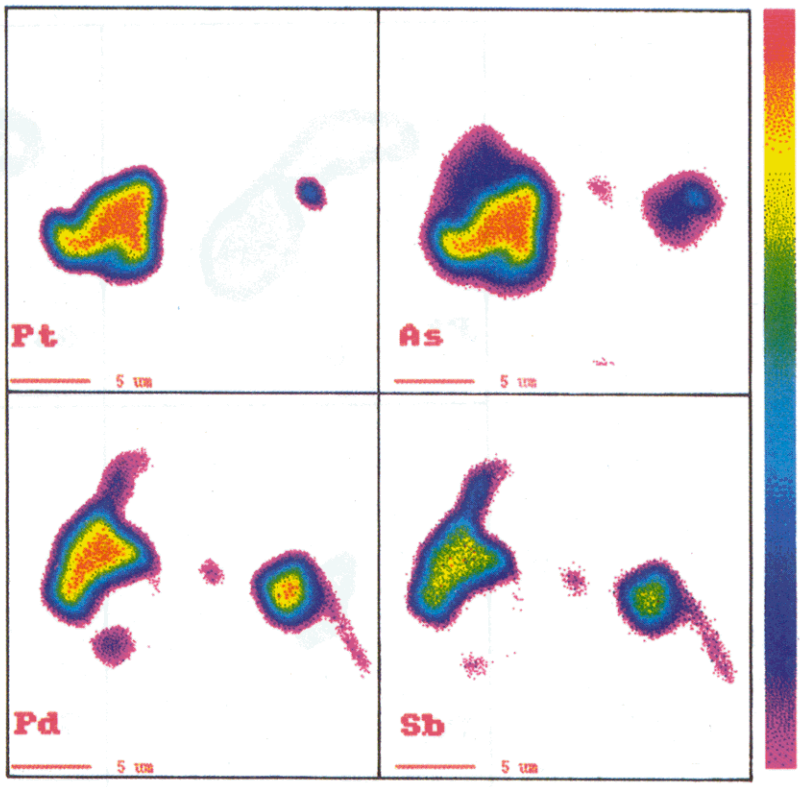

2a (S94924 area 3) Microchemical maps showing the distribution of sperrylite, isomertieite and other Pd minerals

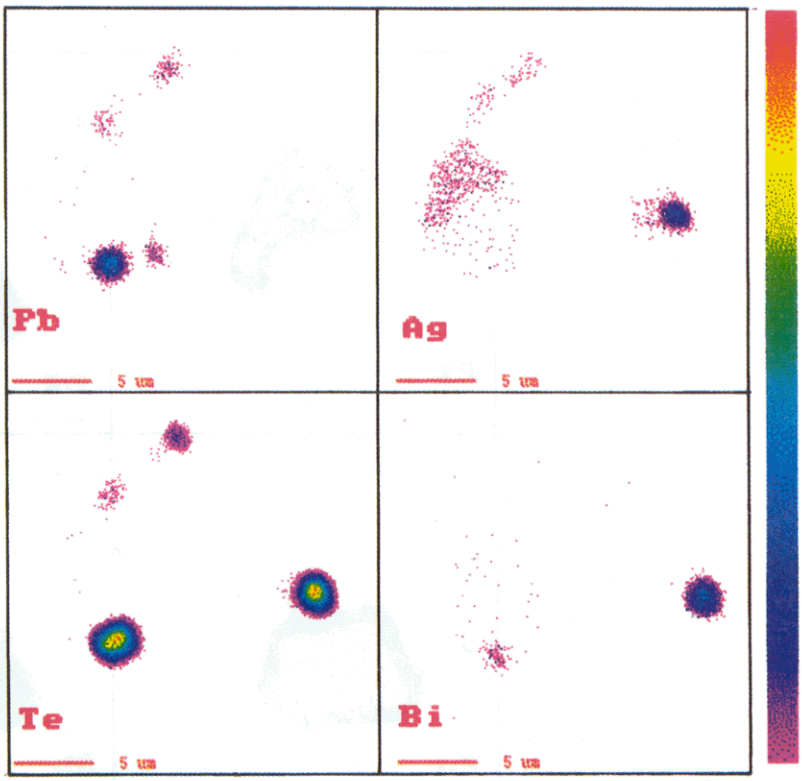

2b (S94924 area 3) Microchemical maps showing the distribution of Pb, Ag, Te and Bi minerals

Plate 3

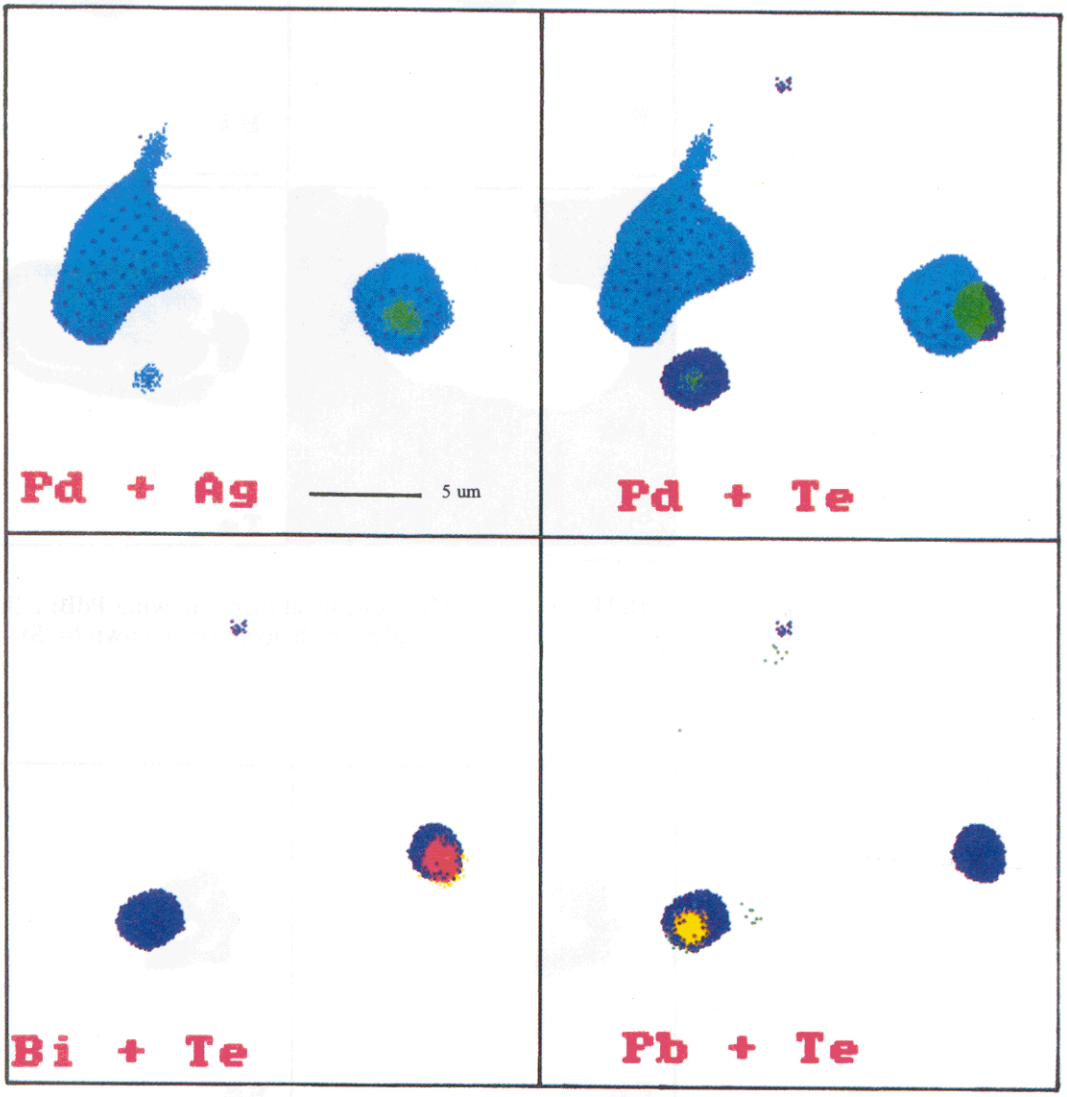

3a (S94924 area 3) Map showing Pd in blue and areas where Ag also occurs in green

3b Map showing Pd, light blue, Te, dark blue and both together in green

3c Map showing Te in blue and where Bi also occurs in red

3d Map showing Te in blue and where Pb also occurs in yellow

Plate 4

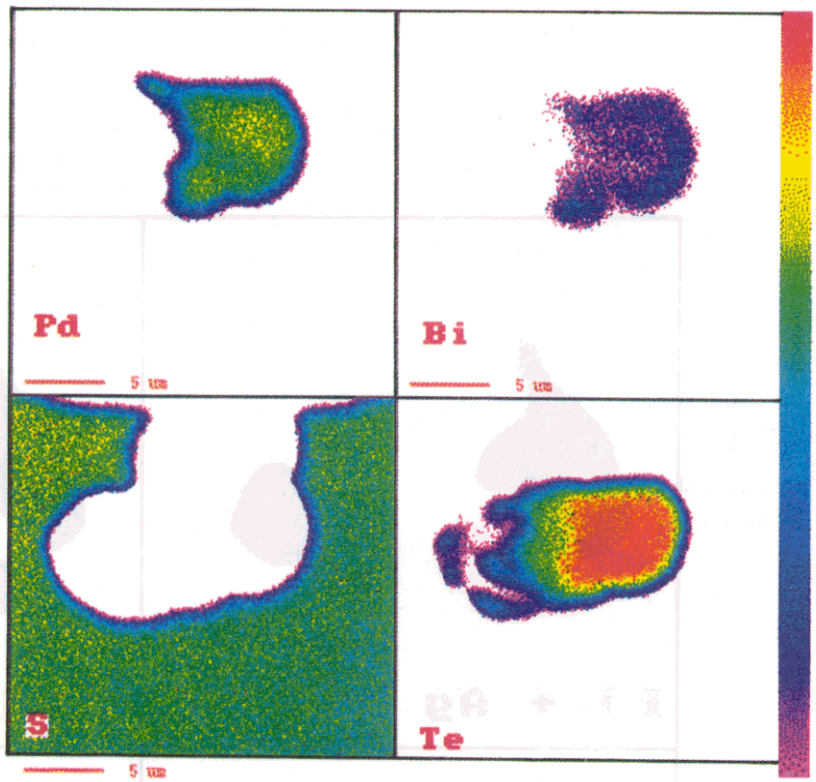

4a (S94920) Microchemical maps showing PdBi telluride included in chalcopyrite (shown by S)

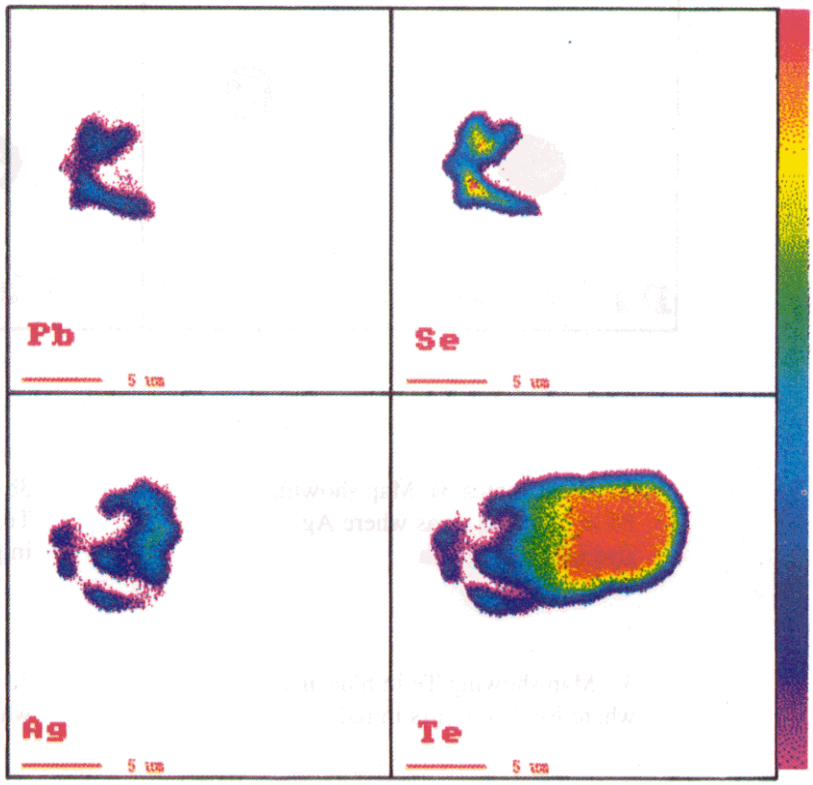

4b (S94920) Microchemical maps showing intergrown PbSe and Ag_4Te

Table 14 Electron microprobe analyses of mineral grains in pyroxenite sample S94920

	1	2	3	4	5
Pd	41.70	26.89	0.00	0.00	0.00
Ag	1.12	4.83	25.61	24.08	25.52
Bi	13.71	21.28	0.00	0.00	0.00
Pb	0.27	0.53	50.21	52.12	38.39
Cu	0.48	20.50	0.11	0.23	2.23
Sb	0.42	0.29	0.00	0.06	0.00
As	0.00	0.00	0.00	0.00	0.00
Se	0.00	0.00	16.20	17.53	13.52
S	0.06	6.30	0.73	0.74	1.75
Te	32.50	17.01	7.78	7.11	8.29
	90.26	97.63	100.64	101.87	89.70
recalculated to totals of 100%					
Pd	46.20	27.54	0.00	0.00	0.00
Ag	1.24	4.95	25.45	23.64	28.45
Bi	15.19	21.80	0.00	0.00	0.00
Pb	0.30	0.54	49.89	51.16	42.80
Cu	0.53	21.00	0.11	0.23	2.49
Sb	0.47	0.30	0.00	0.06	0.00
As	0.00	0.00	0.00	0.00	0.00
Se	0.00	0.00	16.10	17.21	15.07
S	0.07	6.45	0.73	0.73	1.95
Te	36.01	17.42	7.73	6.98	9.24
number of atoms on the basis of X Sb+As+Se+Te+S					
Pd	6.05	3.06	0.00	0.00	0.00
Ag	0.16	0.54	3.28	2.96	3.25
Bi	1.01	1.23	0.00	0.00	0.00
Pb	0.02	0.03	3.36	3.34	2.55
Cu	0.12	3.89	0.02	0.05	0.48
Sb	0.05	0.03	0.00	0.01	0.00
As	0.00	0.00	0.00	0.00	0.00
Se	0.00	0.00	2.84	2.95	2.36
S	0.03	2.36	0.32	0.31	0.75
Te	3.92	1.61	0.84	0.74	0.89
X	4.00	4.00	4.00	4.00	4.00

1: PdTe-rich centre of PbBi telluride (Plate 4a)
2: Bi-rich rim of PbBi telluride
(Cu and S from surrounding chalcopyrite)
3-5: Mixed analyses of finely intergrown Ag4Te and PbSe

Table 15 Ag4Te and PbSe recalculated

	3#	4#	5#	3*	4*	5*
Pd						
Ag	25.61	24.08	25.52			
Bi						
Pb				50.21	52.12	38.39
Cu						
Sb						
As						
Se				16.20	17.53	13.52
S						
Te	7.78	7.11	8.29			
	33.39	31.19	33.81	66.41	69.65	51.91
Normalised wt% element						
Pd	0.00	0.00	0.00	0.00	0.00	0.00
Ag	76.70	77.20	75.48	0.00	0.00	0.00
Bi	0.00	0.00	0.00	0.00	0.00	0.00
Pb	0.00	0.00	0.00	75.61	74.83	73.95
Cu	0.00	0.00	0.00	0.00	0.00	0.00
Sb	0.00	0.00	0.00	0.00	0.00	0.00
As	0.00	0.00	0.00	0.00	0.00	0.00
Se	0.00	0.00	0.00	24.39	25.17	26.05
S	0.00	0.00	0.00	0.00	0.00	0.00
Te	23.30	22.80	24.52	0.00	0.00	0.00
Number of atoms on the basis of X Sb+As+Se+Te+S						
Pd	0.00	0.00	0.00	0.00	0.00	0.00
Ag	3.89	4.00	3.64	0.00	0.00	0.00
Bi	0.00	0.00	0.00	0.00	0.00	0.00
Pb	0.00	0.00	0.00	1.18	1.13	1.08
Cu	0.00	0.00	0.00	0.00	0.00	0.00
Sb	0.00	0.00	0.00	0.00	0.00	0.00
As	0.00	0.00	0.00	0.00	0.00	0.00
Se	0.00	0.00	0.00	1.00	1.00	1.00
S	0.00	0.00	0.00	0.00	0.00	0.00
Te	1.00	1.00	1.00	0.00	0.00	0.00
X	1.00	1.00	1.00	1.00	1.00	1.00

3# - 5# Ag4Te
3* - 5* PbSe

CONCLUSIONS

The internal structure and contact relationships of the Loch Ailsh Complex are consistent with an origin by fractional crystallisation and injection of separate phases of syenitic, mafic and ultramafic magma. Later disruption by high angle faults and thrusts has affected the geometry of the Complex.

Drainage surveys indicate a general enrichment of Pt and Pd associated with pyroxenite bedrock in the Allt Cathair Bhan catchment near the south-eastern margin of the Complex. Elevated Au values are more widely distributed but are especially concentrated in the northern sector of the Complex to the west of Sron Sgaile.

Detailed sampling of basal overburden within the Allt Cathair Bhan catchment indicates localised enrichment of Pt and Pd. Geochemical data show that supergene processes have not produced significant distortion of trace and precious metal distributions. This technique therefore provides an effective method for the discrimination of bedrock type and for the recognition of zones of metal enrichment.

Lithogeochemical data show that the ultramafic pyroxenites are generally enriched in Pt+Pd levels (median value 15 ppb) relative to the other rock types in the Complex and adjacent country rocks. This high background content is interpreted as being of magmatic origin. Local enrichment of the PGE in other lithologies is often associated with attendant enrichment of Au and/or base metals. It is envisaged that this style of mineralisation is due to localised hydrothermal processes.

Mineralogical studies of PGE-enriched samples revealed sperrylite (PtAs) and isomertieite ($Pd_{11}Sb_2As_2$) in association with a suite of arsenides, antimonides, selenides and tellurides. This assemblage occurs in proximity to interstitial biotite, magnetite, apatite and sphene and is often located along grain boundaries and fractures. A derivation from late, volatile-rich magmatic fluids is inferred from these observations. These investigations have indicated that substantial upgrading of the PGE has occurred in spite of sulphur deficiency. These discoveries therefore broaden the range of targets for potentially economic PGE mineralisation.

Geophysical data provide new information on the structure and contact relationships of the Complex. Modelling of ground magnetic data support the existence of compositional heterogeneity within the Allt Cathair Bhan pyroxenite and indicate that it forms an extensive sheet beneath Palaeozoic and Moinian rocks to the east. Resurveying of an IP anomaly previously identified during commercial surveys did not indicate the presence of any significant sulphide mineralisation likely to be enriched in precious metals.

In the northern part of the Complex around Sron Sgaile elevated Au, Pt and Pd levels have been reported in drainage samples and enhanced Au in loose boulders of shonkinite. Detailed sampling of bedrock and float material would be required to establish the source or sources of these anomalies.

Further work is required to define the nature and extent of PGE mineralisation in the central Allt Cathair Bhan. Possible structural traps for the PGE, such as beneath the Durness limestone and along the north-eastern margin of the Allt Cathair Bhan ridge, would be priority targets for drilling.

ACKNOWLEDGEMENTS

The British Geological Survey is indepted to the landowner for allowing access for mapping, geochemical sampling and geophysics. The authors acknowledge the assistance of field geologists Stuart Black, Frankie Curtis, Tim Fletcher, John Mason, Paul Shand and Barrie Young in assisting with surveying, sampling and geophysics.

REFERENCES

COGHILL, B M and WILSON, A H. 1993. Platinum group minerals in the Selukwe Subchamber, Great Dyke, Zimbabwe: implications for PGE collection mechanisms and post-formational redistribution. *Mineralogical Magazine,* Vol. 57, 613-633.

DALY, ELLIOTT, D, and JOHNSON, M R W. 1980. Structural evolution in the northern part of the Moine thrust belt, NW Scotland. *Transactions of the Royal Society of Edinburgh: Earth Sciences,* Vol. 71, 69-96.

ECKEL, E B. 1938. The copper ores of La Plata district, Colorado, and their platinum content. *Colorado Scientific Society, Proceedings.* Vol. 13, 647-664.

ECKSTRAND, O R. 1984. Canadian Mineral Deposit Types: A Geological Synopsis. Geological Survey of Canada Economic Geology Report 36. Section 12.2.c, 41.

FINCH, R J, IKRAMUDDIN, M, MUTSCHLER, F E, and Shannon, S S Jr.. 1983. Precious metals in alkaline suite porphyry copper systems, western North America. *Geological Society of America Abstracts with Programs.* Vol. 15, 572.

GUNN, A G. 1989. Drainage and overburden geochemistry in exploration for platinum-group element mineralisation in the Unst ophiolite, Shetland, U.K. *Journal of Geochemical Exploration,* Vol. 31, 209-236.

GUNN, A G, STYLES, M T, STEPHENSON, D, SHAW, M H, and ROLLIN, K E. 1990. Platinum-group elements in ultramafic rocks of the Upper Deveron Valley, near Huntly Aberdeenshire. *British Geological Survey Technical Report WF/90/9 (Mineral Reconnaissance Programme Report 115).*

HALLIDAY, A N, AFTALION, M, PARSONS, I, DICKIN, A P, and JOHNSON, M R W. 1987. Syn-orogenic alkaline magmatism and its relationship to the Moine Thrust Zone and the thermal state of the Lithosphere in NW Scotland. *Journal of the Geological Society of London,* Vol. 144, 611-617.

MATTHEWS, D W, and WOOLLEY, A R. 1977. Layered ultramafic rocks within the Borralan complex Scotland. *Scottish Journal of Geology,* Vol. 13, 223-236.

NOTHOLT, A J G, and HIGHLEY, D E. 1981. Investigation of the phosphate potential of the Loch Borralan Complex, north-west Highlands, Scotland. *Open File Report, Institute of Geological Sciences (now BGS).*

PARSONS, I. 1965 (a). The sub-surface shape of part of the Loch Ailsh Intrusion, Assynt, as deduced from magnetic anomalies across the contact, with a note on traverses across the Loch Borralan Complex. *Geological Magazine,* Vol. 102, 46-58.

PARSONS, I. 1965 (b). The feldspathic syenites of the Loch Ailsh Intrusion, Assynt, Scotland. *Journal of Petrology,* Vol. 6, 365-394.

PARSONS, I. 1968. The origin of the basic and ultrabasic rocks of the Ailsh alkaline intrusion, Assynt. *Scottish Journal of Geology,* Vol. 4, 221-234.

PEDLEY, R C. 1991. GRAVMAG Interactive 2.5D gravity and magnetic modelling program: User Guide. *British Geological Survey, Keyworth, Nottingham.*

PHEMISTER, J, and ROSS, G. 1926. The geology of Srath Oykell and Lower Loch Shin. *Memoirs of the Geological Survey of Great Britain.*

SHAND, S J. 1910. On borrolanite and its associates in Assynt (second communication). *Transactions of the Geological Society of Edinburgh.* Vol.9, 376-416.

SHAW, M H, GUNN, A G, FLETCHER, T A, STYLES, M T, and PEREZ, M. 1992. Data arising from drilling investigations in the Loch Borralan Intrusion, Sutherland, Scotland. *B.G.S. Mineral Reconnaissance Programme Open File Report Series No. 8.* (2 vols.).

STUMPFL, E F. 1993. Fluids: A prerequisite for platinum metals mineralisation. *In:* Current Research in Geology Applied to Ore Deposits. Fenoll Hach-Ali, P, Torres-Ruiz, J and Gervilla, F (editors). *University of Granada, Granada, Spain.*

STYLES, M T. 1993. A mineralogical study of platinum group element mineralisation in the Loch Ailsh Complex, Sutherland, Scotland. *British Geological Survey Technical Report.* WG/93/7.

SUTHERLAND, D S. 1982. Alkaline intrusions in north-western Scotland. *In: Igneous Rocks of the British Isles pp 203-214.* (John Wiley and Sons Ltd.).

TENENGREN, F R. 1962. The Vassbo lead ore deposit in Idre, western Sweden and its geological setting. *Sveriges Geologiska Undersokning, Ser. C.* Vol. 586, (61 pages).

THIRLWALL, M F. 1988. Geochronology of Late Caledonian magmatism in northern Britain. *Journal of the Geological Society of London,* Vol. 145, 951-967.

VAN BREEMAN, O, AFTALION, M, and JOHNSON, M R W. 1979. Age of the Loch Borralan Complex, Assynt and late movements along the Moine Thrust Zone. *Journal of the Geological Society of London.* Vol. 16, 489-495.

WERLE, J L, IKRAMUDDIN, M, and MUTSCHLER, F E. 1984. Allard Stock, La Plata Mountains, Colorado - an alkaline rock-hosted porphyry copper - precious metal deposit. *Canadian Journal of Earth Sciences.* Vol. 21, 630-641.

WYLLIE, P J. 1984. Constraints imposed by experimental petrology on possible and impossible magma sources and products. *Philosophical Transactions of the Royal Socety of London, A.* Vol. 310, 439-456.